APPLICATION OF ELECTRICAL RESISTIVITY TECHNIQUES TO IDENTIFY AREAS OF GROUNDWATER CONTAMINATION

by

Abdulameer Jaffar Al-Aradi

A dissertation submitted to the University of Wales, Bangor in partial fulfilment of the degree of Magister in Scientia.

GIFT هدية

جامعة البحرين
المكتبة
LIBRARY
University of Bahrain

School of Ocean Sciences
University of Wales, Bangor
Menai Bridge
GWYNEDD
UK

December, 1995

ABSTRACT

The electrical resistivity method has been used to investigate possible groundwater contamination from two different sources at two sites. The first in a coastal aquifer is due to the intrusion of seawater and the second in an aquifer underlying a landfill site is due to possible migration of leachate.

The effectiveness of several different electrode configurations for carrying out Vertical Electrical Sounding (VES) has been investigated in relation to the detection of a saline interface. The Offset Wenner technique was found to be the best option in terms of ease of use, recognising lateral problems and providing error estimates. The Schlumberger array was considered as the next best alternative if the switching box and muliticore cable required for the offset Wenner technique was unavailable.

Investigations on the coastal aquifer site using VES , Wenner pseudosection and Sclumberger AB profiling techniques enabled the lateral variations of the resistivity to be mapped. The VES data provide reasonable vertical resolution at a relatively few sounding locations. The pseudosection data provided good horizontal resolution with a limited depth of penetration (6 to 8 metres). The Schlumberger AB profile showed the lateral changes in apparent resistivity over a small rectangular area and averaged over a depth of about 50m. High resistivity areas were correlated to elevated areas of the site which had a surficial layer of dry sandy gravel overlying alluvium. The lowest resistivity areas occured in the lower regions of the site and were correlated with the alluvium. Repeated VES and pseudosection surveys were conducted to investigate any temporal changes in groundwater conductivity due to the effects of tidal pumping. No significant systematic changes with time were observed.

On the landfill site VES and pseudosection techniques were used and proved capable of detecting the presence of leachate within the waste tip. Leachate contamination away from the base of the waste tip was observed. Some of the plumes of leachate could be correlated with leaks from the side of the tip which had spread out on the surface adjacent to the tip.

The use of these different techniques has given the auther some confidence in their application for delineating and mapping interfaces between fresh and saline water in aquifers in Bahrain.

CONTENTS

ABSTRACT

ACKNOWLEDGEMENT

DECLARATION

CHAPTER ONE 1

1- Introduction 1
1-1 Overview of the seawater intrusion problem in Bahrain 1
1-2 Aims of study 2
1-3 Measures used to achieve intended aims 2
1-4 Outline of the Thesis 3

CHAPTER TWO 5

2- Seawater intrusion and the use of the electrical resistivity method for detecting groundwater contamination 5
2-1Ghyben-Herzberg relation 5
2-2 Mechanism of fresh-salt Water interface 7
2-3 Zone of diffusion 7
2-4 Fresh-salt water interface structure 9
2-5 Resistivity methods for the detection of groundwater contamination 11
2-5-1 Apparent resistivity 13
2-5-2 Types of resistivity methods 14
2-5-2-1 VES method 14
2-5-2-2 CST method 15
2-6 Review of previous electrical investigations 15

CHAPTER THREE 16

3- Description of the test sites used in the study 16
3-1 College Farm, Aber 16
3-1-1 Location 16
3-1-2 Geology 16
3-1-3 Hydrogeology 19
3-1-4 Seawater intrusion study 19
3-1-5 Problems associated with site which might be solved by further surveys 20
3-2 Landfill site 20
3-2-1 Geology 21

3-2-2 Hydrology 21
3-2-3 Hydrogeology 22
3-2-4 History of site waste disposal and problems which might be solved by electrical surveys 22

CHAPTER FOUR 24

4- Methodology and Measurement Programme 24
4-1 Electrical resistivity equipment 24
4-1-1 The Campus Geopulse modular resistivity meter 26
4-1-2 The ABEM Terrameter SAS 300 27
4-1-3 The Terrameter SAS log 200 30
4-2 Electrical resistivity surveying techniques 31
4-2-1 Vertical electrical sounding (VES) 31
4-2-1-1 Schlumberger array 32
4-2-1-2 Wenner array 32
4-2-1-3 Offset Wenner system 33
4-2-1-3-1 Calculation of intermediate and last reading in the resistivity curve 34
4-2-2 Constant separation traversing (CST) 36
4-2-2-1 Lateral changes in resistivity Using successive Schlumberger AB profile 36
4-2-2-2 Resistivity pseudosection 37
4-2-3 Borehole fluid resistivity logging 41
4-3 Electrical surveys carried out at College Farm, Aber 44
4-3-1 VES for constructing a geoelectric section 45
4-3-2 VES for comparing different arrays 45
4-3-3 Mapping the lateral changes in the apparent resistivity using AB profiles 45
4-3-4 Pseudosection 46
4-3-5 Borehole resistivity logging 47
4-4 Electrical surveys carried out at the landfill site 47
4-4-1 VES surveys 48
4-4-2 Pseudosection 48
4-5 Errors involved in electrical surveys 49
4-5-1 VES errors 49
4-5-2 Pseudosection errors 51
4-6 Positional site survey 51
4-6-1 Positional surveying equipment 53
4-6-1-1 The Hilger Watts level 53
4-6-2 Positioning and levelling surveys carried out at College Farm, Aber site 53
4-6-3 Errors involved in positioning and levelling surveying 53

CHAPTER FIVE 55

5- Interpretation of Electrical Measurements 55
5-1 Interpretation of VES resistivity curves 55
5-1-1 Ambiguity of Interpreting the VES resistivity curves 56
5-1-1-1 Principle of equivalence 56
5-1-1-1-1 Examples of principle of equivalence 57
5-1-1-2 Principle of suppression 57
5-1-1-2-1 Examples of principle of suppression 58
5-1-1-3 Relative thickness of a layer 58
5-2 Interpretation of resistivity pseudosections 58
5-2-1 The inversion program used in this study 60
5-2-1-1 Processing data using the inversion program 60
5-3 Interpretation methods of the surveyed AB profiles 63

CHAPTER SIX 65

6- Results of surveys 65
6-1 Data from College Farm, Aber 65
6-1-1 The VES resistivity surveys 65
6-1-1-1 Comparison of different VES configurations 65
6-1-1-2 Geoelectric section derived from the VES data 75
6-1-1-3 Temporal changes in groundwater conductivity 78
6-1-2 Pseudosections and inverted resistivity depth profiles 79
6-1-2-1 Pseudosection Ps1 for the delineation of saline interface 81
6-1-2-2 Spatial variations in resistivity 84
6-1-2-3 Monitoring tidal effect on the groundwater conductivity 89
6-1-3 Schlumberger AB Profiles 89
6-2 Data from the landfill site 93
6-2-1 VES resistivity curves 93
6-2-1-1 VES S1 93
6-2-1-2 VES S2 94
6-2-1-3 VES S3 94
6-2-1-4 VES S4 96
6-2-2 Pseudosections sections and resistivity-depth profiles 96
6-2-2-1 Pseudosection Ps1 96
6-2-2-2 Comparison of pseudosections Ps2 and Ps3 100

CHAPTER SEVEN 104

7- Discussion 104
7-1 College Farm, Aber 104
7-1-1 Comparison of VES array configurations 104
7-1-2 Comparison of geoelectric section and pseudosection ps1 105
7-1-3 Spatial variation in resistivity across the site 107
7-1-4 Temporal variation in groundwater conductivity 108
7-2 Landfill site 109
7-2-1 Comparison of the VES and pseudosection surveys 109
7-3 Comparison of the results from both sites 111

CHAPTER EIGHT 113

8- Conclusions 113

APPENDICES

REFERENCES i-v

ACKNOWLEDGEMENT

I am grateful to Dr Jim Bennell who spared no effort to supervise this project and enlightened me with useful ideas during discussions throughout the project period. I am also thankful to him for designing the multi-core cable for performing 2-D pseudosection surveying which has facilitated the acquisition of data. Besides, thanks are due to him for his assistance in the field where his experience has been very benificial.

Thanks are also due to Dr Angela Davis, the MSc course director of Marine Geotechnics, for her continued encouragement through the first part of the MSc course and this study as well. I thank all the Geotechnics' staff who were involved in teaching this course where I gained a lot of knowledge and experience. Thanks are specially due to Mr. Geraint Williams who helped in technical and field work. I acknowledge with many thanks the special permission granted by the owner of the landfill site for conducting the electrical resistivity surveys.

I would like to thank the British Council in Bahrain for granting me a scholarship for reading in the University of Wales, Bangor, and in this regards thanks are also due to British Gas who jointly funded this scholarship.

I thank Mr. A. Bucheeri, the director of Water Resources Directorate (WRD) for allowing me to pursue my study and would like to thank all my colleagues at WRD with special thanks to Mr. Mubark Aman, my supervisor, for his encouragement and moral support.

I am extremely grateful to my wife and children Jaffar, Fatima and Hussain who patiently tolerated being away from me during the study period and for their moral support which encouraged me to pursue my higher degree. I am highly indebted to my mother, sisters and brothers, especially Mohammed for their moral support and encouragement throughout my study. I also thank all friends, in and outside Bahrain, who encouraged me to take this opportunity of doing my degree.

DECLARATION

This work has not previously been accepted in substances for any degree and is not being concurrently submitted in candidature for any degree.

Signed .....(candidate)
Date 7.12.95

STATEMENT 1

This dissertation is being submitted in partial fulfilment of the requirements for the degree of MSc.

Signed .....(candidate)
Date 7.12.95

STATEMENT 2

This dissertation is the result of my own independent work/investigation, except where otherwise stated.

Other sources are acknowledged by footnotes giving explicit references. A bibliography is appended.

Signed .....(candidate)
Date 7.12.95

This is to certify that the work here submitted was carried out by the candidate himself. Due acknowledgement has been made of assistance received.

Signed J. D. Bennell .....(supervisor)
Date 7/12/95

STATEMENT 3

I hereby give consent for my dissertation, if accepted, to be available for photocopying and for interlibrary loan, and for the title and summary to be made available to outside organisations.

Signed .....(candidate)
Date 7.12.95

CHAPTER ONE

1- INTRODUCTION

Over the past few decades there has been considerable concern about groundwater deterioration, particularly in arid and semi-arid regions, where this forms the major exploitable source. Coastal areas are of special interest because of the phenomenon of seawater intrusion .

1-1 Overview of the Seawater Intrusion Problem in Bahrain

Bahrain suffers seriously from this phenomenon where its fresh groundwater resource is threatened by a major invasion of seawater. Many agricultural areas and some water pumping stations along the east coast, where the groundwater flow is oriented, have already been abandoned.

An integrated groundwater modelling programme, consisting of a number of sub-models, was constructed in 1980 and is currently under use to monitor the groundwater conditions. One of these models is called the Khobar Saline Water Model, which is concerned with the behaviour of the Dammam aquifer in northern Bahrain in terms of water quality. It is intended to predict changes in groundwater with time in this aquifer, which until 1984 was the main supply of water for domestic and agricultural use. The model requires a number of input variables, such as piezometric levels and groundwater abstraction rates, to predict the theoretical position of the saline interface. The model has been partially validated by well pumping experiments and limited borehole logging to monitor the movement of the seawater front during periods of heavy groundwater abstraction.

However, the limited borehole logging is not capable of locating the fresh-saline water interface everywhere. In addition, the areal extent of the seawater intrusion, as predicted by the model, has not yet been verified by an extensive measurement programme.

The ongoing programmes for monitoring the Dammam aquifer through a network of boreholes, in terms of piezometric levels, water quality, and water abstraction do not

adequately predict groundwater conditions between these boreholes.

In this respect there is a substantial need to use a fast and effective surface technique that is able to map global groundwater conditions between the available boreholes.

1-2 Aims of Study

The ultimate goal of this study is to investigate the feasibility of different electrical resistivity techniques to define areas of contamination in groundwater. There was also the intention to study the possibility of using these methods to monitor the movement of the fresh-salt water interface due to tidal pumping effects. If the techniques prove to be successful it is intended that they should be used back in Bahrain, at the conclusion of this study, as a means of monitoring groundwater contamination and validating the Khobar Saline Water Model. A secondary aim of the research was to determine the most effective way of carrying out a Vertical Electrical Sounding (VES). A similar conclusion is hoped to be reached concerning the determination of lateral changes in resistivity by the means of either the equipotential method or pseudosection techniques.

1-3 Measures Used to Achieve Intended Aims

Spatial and temporal surface electrical resistivity surveys have been conducted at two different contrasting sites to achieve the above objectives.

The first site at Aber, Gwynedd, UK consists of a small coastal aquifer composed of sands and gravels underlain by glacial deposits. The site has already been investigated as a part of a Ph.D research project on saline intrusions (Soomro, 1993). A suite of boreholes have been installed on the site for permeability measurements. Since the site is relatively well investigated it makes an ideal test bed for this particular study of the comparison of various electrical resistivity techniques for detecting groundwater contamination. The investigation involved carrying out different types of electrical surveys to study how the intrusion of seawater into the aquifer varied both spatially and temporally. To achieve the latter objective measurements were made at the same point on different days. In addition, measurements were made at the same location; at a closer time interval (about one hour) on the same day

in order to assess the effect of tidal pumping on the groundwater conductivity (i.e. to see if the saline intrusion flowed further inland as the head of seawater increased).

The second site is an inland Landfill area the location of which is to be kept confidential to protect the interests of the site owner. The main aim of this investigation was to see first if resistivity techniques could detect contamination of the groundwater and second to determine which techniques would be best suited for the detection of any seepage of leachate into the local drainage system (if any leakage actually occurs). The site is monitored regularly, through a network of widely spaced shallow boreholes, by the local council, and the results show there is no major escape of leachate from the site. The boreholes are, however, fairly widely spaced so surface resistivity methods could be useful for monitoring any leachate flow that might occur between the boreholes.

From a comparison of the techniques and results of investigations at both of these sites it is hoped to assess the best ways of carrying out surface electrical surveys for mapping groundwater contamination. It is then expected that similar types of surveys can be used back home in Bahrain to complement the existing network of boreholes used for monitoring groundwater contamination.

1-4 Outline of the Thesis

In the **next chapter** a general introduction to the theory of seawater intrusion is given together with a review of the methods available to detect and delineate the fresh-salt-water interface. A brief review of the electrical resistivity method is introduced here but a complete description of the equipment, methodology and surveys undertaken is given in **chapter four**.

Chapter three will be assigned to the description of the test sites and problems associated with each of them that might be solved by further surveys.

Chapter five describes how the field data has been processed and inverted to produce the necessary data on the vertical and areal distribution of ground resistivity or conductivity.

Chapter six presents the results obtained at each of the sites in terms of geoelectric sections

and contour maps along with any changes in groundwater conductivity with time that have been detected.

The results are then discussed in relation to what is already known about the sites in **chapter seven.**

Finally **chapter eight** compares the data obtained at each site and makes recommendations on the techniques which would be most applicable for detecting groundwater contamination in Bahrain.

2- SEAWATER INTRUSION AND THE USE OF THE ELECTRICAL RESISTIVITY METHOD FOR DETECTING GROUNDWATER CONTAMINATION

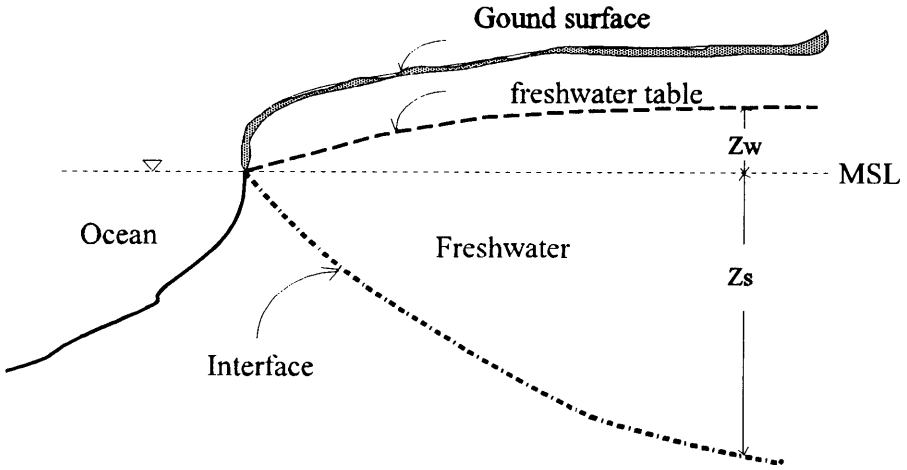
Where the freshwater and saltwater come into contact, an interface zone develops. In the interface zone, the salt concentration changes from that of the saltwater to that of the freshwater.

2-1 Ghyben-Herzberg Relation

Badon Ghyben (1888) and Herzberg (1901) established the theory of hydrostatic equilibrium for the salt-fresh-water interface in a homogenous, unconfined coastal aquifer.

They showed that the interface separating salt water of density ρ_s and freshwater of density ρ_f must project into the aquifer at an angle $\alpha < 90°$ (fig. 2.1). Under hydrostatic conditions,

Figure 2.1



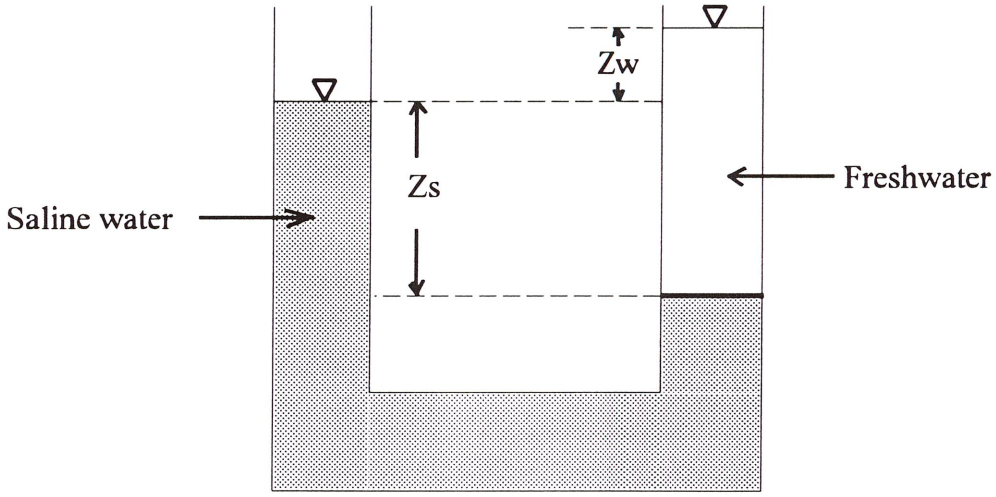
Idealized sketch of occurence of fresh-salt water

Interface in an unconfined coastal aquifer (after Todd, 1980)

the weight of a unit column of fresh-water extending from the water table to the interface

is balanced by a unit column of salt-water extending from sea level to the same depth as the point on the interface (Freeze and Cherry, 1979). Fig. 2.2 shows the hydrostatic balance between freshwater and saline water as illustrated by a U-tube given by Todd, (1980).

Figure 2.2
Hydrostatic balance between fresh and saline water in a U-tube
(After Todd, 1980)



$$\rho_s g Z_s = \rho_f g(Z_w + Z_s) \qquad 2.1$$

where Z_s is depth to the interface,

Z_w is depth to freshwater table,

ρ_f is density of freshwater,

ρ_s is density of seawater, and

g is the acceleration due to gravity.

The result of this theory is the Ghyben - Herzberg relation which is:

$$Z_s = (\rho_f / (\rho_s - \rho_f)) Z_w \qquad 2.2$$

If a typical seawater density of 1.025g/cm^3 and a freshwater density of 1.000g/cm^3 are used, then equation 2.2 becomes:

$$Z_s = 40\ Z_w \qquad 2.3$$

This depth may vary from place to place dependant upon the density values of salt and

fresh water. In Bahrain, for instance, $\rho_s = 1.029$ and $\rho_f = 0.998$ have been used to provide a local value of $Z_s = 32\ Z_w$ (GDC, 1980).

2-2 Mechanism of Fresh-Salt water Interface

Since the issue of this theory, some scientists have observed an agreement to the predictions of this theory, that assumes an abrupt interface between the salt and fresh water which act as immiscible fluids under the steady state condition, (Volker and Rushton, 1982; Singh and Stammer, 1989), while others have observed evidence for a more dynamic situation rather than hydrostatic equilibrium of the fresh-salt-water interface (Hubbert, 1940; Harris,1967).

However, Harris (1967) finds that the assumption of a static system is only reasonable in the absence of any substantial fresh groundwater movement. His study indicates that under steady-flow conditions, the interface would be sharply defined, but tidal action and rise and fall of the water table would maintain a zone of diffusion between the fresh and salt water.

Soomro (1993) summarised the work of many scientists whose published results were in agreement with the theory of hydrostatic equilibrium and also those which were in disagreement with the theory.

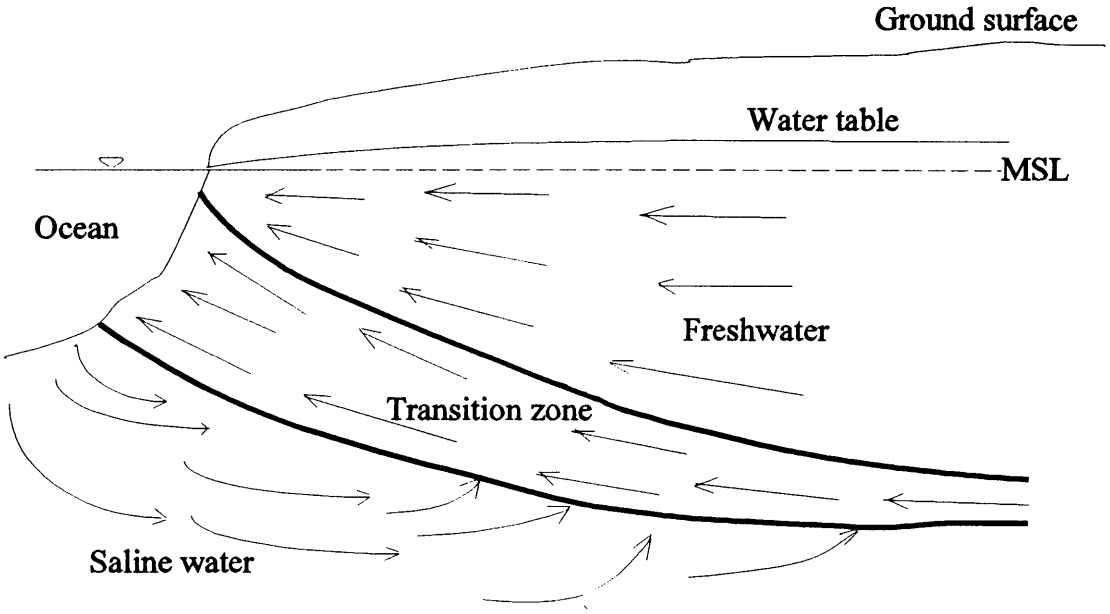
2-3 Zone of Diffusion

The presence of zone of diffusion was suggested earlier by Kohout (1964) and Cooper et al., (1964) who revealed that there was a cyclic circulation of salt water from the floor of the sea to a zone of diffusion and thence a return of salt water which is now diluted with freshwater, through the freshwater section to the sea. This circulation is induced by the dispersion of salts produced by the reciprocative motion of the salt water front caused by the tides and by any variation in freshwater recharge in the diffusion zone (Harris, 1967; Todd, 1959). Pumping from wells or tidal will promote this circulation (Cooper, 1959).

> "Where a zone of diffusion exists, the salt water is not static but flows perpetually from the sea floor into the zone of diffusion and back to the sea, and this flow tends to lessen the extent to which the salt water occupies the aquifer" (Cooper, 1959).

The diffusion, or mixing zone between fresh and salt water, is defined as the result of the contact between the two fluids where molecular dispersion takes place. Thus freshwater and salt water initially in contact show relatively high diffusion rates, which become progressively smaller as the diffusion zone (transient zone) increases and the concentration gradient decreases (fig. 2.3) (Soomro, 1993).

Figure 2.3
Vertical cross section showing flow pattern of fresh and saline water in an unconfined coastal aquifer (after Todd, 1974)



Generally speaking, the thickness of this zone may vary from less than a metre to more than 100 m (Soomro, 1993). It depends upon the properties of the fluids and the porous medium and the relative predominance of diffusion and dispersion (Singh and Stammers, 1989). In inhomogeneous coastal aquifers, stratification and irregularities in the distribution of fresh and salt waters occur (Harris, 1967).

The mechanical cyclic flow suggested by Cooper (1959) governs the flow between fresh and salt water within the transient zone;

"this is the powerful mechanism causing sufficient mixing" (Cooper, 1959).

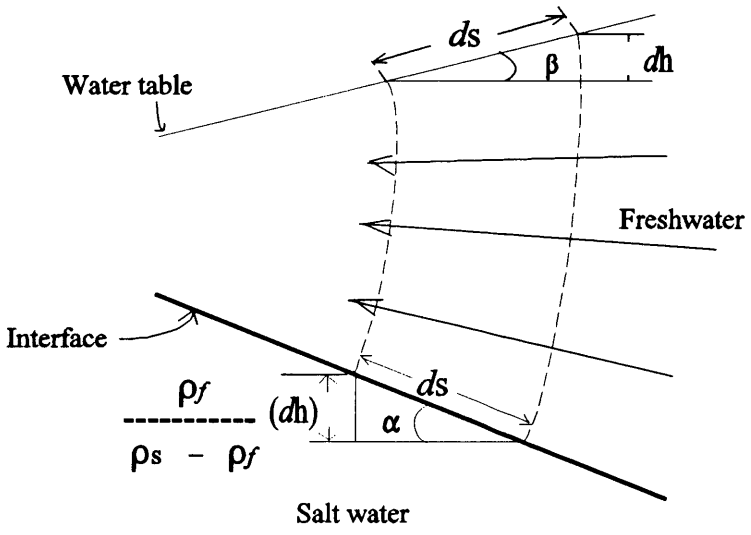
Freeze and Cherry (1979) quoted Henry (1960) as being the first to present a mathematical solution for the steady-state case that also includes a consideration of dispersion. For non-

homogenous or anisotropic coastal aquifers where permeability is different in different directions, stratified zones of fresh and salty water may arise (Harris, 1967).

2-4 Fresh-Salt Water Interface Structure

The Ghyben-Herzberg relation assumes that the interface slopes downward from the coast. The interface shape and slope can be inferred for the case where the flow occurs only in the freshwater zone (fig. 2.4).

Figure 2.4
Relation between slopes of the water table and the fresh-salt water interface (from Soomro, 1993)



The shape and slope of the interface is obtainable from Darcy's law:

$$v = k\,i \qquad 2.4$$

where v is the velocity of the interface movement,
k is the coefficient of permeability, and
i is the hydraulic gradient.

From fig. 2.4 we find:

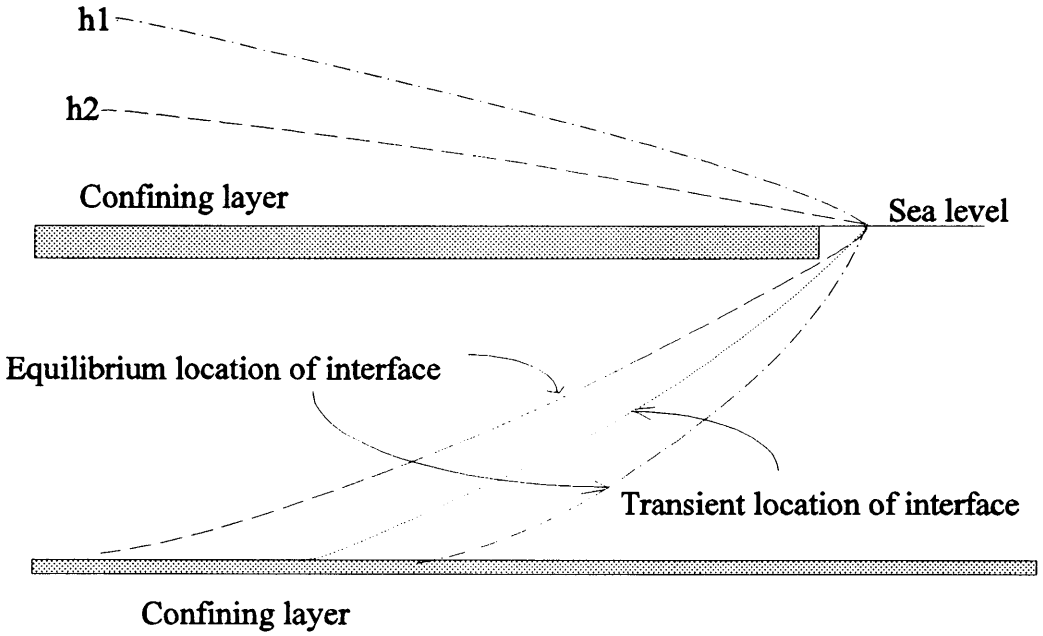
$$\sin\beta = dh/ds = v/k \qquad 2.5$$

According to equation 2.2 the slope of the fresh-salt-water boundary is then given as:

$$\sin\alpha = [\rho_f/(\rho_s-\rho_f)]\ v/k \qquad 2.6$$

Because of the steeper density gradient in the saline water than in the fresh, the pressure gradient increases with depth. It follows then that for an aquifer of uniform horizontal permeability, v increases with depth (GDC, 1980). This is illustrated in fig. 2.5 where the theoretical motion of the interface is shown at the equilibrium positions corresponding to head conditions h1 and h2.

Figure 2.5
Motion of the interface corresponding to
head conditions h1 and h2 (after GDC, 1980)



The length of the intruded wedge for a confined aquifer can be obtained from Darcy's law with the help of fig. 2.6.

$$q = 1/2(\rho_s-\rho_f/\ \rho_f)(\ k\ b^2\ /\ L) \qquad 2.7$$

where q is the seaward fresh water flow per foot of ocean front,

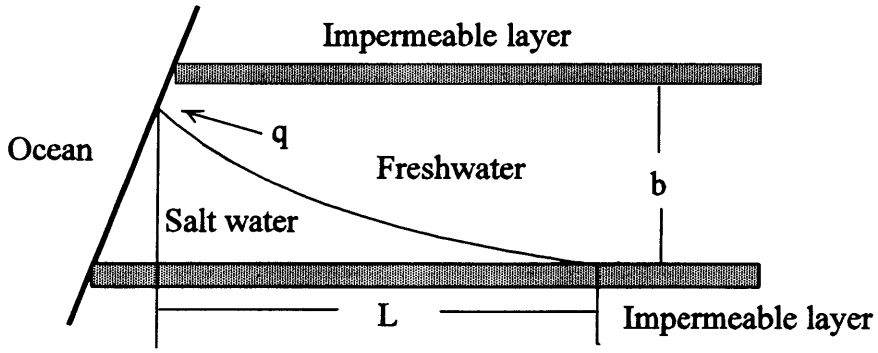
L is the length of the wedge, and

b is the thickness of the aquifer.

This equation is also applicable to an unconfined aquifer where b is replaced by the saturated thickness, provided that the flow does not deviate greatly from the horizontal (Soomro, 1993). From equation 2.7 the length of the intruded wedge is inversely proportional to the fresh water flow.

Figure 2.6

Salt water wedge in a confined aquifer (after Soomro, 1993)



Goswami (1968) observed that spring tides resulted in a considerable shift in the saline front, but the daily tidal effect only caused a minor movement of the interface. Pumping, on the other hand, is a major factor causing advancement of the saline front landward and may result in what is called upconing when the saline front is raised locally below the pumping well. This situation has been encountered in several wells in areas influenced by seawater intrusion in Bahrain (GDC, 1980).

In general, the degradation of groundwater quality is mainly caused by water extraction (Gonzalez and Romero, 1991), especially from coastal aquifers. This is because of the inability of freshwater sources, from rain and rivers, to replace the extracted water allowing the invasion of seawater to maintain the pressure balance.

2-5 Resistivity Methods for the Detection of Groundwater Contamination

As groundwater becomes more important as a source of uncontaminated water, methods for locating good aquifers must become more efficient. Partly for this reason, geophysical methods are playing an increasingly important role in groundwater investigation. (Kosinski and Kelly, 1981).

Since the electrical properties of most rocks in the upper part of the Earth's crust are dependent primarily upon the amount of water in the rock, the salinity of the water, and the

distribution of the water in the rock, the electrical resistivity methods are unique in furnishing information concerning the depth of the fresh-salt water interface (Zohdy et al., 1974).

The only geophysical exploration techniques that enables variations in water salinity to be delineated are electrical methods (Overmeern, 1989).

In recent years the use of the Electromagnetic (EM) techniques have gained considerable attention in groundwater applications. This technique solves some of the field problems like induced polarisation that is attributed to the use of electrodes, because it does not rely on any ground contact. It also solves the logistic problem of carrying large and heavy cables.

However, like the electrical resistivity method, the EM technique suffers from the same interpretation problem in its lack of a unique solution due to the principles of equivalence and suppression.

Because the conductivity of water increases with chloride concentration, electrical methods are well-suited for mapping chloride concentration in groundwater (Mills et al. 1988). It is well known that the surface electrical resistivity method is capable of distinguishing between zones of fresh water and saline water in a saturated granular formation (Zohdy et al. 1974).

The surface electrical method is based on introducing an artificial electrical current into the ground through a current electrode (source) and receiving it at a second current electrode (sink). The potential drop of this current is measured between two potential electrodes located somewhere between the current electrodes as the case in most electrode configurations (eg. Schlumberger and Wenner etc.)or outside the current electrodes as in some of the Dipole-Dipole arrays .

The idea of measuring the potential difference between the current electrodes is based on Ohm's Law for measuring the potential V in an electrical circuit:

$$V = IR \qquad 2.8$$

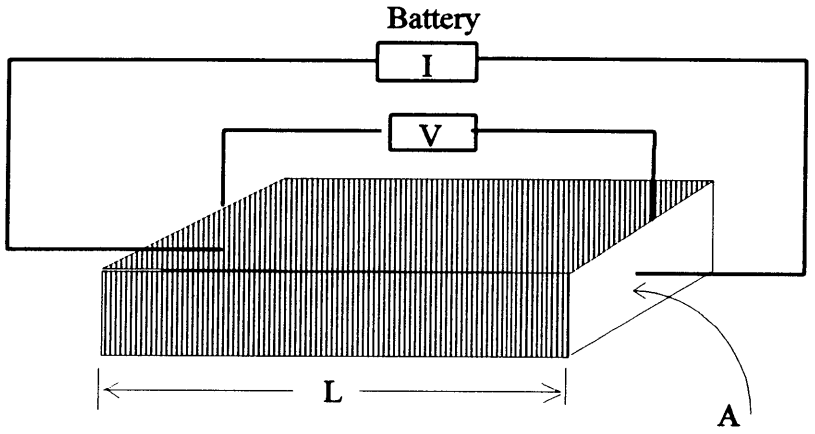
where I is the current flowing through the circuit, and

R is the resistance encountered by the flow of the current in the resistor.

The electrical current flowing through the resistor (fig. 2.7) encountered resistance (R) described in terms of the length, L of the path of the flowing charges, the cross-sectional area A, and the resistivity ρ, which is a physical property of the substance used to make the resistor.

$$R = \rho L/A \qquad 2.9$$

Figure 2.7
Electrical resistor consisting of a rectangular bar (after Robinson & Coruh, 1988)



In a homogenous medium, the potential V due to a point source is inversely proportional to the distance r between two closely spaced points; it is also directly proportional to the current I emanating from the source and to the resistivity ρ of the medium (Kunetz, 1966). If one assumes the earth to be a homogeneous half space of infinite extent, the constant of proportionality equals ½ ρ (Kunetz, 1966; Zohdy et al. 1974) and the potential then becomes:

$$V = I \rho / (2\pi r) \qquad 2.10$$

2-5-1 Apparent Resistivity

When subsurface inhomogeneities exist, the resistivity will vary with the relative positions of the electrodes, and any measured value is then known as the apparent resistivity ρ_a and will be a function of the form of the inhomogeneity (Kerry and Brooks, 1991). The value

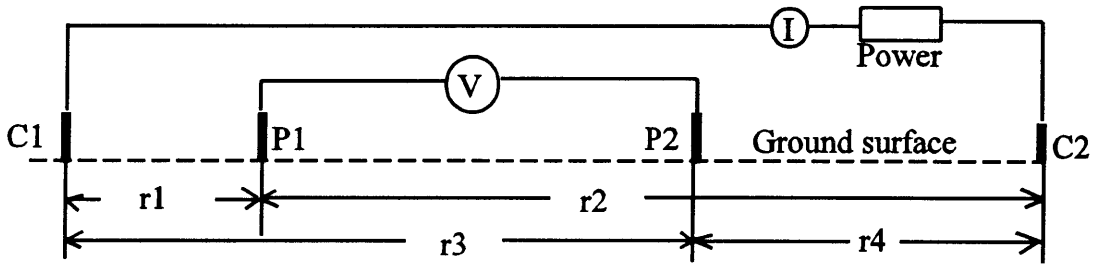
of the apparent resistivity is a function of several variables: electrode spacing, the geometry of the electrode array, the true layer resistivities and other characteristic of the subsurface materials such as layer thicknesses, angles of dip, and anisotropic properties (Zohdy et al. 1974).

A general equation, eq. 2.11, is available to determine apparent resistivity for all kinds of electrode configurations (fig. 2.8) [Telford et al., 1990].

$$\rho_a = (2\pi\Delta v/I)\{1/[1/r_1-1/r_2-1/r_3+1/r_4]\} \qquad 2.11$$

Figure 2.8

Two current and two potential electrodes on the surface of homogenous isotropic ground of resistivity ρ (after Telford et al., 1990)



2-5-2 Types Of Resistivity Methods

Two surface resistivity techniques are commonly used in groundwater applications. These are Vertical Electrical Sounding (VES) or Depth Probing and the Constant Separation Traversing (CST) or Resistivity Profiling methods.

2-5-2-1 VES Method

This method involves expanding the electrode array about a central point so as to determine the depth to successive layers within the earth. The apparent resistivity values are plotted against the spacing between the current electrodes on a bi-logarithmic chart. The resulting sounding curve can then be interpreted in terms of layers of different true resistivities.

Several electrode configurations are suitable to use for this technique. The most common and widely used arrays are Schlumberger and Wenner. In this study, the Offset Wenner system has also been used alongside the aforementioned configurations.

2-5-2-2 CST Method

This technique maintains a constant electrode spacing while carrying out a set of measurements as the array is moved along a straight line. The main objective is to determine the lateral variation of apparent resistivity.

If the process is repeated along the same line while increasing the spacing, greater depths are explored and the apparent resistivity values can be contoured in what is known as **Resistivity Pseudosection**.

2-6 Review of Previous Electrical Investigations

The surface resistivity method has been employed successfully for detecting and mapping groundwater contamination under a variety of conditions (Kelly, 1976).

Recently the resistivity method has been used in the Azraq basin, in Jordan and led to the determination of the boundary between saline and freshwater zones with reasonable accuracy (Elwaheidi et al., 1992). The method has been widely used in many parts of the world and has proved an excellent technique for detecting the fresh-salt water interface. Recent examples are found in Al Ruwaih (1992), Sarma et al (1993), Soomro (1993) and Wu et al.,(1993) among others.

3- DESCRIPTION OF THE TEST SITES USED IN THE STUDY

This chapter will briefly present the previous work that has already been carried out on both sites that will be of benefit to this study.

3-1 College Farm, Aber

3-1-1 Location

This site is a farm for grazing animals and assigned for academic research. It belongs to the school of Agriculture at the University of Wales, Bangor. The farm consists of six fenced fields (fig. 3.1). The study area is in the northeastern part of the farm adjacent to the shore. It is situated on the north coast of Wales, about one kilometre northwest of the village of Aber (post office). Approximate Grid coordinates are: 373500 N and 265500 E. The site is almost flat with only minor undulations of the local topography.

3-1-2 Geology

The geology of the area was determined by a study of the glaciogenic deposits along the eastern Menai Strait by Pointon and Hart (Soomro, 1993). This original study could not be obtained but details have been obtained from a Ph.D thesis by Soomro (1993). The interpretation of the site lithology is based on data from the geology of Glan-y-Mor-Isaf that lies to the southwest and also the exposure associated with the A55, North Wales Coast Road, near Llanfairfechan which lies to the northeast. The lithology can be divided into two geological Epochs, the Holocene and the Pleistocene, of the Quaternary Era.

A- **The Holocene** (<10,000 years BP) contains four layers:

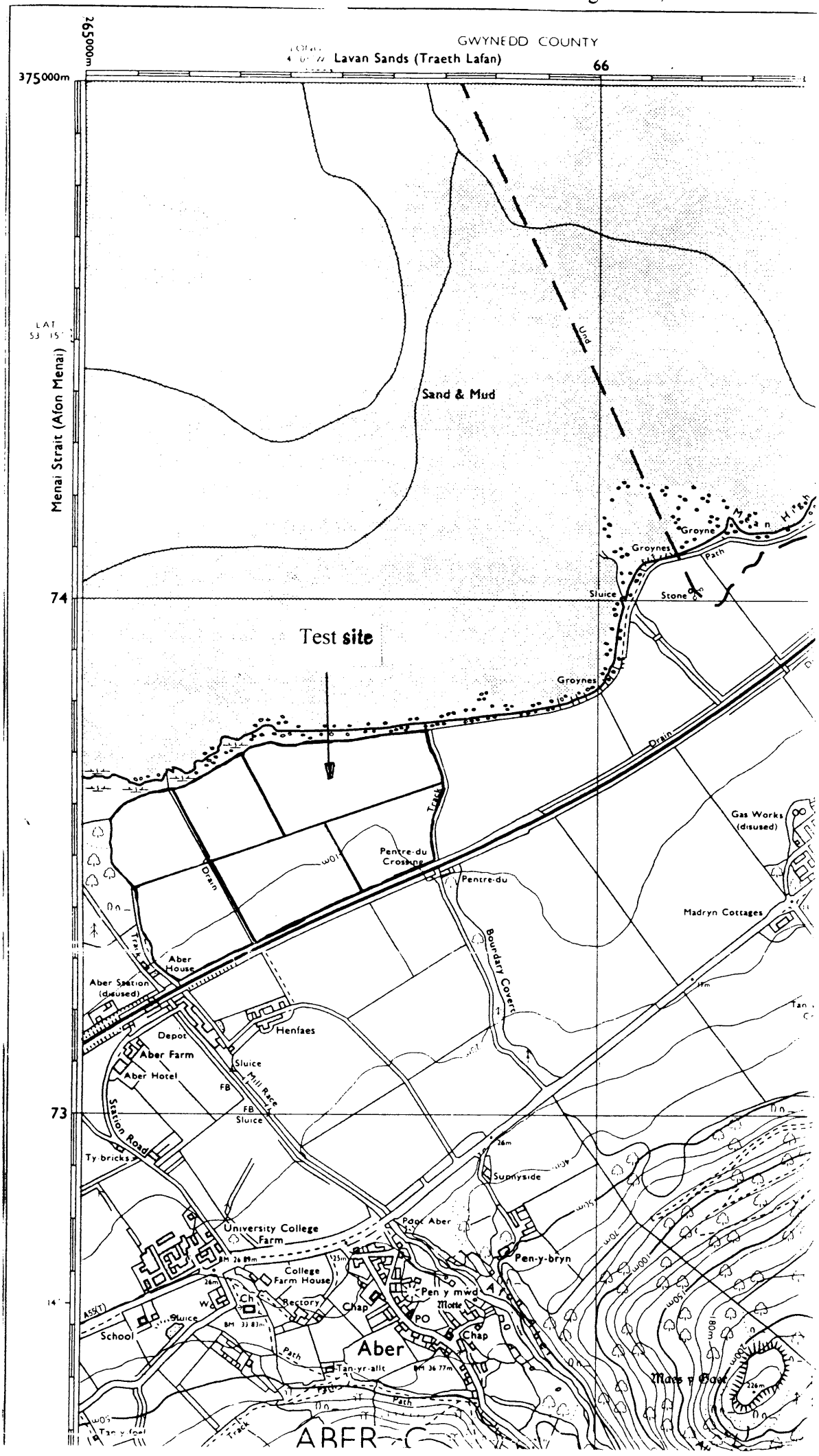
1- *Surface Fill.*

2- *Fluvial Sand and Gravel.*

3- *Marine Clays and Silts.* Occasional existence of sand and gravel.

4- *Peat.* (its base forms the junction between lower Holocene and the upper Pleistocene).

FIG. 3.1. College Farm, Aber



B- **The Pleistocene** (>10,000 years BP) contains four strata:

1- *Fluvial Gravels.* (pebbles and cobble are abundant, and boulders are occasionally found).

2- *Irish Sea Till.* It is matrix-supported diamicton that is a poorly sorted gravel-sand-mud admixture which is highly over consolidated. This till is likely to be deposited in association with ice movement southwards into the Irish Sea Basin. It contains coarse clasts of cobble and boulder, but characteristically far less than the coarse material in the Welsh Till.

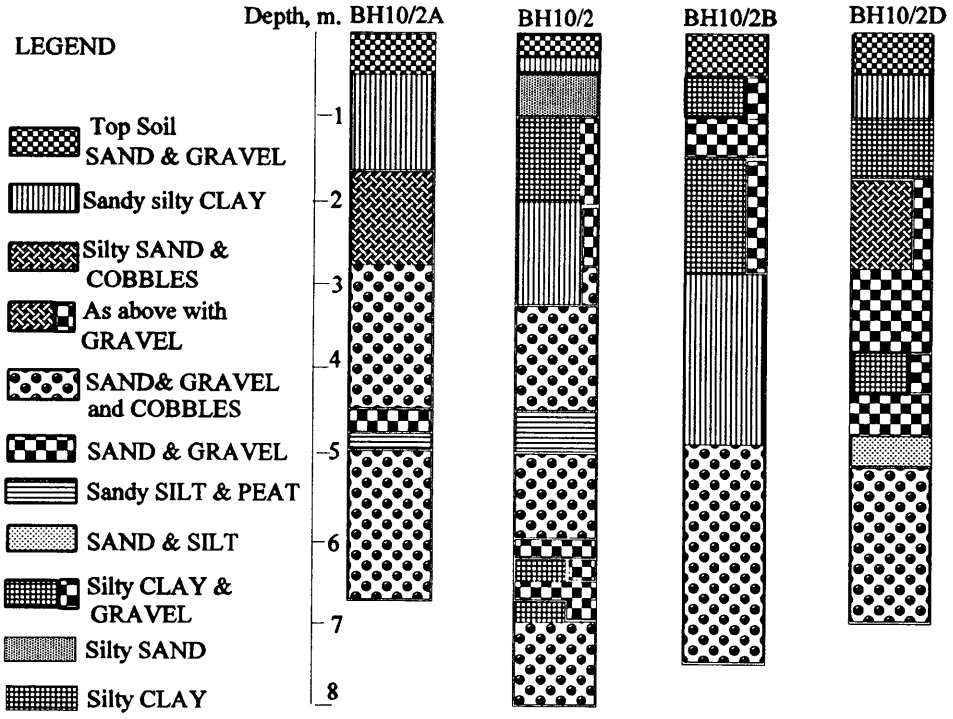
3- *Welsh Till.* It is matrix-supported diamicton with abundant coarse clasts of cobble, boulder, and frequent thick gravel intra-beds. It is typically highly over consolidated and its depositional environment is associated with ice moving northwards out from the mountains of Snowdonian .

4- *Irish Sea Till*

Gilchrist (1993), a BSc student, who ran several geophysical seismic surveys, described the lithology of four boreholes on the site (fig. 3.2) which can be correlated with the general geology of the area. The location of these boreholes will be shown in chapter 4.

Figure 3.2

Lithology of boreholes



3-1-3 Hydrogeology

A previous study by Soomro (1993) revealed two aquifers to be present in the area. The upper aquifer, composed of unconsolidated fine to coarse grained sand and gravel is intercalated with one or two thin soft clay and peat lenses and extends from a depth of two to seven metres. This information is based on data from shallow auger boreholes in the area.

This aquifer is considered to be confined where it is overlaid by Surface Fill material, which is a silty and clayey soil mixed with fine sand and gravel at the top becoming coarser at its base. The aquifer is underlain by an impervious glacial till that contains an admixture of boulders, cobbles, gravel, sand, and mud.

A second aquifer lying below the glacial till was evident from geophysical data.

Although Soomro's study considered the upper aquifer to be confined, he showed that local recharge from the rain water that percolates through the 50% granular material at the surface could replenish the aquifer. It infiltrates further down to the second aquifer. This suggests that what are considered confining beds at the top and the bottom of the first aquifer are likely to be semi-confining layers.

3-1-4 Seawater Intrusion Study

The electrical resistivity method and the electromagnetic method were used by Soomro (1993) to study the seawater intrusion and to delineate the fresh-salt water interface. He used sounding techniques (Wenner and Offset Wenner) to run several depth probes along lines perpendicular to the coast to produce what is known as geoelectrical sections. These sections show plots of the interpreted data (resistivity and thickness) from the processed sounding curves. Two out of five of these geoelectrical sections lie within the present study area. In these two sections two aquifers have been shown to exist.

The fresh-salt water interface could be delineated in these sections that also show the mixing zone and the fresh water boundaries in the upper and lower aquifers.

Seawater intrusion was monitored during a spring tide by taking nine water samples from one borehole at intervals of one hour. The chemical analysis results of these samples were compared with the fluctuations of the groundwater levels recorded by a portable water level recorder. The result showed that the rise and fall in the groundwater level (the water level in the borehole) almost coincided with the rise and fall of the tide. On the other hand the highest salinity was recorded about 1 1/2 hours after high tide.

To assess the tidal effect on the salt-fresh water interface the electrical method was used. During this spring tide temporal resistivity soundings (five soundings made at hourly intervals) were made at one fixed location where resistivity changes were recorded. The impact of the spring tide on the movement of the saline water front in both aquifers has been shown in changes in the earth models (resistivity/thickness) interpreted from each of the temporal soundings. The interpreted models showed a rise and falling trend in the resistivity/thickness of the upper aquifer attributed to the rise and fall of groundwater level due to the tide.

The usefulness of the resistivity method to detect changes in groundwater salinity due to a saline intrusion has been proved from these results (Soomro, 1993).

3-1-5 Problems Associated with Site Which Might Be Solved by Further Surveys

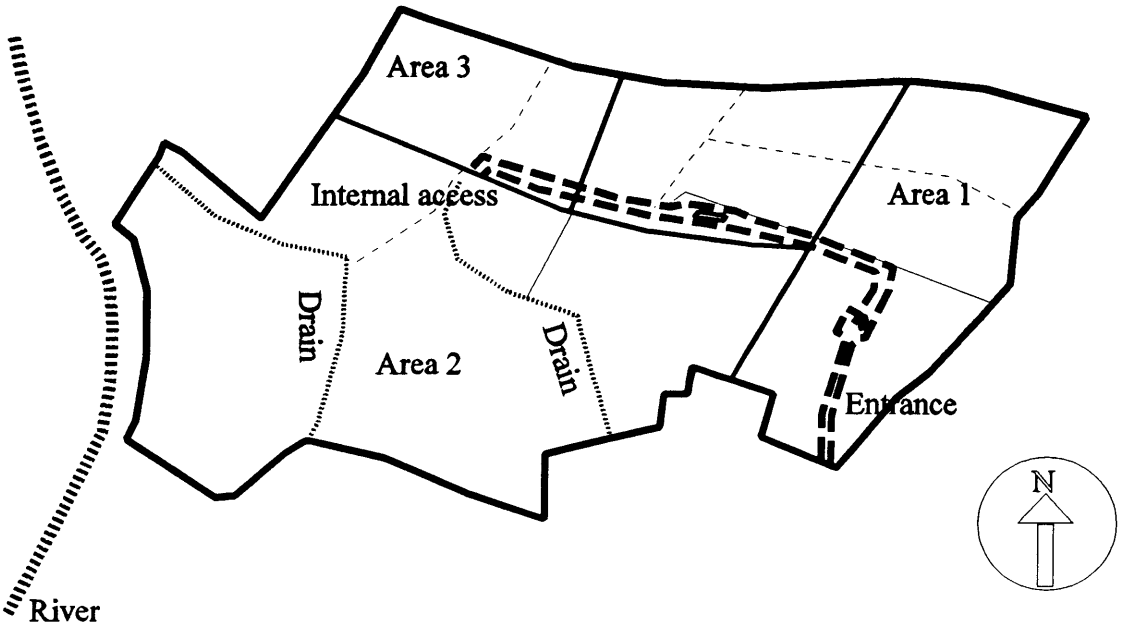
The site itself is very complicated in its geological and hydrogeological properties which show considerable lateral variability. By concentrating measurements in a small area, i.e. the field with the boreholes, it should be possible to map lateral variations in both the hydrogeological conditions and the geological strata.

3-2 Landfill Site

The intention of this study on this site was to verify the effectiveness of resistivity techniques in defining areas of groundwater contamination arising from a different source than seawater. Fig. 3.3 shows a schematic plan of the landfill site and the location of the river that runs adjacent to the area surveyed in this investigation.

Figure 3.3

Schematic plan of the Landfill site with main entrance and internal minor accesses



3-2-1 Geology

This study area is a part of a valley covered with marshy ground that is underlain by poorly sorted alluvial sands and gravels resting on schist bedrock. There is a relatively impervious alluvial clay covering the sands and gravels on the western parts of the study area. In the eastern parts of the test area the sands and gravels are underlain by boulder clay.

3-2-2 Hydrology

The land surrounding the site is low-lying, and is drained by a number of ditches which generally discharge in a southerly direction towards the river. One such drain crosses Area 3 of the site and is carried in a culvert beneath the waste in Area 2. Much of the surrounding land, including the western part of Area 3 and the land to the southwest of Area 2, is boggy and is subjected to flooding. This is attributed to the presence of the relatively impervious alluvial clay above the sands and gravels.

3-2-3 Hydrogeology

The sands and gravels comprise a minor confined aquifer where it is overlain by the clay. Where this clay is absent the aquifer is in direct hydraulic connection with the surface. In the parts of the site for which the alluvial clay is absent the base of the aquifer lies on the boulder clay. Leachate within the waste is perched above the alluvial clay, where it is present, and is isolated from the groundwater system, but it enters the aquifer where the clay is absent.

In the western part of Area 2, leachate within the waste is perched above the alluvial clay and is effectively isolated from the groundwater system in the sands and gravels. Leachate then emerges at the foot of the waste and enters the surface drainage system, draining eventually to the river. Where this clay is absent in the east of Area 2 and beneath Area 1, leachate in the waste is in direct hydraulic continuity with groundwater in the sands and gravels.

The uppermost levels of the metamorphic bedrock are fractured, and have a relatively high permeability. This unit is effectively isolated from groundwater in the overlying sands and gravels by the boulder clay which underlies most of the site; however, some hydraulic continuity is possible to the west of the site, where the sands and gravels rest directly on the bedrock.

3-2-4 History of Site Waste Disposal and Problems Which Might Be Solved by Electrical Surveys

Presently the site is being properly managed, monitored and regulated taking care to provide clay layer and bunds to constrain the waste and leachate.

The main flow of groundwater is expected to be southwards. Groundwater analyses from the sands and gravels beneath Area 2 confirm that leachate contamination is occurring. Data from one borehole to the west of this area indicates moderate contamination despite the presence of the alluvial clay above the aquifer in this area. It is postulated that this may be due to the presence beneath the landfill in this area of an old ditch excavated through the

clay and into the sands and gravels. Alternatively it is possible that groundwater under artesian pressure is entering the landfill via this route, thus contributing to the leachate generation.

Analysis of groundwater taken from the sands and gravels in a borehole situated 300m southwest (down gradient) of Area 2, showed few signs of leachate contamination. This was expected, since the contamination plume from the landfill was not expected to have reached this location at the time of the investigation (1988).

The monitoring wells are, however, spaced fairly well apart so leakage could be occurring between them. Electrical Resistivity profiles could be used to examine these areas.

Another cause of concern was that leachate could be discharging into the adjacent river not only by surface drainage but also through the aquifer. Between the site and the river there is an extensive reed bed which could be absorbing the contamination. Again electrical resistivity profiles could examine how far the leachate is penetrating into the reed bed. It would also be useful in seeing if leachate leaks were more of a problem in the unconfined (uncontained) part of the site compared to the more recent contained areas of the site.

In fact most of the surveys were undertaken on the west side of the site between the river and the landfill where it was possible to directly compare the ground adjacent to the unconfined landfill and the ground close to an area that had only just begun to be used for landfill and which had been protected by an impervious clay bund.

It would have been interesting to investigate other areas to the south of the site but access was difficult due to the marshy nature of the ground and the limited space available to layout the electrode spreads (usually a straight line profile of between 100 to 200m is required).

4- METHODOLOGY AND MEASUREMENT PROGRAMME

Various electrical resistivity techniques have been used to achieve the goals mentioned in chapter one. Table A4T1, in appendix 4.1, shows all types of field work that have been carried out in this study. The purpose of using each technique is briefly given in this table.

4-1 Electrical Resistivity Equipment

Two resistivity meters, the Campus Geopulse and the Terrameter SAS 300, were used for conducting all resistivity surveys on the test sites. A set of complementary tools were used with the aforementioned resistivity meters to make the resistivity measurements.

The followings are the tools used in resistivity soundings (VES) and the Schlumberger AB profiles in addition to the Campus Geopulse:

a- Four drums of single core cable, each about 200 m long,

b- Four stainless steel electrodes.

c- Four short (about 2 m in length) flying leads for connecting the terminals of the resistivity meters to the drums that are connected to the electrodes.

d- Two measuring tapes, each 100 m long.

The above equipment are shown in photographic plate 4.1. The Campus Geopulse was also used along with the Terrameter SAS LOG 200 for the borehole fluid resistivity logging (see photographic plate 4.2)

On the other, hand the following tools were used in the resistivity pseudosection surveys alongside the Terrameter SAS 300 (see photographic plate 4.3 & 4.4):

a- A multicore cable with 2 m spaced contacts

b- Fifty four steel electrodes

c- Switching box

d- A set of connecting wires, to connect the terminals on the resistivity meters with the switching box and wires to connect the electrodes to the multicore cable.



Photographic plate 4.1. The Campus Geopulse resistance meter and tools required to perform a VES survey.

Photographic plate 4.2. The Campus Geopulse resistance meter, Terrameter SAS LOG 200 and tools required to perform borehole fluid resistivity logging.



4-1-1 The Campus Geopulse Modular Resistivity Meter

This instrument is a general purpose earth resistance meter capable of accurate measurement over a wide range of conditions (CGIL, 1992). It has a maximum power output of 18 watts, manual selection of current in steps up to 100 mA, a choice of signal averaging length and three frequency settings. The receiver incorporates automatic gain steps that provide a range of measurements from 200 kΩ down to 0.001Ω.

The Campus Geopulse is housed in a fully watertight fibreglass impact resistant case and powered by a rechargeable battery that is also inside the case. It has a front panel with several buttons (functions described below) and four electrode terminals; two for the current and two for the potential. The right half of the front panel has slots for additional modules to connect special ground imaging cables for automatic acquisition of resistivity pseudosection data by computer switching.

The transmitter/receiver controls and display occupy the left hand half of the panel . This control unit has an " on" switch and a "Go" or "initiate measurement" button and three other button switches marked, mA, *, and ~. The button marked, mA is used to select the desired current of which the available values are: 0.5, 1, 2, 5, 10, 20, 50 and 100mA. The instrument was set to a current of 20 mA for almost all the resistivity measurements in this study.

The mark "*" selects the units (quantity) of measurement which are"Ω" for ground resistance, "V" for volts (eg. self potential), "bat" for checking battery voltage, and "°C" for checking the internal temperature of the instrument box.

The unit "Ω" has been used all through the measurements. The button marked "~" selects the number of readings to be averaged which are: 1, 2, 4, and 16 (details of how the signal is processed to obtain a single measurement of ground resistance are given in appendix 4.2).

For most measurements the 4-cycle option was used but when the measurement seemed to be very consistent, which indicates a non noisy environment, the 2-cycle option was used to accelerate the speed of surveying. In contrast to this, when the measured resistance seemed to change a lot (i.e. very noisy environment) the 16-cycle option was chosen to

allow further averaging to provide a more consistent reading. The 8-character liquid crystal display, in the panel, provides space for a 4-digit resistance measurement, and the unit Ω or mΩ is indicated after the resistance value. A negative sign appears on the screen preceding the reading if the potential and the current connections have been incorrectly made. This may also be due to ground conditions.

"G0", "G1", "G2" or "G3" before the reading indicates the amplifier gain settings which are: 20, 2, 0.2, and 0.02 respectively. Sometimes a low gain reading was encountered. This seems to be a result of dry ground or bad contacts between the ground and the electrodes. In these cases attempts were made to repeat the measurements with the electrodes re-positioned slightly. Sometimes even this would not resolve the problem and an unavoidable low gain reading was recorded.

Some examples will be shown in the next chapters where some data had to be corrected because the values are affected by the noisy environment. These values appeared inconsistent with the general pattern of the resistivity behaviour.

4-1-2 The ABEM's Terrameter SAS 300

The ABEM TERRAMETER SAS system is a family of instruments used for surveying resistivity, self potential and temperature. The Terrameter SAS 300 unit is a complete transmitter/receiver system in one single box which can be used alone or as a master for the Terrameter SAS 2000 booster transmitter to extend the voltage and current ranges of the SAS 300. It can also be used as a separate transmitter. The Terrameter SAS LOG 200 is a well logging unit for downhole resistivity, self potential and temperature measurements.

The ABEM SAS 300 Terrameter was recommended by Turnbull in his Ph.D thesis as the most suitable instrument for routine 2-D resistivity surveys where the depth of exploration is limited to 500 metres (Turnbull, 1986).

In this study the Terrameter SAS 300 unit has been used for carrying out the measurements of the resistivity pseudosection at both sites and used as a master unit for the Terrameter SAS LOG 200 for borehole logging in College Farm, Aber.



Photographic plate 4.3. The Terrameter SAS 300 resistiance meter, multicore cable and tools required to perform a pseudosection survey.

Photographic plate 4.4. The Terrameter SAS 300 resistance meter, switching box, stripboards and the multicore cable.



SAS stands for Signal Averaging System, a method by which consecutive readings are taken automatically, results are averaged at each stage and the updated running average is presented automatically on the display.

The basic unit (SAS 300) contains three main units, all housed in a single casing: the transmitter, the receiver and the microprocessor.

The electrically isolated transmitter sends out a well-defined and regulated signal current. The receiver discriminates against noise and measures voltages correlated with the transmitted signal current (resistivity surveying mode) and also measures uncorrelated DC potentials with the same discrimination and noise rejection (voltage measuring mode). The microprocessor monitors and controls operations and calculates results.

The ABEM Terrameter SAS 300 has the following controls:
1- SAS selector with four position selectors being: 1-cycle, 4-, 16- and 64-cycle.
2- Voltage/resistivity range selector (range selector). It has a 9-position selector, four in the resistivity range: 1Ω, 100Ω, 10KΩ, 1M Ω; four in the voltage range: 1V, 10V, 100V, 500V; and the " bat" position for checking battery voltage.
3- On/Off switch.
4- Current selector: can be set to 0.2, 0.5, 1, 5, 2, 10, and 20 mA at 150 V maximum current electrode potential; the range can be extended to 500 mA or to 500 V by using the optional Terrameter SAS 2000 Booster.
5- Measure push-button. This button is depressed when making the measurement where the microprocessor runs through its automatic diagnostics programme and, if everything is satisfactory, automatically starts the Terrameter SAS 300 measurement procedure. When the measurement is complete, the SAS is returned to the standby mode with the result on the digital display. Current electrode terminals are located at the right on the control panel while the potential electrode terminals are at the left. All controls are shown in fig. 4.1.

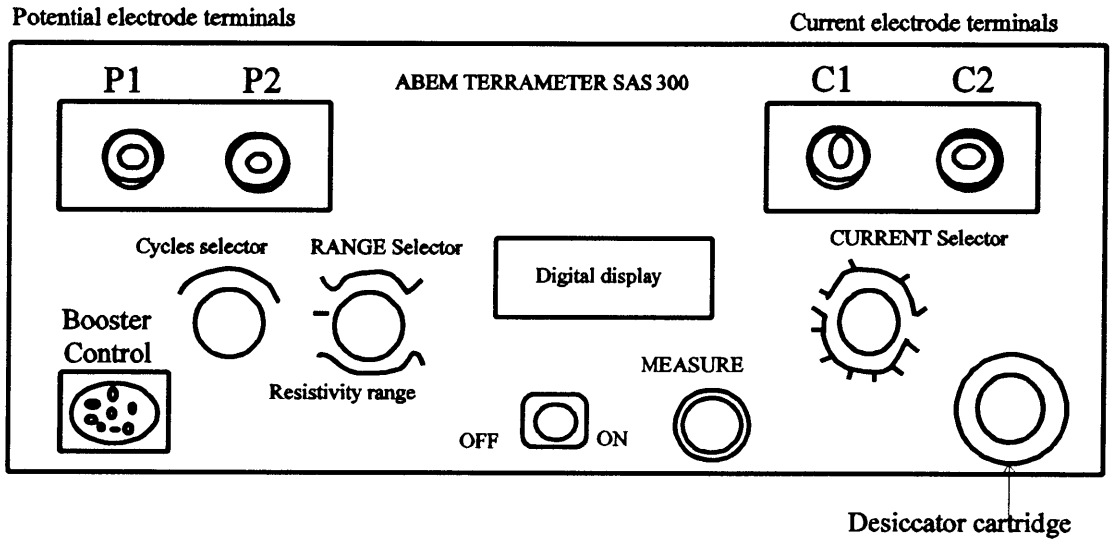
Accuracy of the instrument

The accuracy of this device (with or without the SAS 2000) is ±2% of the reading plus 2 digital increments (ΔV or ΔR). For the resistivity measurements the value of one digital

increment (ΔR) varies with the current and resistance settings as in table A4T2, appendix 4.1. For example, for the current range 20 m A and resistivity range 1 ohm, the setting

Figure 4.1

Schematic diagram of SAS 300 controls and terminals



used for all measurements in this work unless otherwise stated, the increment is 250 μ Ω plus ±2% of the reading.

4-1-3 The Terrameter SAS LOG 200

The instrument is shown in photographic plate 4.2. This unit is intended for downhole logging to depths of 200 m and can be used to measure:

1- Short normal (16") resistivity

2- Long normal (64") resistivity

3- Lateral (18') resistivity

4- Self potential

5- Temperature

6- Fluid resistivity

The SAS LOG 200 consists of a 200 m long cable, marked at 1 m intervals, with a logging probe, a 6-position MODE selector and circuitry for connecting a Terrameter SAS 300, a current return electrode and a potential reference electrode, temperature transducer and resistivity cell, all mounted on a backpack frame. The instrument is provided with a 4-conductor cable that can be connected to the potential (P1, P2) and current (C1, C2) terminals on the Terrameter SAS 300.

To make a measurement with the SAS LOG 200 it must be connected to the SAS 300; the return current terminal to a return current electrode and the potential reference terminal to a reference potential electrode. A selector switch on the backpack frame can be then used to select any of the above modes of operation. In this study modes 5 and 6 were used.

4-2 Electrical Resistivity Surveying Techniques

The following electrical resistivity techniques were used in this study:

1- Vertical electrical sounding:

a- Schlumberger array

b- Wenner array

c- Offset Wenner system

2- Constant separation traversing:

a- Resistivity pseudosection

b- Equipotential using Schlumberger AB profiling

3- Borehole Fluid resistivity Logging

4-2-1 Vertical Electrical Sounding (VES)

The electrical resistivity sounding has been widely used in many parts of the world and is particularly useful in groundwater applications.

A VES consists of a succession of apparent resistivity measurements made with an increasing electrode separation; the centre of the configuration and orientation remaining fixed (Kunetz, 1966). Three types of electrode configuration have been used here: Schlumberger, Wenner, and Offset Wenner.

4-2-1-1 Schlumberger Array

This array is the most widely used in electrical prospecting. Four electrodes (A, M, N and B) are placed along a straight line on the earth surface so that AB≥ 5 MN (fig. 4.2). A current I is passed between the outer electrodes A, B and the potential drop ΔV measured between the two inner electrodes M, N.

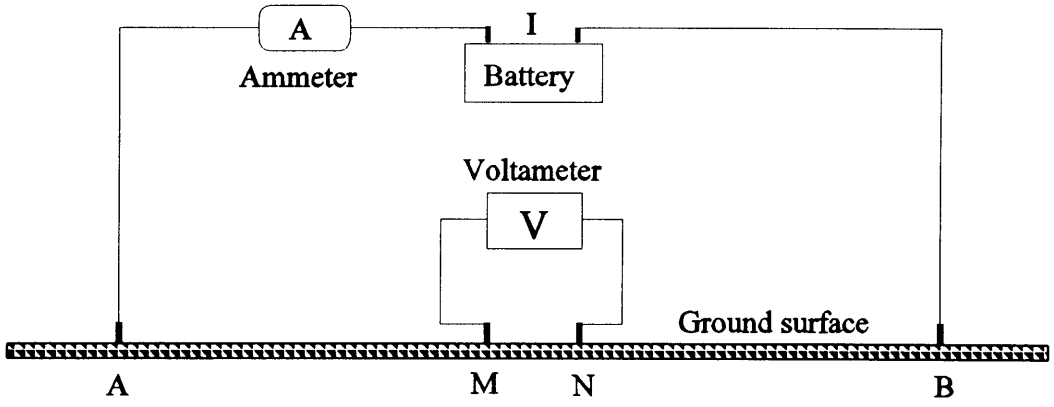
Apparent resistivity can now be calculated from the general equation 2.11 as follows:

$$\rho_a = \pi \{[(AB/2)^2 - (MN/2)^2]/ MN\}(\Delta V/I) \qquad 4.1$$

This equation is applicable when MN is midway between AB, like the surveys carried out in this study.

Figure 4.2

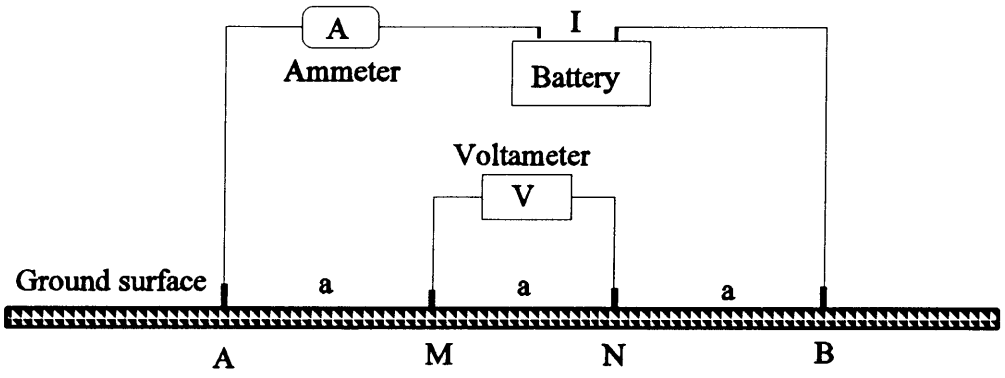
Schlumberger configuration



4-2-1-2 Wenner Array

This well-known array was first proposed for geophysical prospecting by Wenner (1916). The four electrodes A, M, N and B are placed at the surface of the ground along a straight line so that AM = MN = NB = *a* (fig.4.3).

Figure 4.3
Wenner Configuration



The apparent resistivity can be calculated from equation 2.11 as follows:

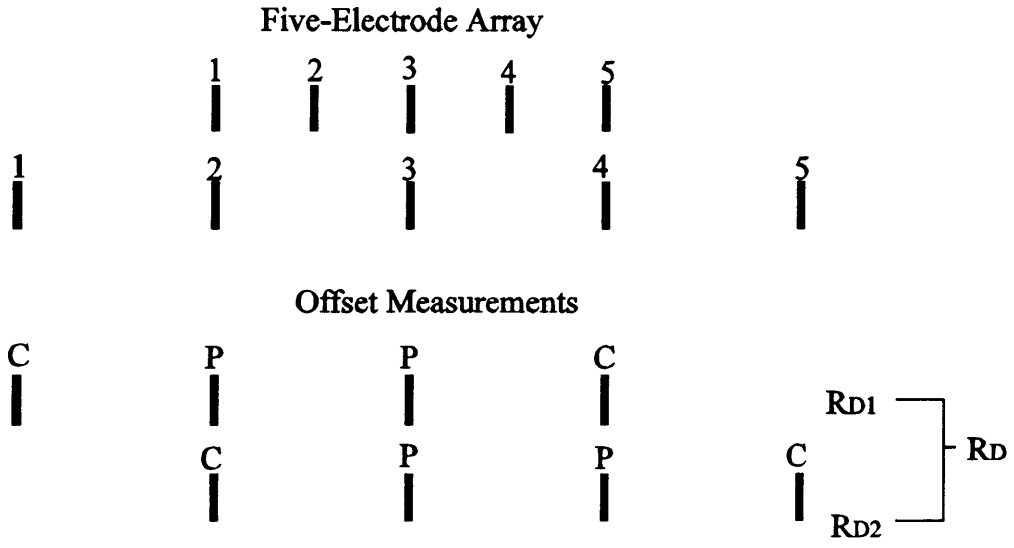
$$\rho_a = 2\pi\, a\Delta V/I \qquad 4.2$$

4-2-1-3 Offset Wenner System

This system has been developed by the University of Birmingham. Vertical sounding using the Offset Wenner technique is conveniently conducted using a five-electrode array. If, using this array, the spacing is increased according to the series: a = 1, 2, 4, 8, .. 2^n .. 64m so that the inner electrode always falls on a position previously occupied by a current electrode (fig. 4.4a), seven " high quality", i.e. low noise, resistance measurements are obtained using a total of only eight electrode positions per half spread.. In practice this is no more difficult than a normal sounding for the additional electrode remains fixed at the centre of the spread (Barker, 1981).

Resistances (R_{D1} and R_{D2}) are measured with each of the normal Wenner arrays, the mean of these two values provide the "Offset Wenner" resistance, R_D.

Figure 4.4a



Principles of sounding with Offset Wenner system
(After Barker, 1981)

The Campus Geopulse resistivity meter was used to carry out this survey at College Farm, Aber where manual switching was used to change from one set of four electrodes to the other.

4-2-1-3-1 Calculation of Intermediate and Last reading in the Resistivity Curve

Barker (1981) explained how additional points on the apparent resistivity curve may be obtained not by changing the spacing but by changing the electrode arrangement. This is possible by measuring resistances with the electrode arrangements R_B and R_C as illustrated in Fig. 4.4b. The same basic five-electrode array is employed with the same spacing series but the roles of the current and potential electrodes are interchanged.

From equation 2.8 (chapter 2) the measured resistance may be defined as:

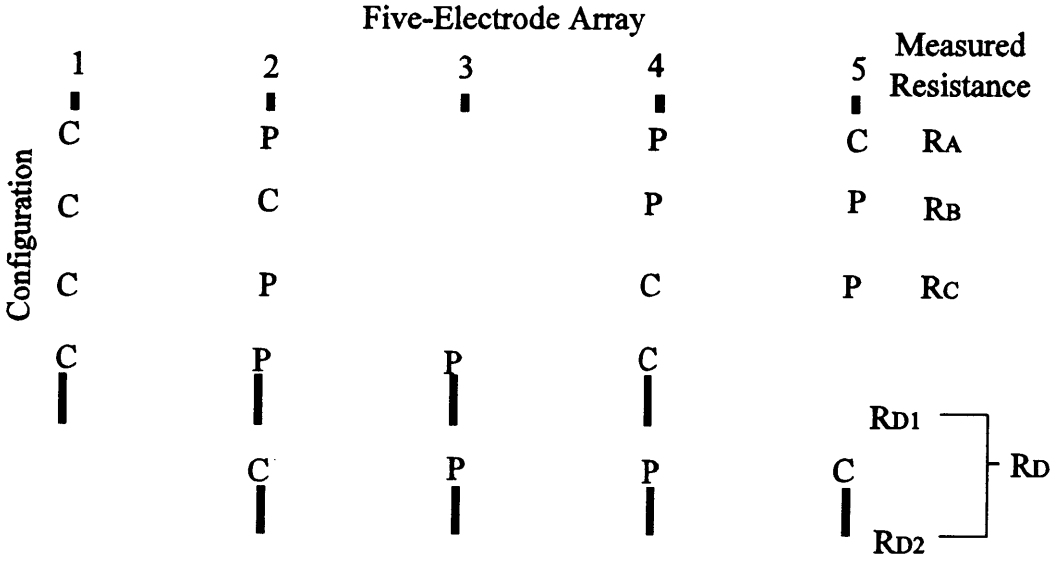
$$R_W(a) = \Delta V/I = (V_{P1}-V_{P2})/I$$

$$= [(V_{P1C1}-V_{P1C2})-(V_{P2C1}-V_{P2C2})]/I \qquad 4.3$$

where V_{P1C1} is the potential at P1 due to current entering the ground at C1, and

$R_W(a)$ is the Wenner resistance measured with spacing a.

Figure 4.4b



Resistance measured with the five-electrode array necessary for the computation of additional Wenner resistances in Offeset Wenner sounding. (After Barker, 1981)

If C1 is a unit source of current V_{P1C1} may be represented by $\phi(a)$, the potential at distance a from a point source. For a horizontally layered subsurface:

$V_{P1C1} = V_{P2C2} = \phi(a)$ and

$V_{P2C1} = V_{P1C2} = \phi(2a)$

The various terms may be combined to provide the following definition of the Wenner resistance (Carpenter 1955).

$$R_W(a) = 2[\phi(a) - \phi(2a)]/I. \qquad 4.4$$

Now resistances R_B and R_C may be defined in a similar fashion.

$$R_B(a) = [\phi(2a) + \phi(4a) - 2\phi(3a)]/I, \qquad 4.5$$

$$R_C(a) = [2\phi(a) - \phi(2a) - \phi(4a)]/I \qquad 4.6$$

These expressions may be combined to calculate Wenner resistances not measured directly. For example:

$$R_C(a) - R_W(a) = [\phi(2a) - \phi(4a)]/I$$

$$= 1/2\ R_W(2a),$$

therefore

$$R_W(2a) = 2[R_C(a) - R_W(a)]. \qquad 4.7$$

Equation 4.7 is used to obtain the last point on the Wenner apparent resistivity curve. In this survey this equation was used to calculate the last point, at 64m spacing, from resistance measurement made with the maximum spacing of 32m.

The intermediate Wenner points were computed by use of the relationship given by Barker (1981).

$$R_W(3a) = 1/2\ R_W(2a) + R_B(2a) - R_B(a) + 1/2\ R_W(4a) \qquad 4.8$$

This equation was used to calculate Wenner resistances at spacing 3, 6, 12 and 24 where the measured resistance obtained at spacing points 1, 2, 4 and 8 were used as appropraite.

All the resistance measurements (measured, intermediate and last point) were converted to apparent resistivity using the same equation, eq. 4.2, that is used for calculating Wenner apparent resistivity.

4-2-2 Constant Separation Traversing (CST)

It is also known as electrical profiling or horizontal profiling or electrical trenching. This technique is used for the determination of lateral variations of resistivity. The current and the potential electrodes are maintained at a constant separation for a set of measurements as the centre of the array is moved in equal steps along the profile.

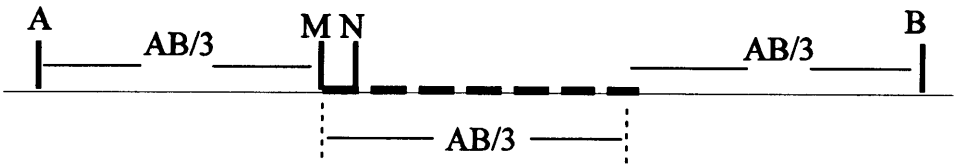
4-2-2-1 Lateral Changes in Resistivity using Successive Schlumberger AB Profile

The Schlumberger AB profile technique is suitable for mapping the lateral variation of ground resistivity over a long profile where only the potential electrodes are moved along the middle third of the line A B (Kunetz, 1966) (fig. 4.5). The two current electrodes may be placed a large distance apart (1-6 Km) (Zohdy et al., 1974).

A constant distance between the potential electrodes is maintained throughout the survey while the current electrodes are kept stationary. The potential difference is measured between the potential electrodes, M and N, and is automatically converted to a resistance value by the resistivity meter.

Figure 4.5

Schlumberger AB Profile



Same procedures can be repeated to survey several profiles at different distances from the first profile (see section 4-3-3).

The general equation (eq. 2.11) can be used to convert the resistance values to apparent resistivities. These values can then be used along with the distances in the x-axis and y-axis to plot an apparent resistivity map of the surveyed area (see section 5.3 in the next chapter).

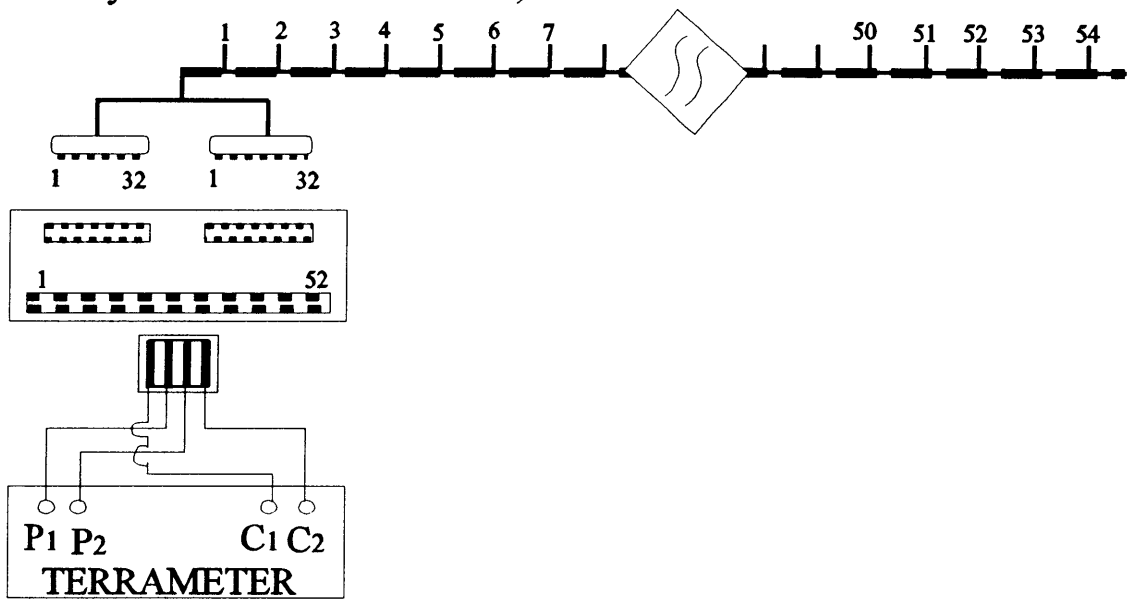
4-2-2-2 Resistivity Pseudosection

To investigate the resistivity variation in two dimensions, a traverse in the cross-strike direction must be profiled repeatedly with a co-linear array of electrodes, increasing the electrode separation each time. In this way an apparent resistivity space section (**pseudosection**) can be built up (Griffiths and Turnbull, 1985) by carrying out successive CST profiles with an increasing electrode separation, and hence increasing depth.

To speed up the collection of data to construct an electrical pseudosection, a special cable and a switch box was fabricated (fig 4.6). A 54-core cable was adapted so that there was an electrical takeout every two metres along its length (106 m between first and last takeouts). Each takeout consisted of a bare wire, connected to a particular core, which is closely wrapped several times around the circumference of the cable to form an electrical contact. The cable sheath has been resealed using self amalgamating tape.

Figure 4.6

Layout of the multicore cable, switch box and the Terrameter.



The electrodes, mild steel stakes, can be directly connected to the cable takeouts using flying leads with crocodile clips attached at both ends. The electrodes can be accurately positioned in the ground by placing them adjacent to each takeout, i.e. a tape measure is not required for accurate electrode location.

The free end of the cable is connected to the switch box via two 32 way 'D' connectors. Inside the box sequential connections are made from each numbered electrode takeout to the terminals of a circuit strip board connector. Thus electrode one is directly connected to edge connector pin 1, electrode 2 to pin 2 and so on. To achieve sequential electrode connections to the ABEM Terrameter several short sections of stripboard were made up with 4 attached leads which can be connected to the current and potential terminals of the Terrameter using "banana" plugs.

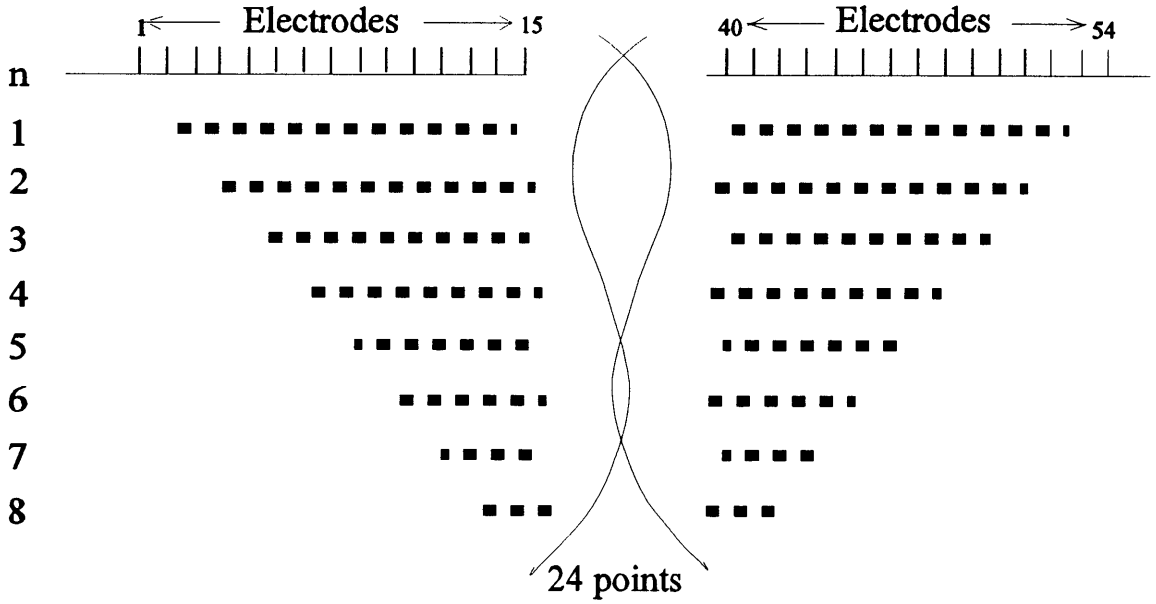
To perform a profile using a Wenner array with a 2m electrode spacing a piece of strip-board with four copper strips is used to connect the electrodes to the Terrameter. The first measurement is made with the strip-board inserted into contacts 1 to 4. Subsequent measurements along the profile are made by moving the strip-board along the edge connector one contact at a time, i.e. 2 to 5, 3 to 6, 4 to 7 etc.

To achieve greater penetration a Wenner array with an electrode spacing of 4 m can be profiled by using a slightly longer piece of strip-board with 7 copper strips. In this case the leads to the Terrameter are connected to every other strip. This allows electrode positions 1, 3, 5, 7; 2, 4, 6, 8 etc to be profiled by moving the strip-board along the strip-board one contact at a time.

This sequence of measurements can be continued by other pieces of strip-board allowing successively greater electrode spacing , i.e. the series 6, 8, 12, 14 and 16 m.

This then allows the construction of a pseudosection by plotting the measured apparent resistivity at the centre of each array position along the profile. Each successive increase in electrode separation can be plotted vertically below the preceding separation to build up a pseudodepth section as illustrated in fig. 4.7.

Figure 4.7



The measurement sequence for building up a pseudosection

The deployment of the cable is very quick and straightforward. First the start and direction of the profile should be located. The cable can then be laid out on the ground from its drum in a straight line so that it is stretched taut. The 54 electrodes are then pushed into the

ground adjacent to each takeout. If the ground is dry each electrode can be "watered in" to provide a good electrical contact. Each electrode is then connected to the cable with the crocodile clips on the flying leads.

The end of the cable is connected to the switch box via the 2 'D' connectors and the flying leads on the smallest strip-board are connected to the Terrameter (or the Geopulse). The strip-board is then sequentially scanned along the edge connector to gather the required sequence of resistance measurements.

To use the full capabilities of the cable a total of 324 measurements can be made for eight successive profiles where the spacing 'a' is increased from 2 to 16 m in steps of 2 m (51, 48, 45, 42, 39, 36, 33, 30 measurements at each level of the pseudosection). Table A4T3, appendix 4.1 shows the details of this technique.

The basic resistance values can be entered into a specially prepared spreadsheet to convert them to apparent resistivities by using equation 4.2 of the Wenner configuration. Table A4T4, appendix 4.1 shows a set of field data along with the converted apparent resistivity values. These parameters are then stored in an ASCII data file suitable for entry in the pseudosection inversion programme (details of processing will be explained in chapter five).

The sequence of measurements can be carried out by a single operator in about 2 hours. A team of three can set up the array in 15 to 20 minutes. A single operator can complete an entire section, from installation to removal,in a period of 3 hours.

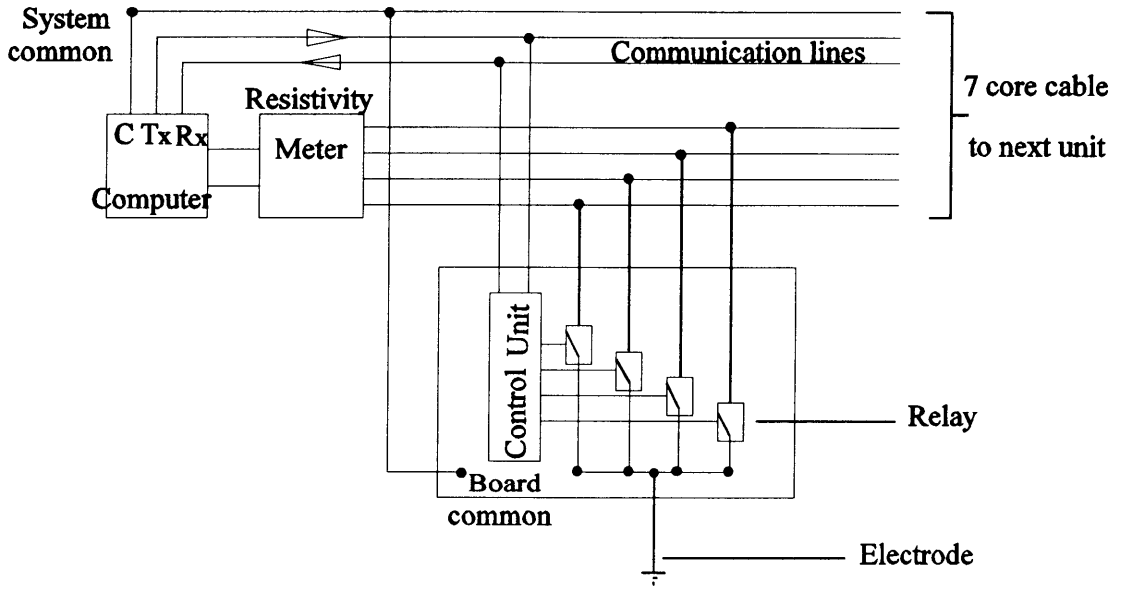
Nawawi and Loke (1995) presented an abstract of their work in the Universiti Saints Malaysia to the EAGE 5th Conference and Technical Exhibition, Glasgow, Scotland, where a similar pseudosection technique was used. The Campus Geopulse resistivity meter and a multicore cable as described by Griffiths and Barker (1993) with 25 electrodes and 2 metre electrode spacing were used in that study. They mentioned that each survey took about one hour. This shows that the multicore cable with 54 electrodes and the manual switching control used in this study is as efficient as the computer controlled switching methods.

The multicore cable with the manual switching control system compares favourably with the

computer switching MRT system described by Griffiths et al., (1990)(fig 4.8).

Figure 4.8

Layout of one switching unit of the MRT system,
showing connections to the resistivity meter and the compter (after Griffith et al, 1990).



4-2-3 Borehole Fluid Resistivity Logging

The physical properties of rocks measured by resistivity logging are principally electrical resistivity and self potential (Telford et al., 1990).

A well-known parameter in electrical borehole logging is the formation factor (= formation resistivity/pore-water resistivity) and it's relationship to formation porosity (or void ratio) (Jackson, 1975).

$F = \rho_o / \rho_w$ 4.9

where F = Formation factor

ρ_o= bulk resistivity of the medium

ρ_w = resistivity of the water contained in the pores.

Formation factor, F, is normally presumed constant throughout the entire aquifer and ρ_w could be calculated directly from an interpreted value of ρ_o at any point of a geoelectric section (Worthington, 1976). Worthington (1976) considered the assumption of a constant

'F' as the major weakness of the quantitative geoelectrical approach to the mapping of water salinity. According to him, this assumption is strictly justified only if the aquifer is texturally uniform, and is effectively clean, i.e. the solid constituents do not contribute significantly to the passage of an applied current by way of ion exchange and surface conduction.

In downhole electrical logging a short (16") normal electrode array is suitable for measuring the resistivity of the fluid (ρ_w), or the porous zone flushed by mud filtrate, and hence for determination of formation porosity. The long (64") normal array can measure an intermediate resistivity which permits calculation of both the invaded zone and the true bulk resistivity (ρ_o) (Telford et al., 1990).

Formation factor can be obtained in the laboratory by using the resistivity cell developed by Jackson (1975) where soil samples are required. If borehole logging is not available this value of 'F' can then be used in equation 4.9 to obtain ρ_w from the bulk resistivity that is estimated from the sounding.

Tonks et al., (1993) has used a conductivity probe, instead of resistivity logging, in boreholes to evaluate groundwater contamination by the use of equation 4.9 with C_w, the conductivity of the pore fluid, replacing ρ_w and C_s, the bulk conductivity of the medium as measured by the probe, replacing ρ_o.

Archie (1942) recognized that formation factor F, is directly influenced by the bulk formation porosity (ϕ), the degree of matrix cementation (m), and a pore geometry coefficient (a), dependent upon the type of porosity present.

$$F = a / \phi^m \qquad 4.10$$

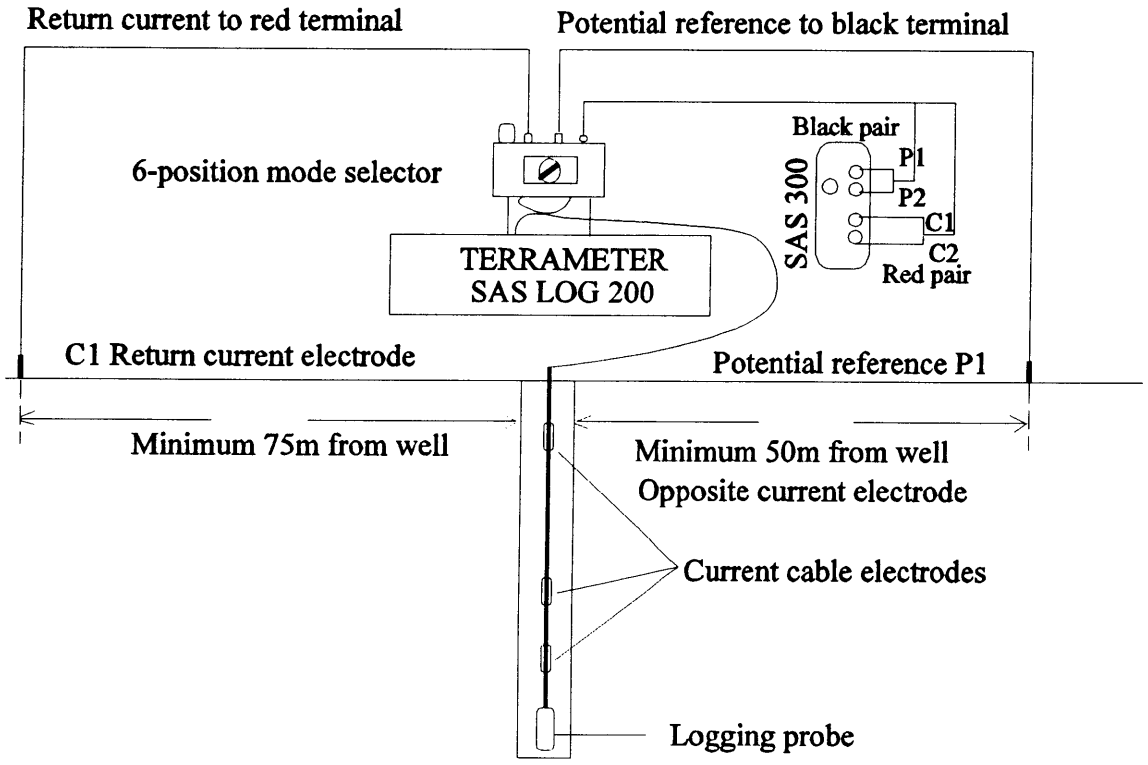
From equations 4.9 and 4.10 bulk porosity can be estimated.

The borehole fluid logging is made in accordance with the Terrameter SAS LOG 200 instruction manual (see appendix 4.6). The logging set up of the probe in the well and the electrode configuration on the surface is shown in fig 4.9. The measurement is taken when

the probe is submerged in the water. Discrete measurements can be made at several depths.

Figure 4.9

Terrameter SAS LOG 200 well logging setup



The instrument displays readings of resistivity so there is no need for data conversion. However, correction factors are available to correct for the effect of small borehole diameters (see appendix 4.3). The collected data, from College Farm, Aber, and the necessary corrections are given in table A4T5, appendix 4.1.

For the test borehole with a diameter of 90 to 100 mm a factor of 1.01 was used to make the necessary correction. The corrected resistivity can then be used to determine the total dissolved solids (TDS) in the fluid.

Resistivity is a function of water temperature. Therefore, a standard temperature, 25°C, should be specified for reporting resistivities or conductivities. The following equation is

used to standardize the resistivities to 25 °C (Terrameter Instruction Manual)

$$\rho_{25} = \rho_T (0.48 + 0.021T) \qquad 4.11$$

where T is the temperature within the 5-50 °C range.

The concentration of the common ions found in groundwater are often reported by weight in parts per million (ppm). The TDS estimation for an average of natural groundwaters is:

$$TDS\ (ppm) = 6400/\rho_{25} \qquad 4.12$$

The above procedures, correction for diameters, standardizing resistivity readings at temperate of 25 °C, and determining TDS, have been shown in table A4T5.

4-3 Electrical Surveys Carried Out At College Farm, Aber

It is known from previous studies that this site is composed of two aquifers. The top, small, aquifer proved to experience a movement of the saline intrusion during spring tides (Soomro, 1993). Electrical and electromagnetic methods were used by Soomro to delineate the fresh-salt water interface.

Based on this knowledge various electrical resistivity techniques were used on this site in order to determine which of them would be most appropriate for identifying areas of saline intrusion. Figure A4F10, appendix 4, illustrates the location of all the resistivity work carried out on the site along with their elevations relative to the lowest point in the site which is a permanent concrete drainage pit (see photographic plate 4.5).

The VES method has been applied to determine depths to different layers. The impact of the saltwater intrusion was hoped to be detected as a conductive zone (low resistive boundary) within these aquifers.

The pseudosection technique was used to spatially delineate and map the saline interface and to monitor any motion of this interface that may occur due to the pumping action of the tide.

4-3-1 VES for Constructing A Geoelectric Section

The Schlumberger configuration was used to make three soundings, (S1, S2 and S3 as given in table A4T1, appendix 4.1) on a line perpendicular to the coast so to draw a geoelectric section. Each sounding was oriented so that the electrode expansion was parallel to the coast (see photographic plate 4.1). This section will help to delineate the fresh-salt water interface.

The first of these soundings was made just three meters to the southeast of borehole BH10/2 (fig.A4F10). The geological information of the top seven to eight metres obtained from this borehole, in previous studies, can be compared to this sounding so to resolve the ambiguity arising from the resistivity technique and consequently improve the interpretation. The second sounding was carried out adjacent to the landward fence in the northeast side, about 52 m from BH10/2, while the third sounding was made at about 55m to the north west of this borehole (about 30m from the seaward fence).

A maximum AB/2 spacing of 100 m was used for these soundings where a depth of about 50m could be expected to be explored.

4-3-2 VES For Comparing Different Arrays

The Schlumberger array was used once again on this site alongside Wenner and Offset Wenner in an attempt to study the practical and interpretational features of these configurations for this sort of application. These surveys were carried out in the same position as sounding S1, (about three metres south east borehole BH10/2). Schlumberger sounding S4 had a maximum spacing, AB/2, of 100m while the Wenner maximum spacing, a, was 80 m. Although the maximum spacing for the Offset Wenner system was 32m a last reading at 64m spacing was calculated as explained in section 4-2-1-3 (see table A4T6, appendix 4.1).

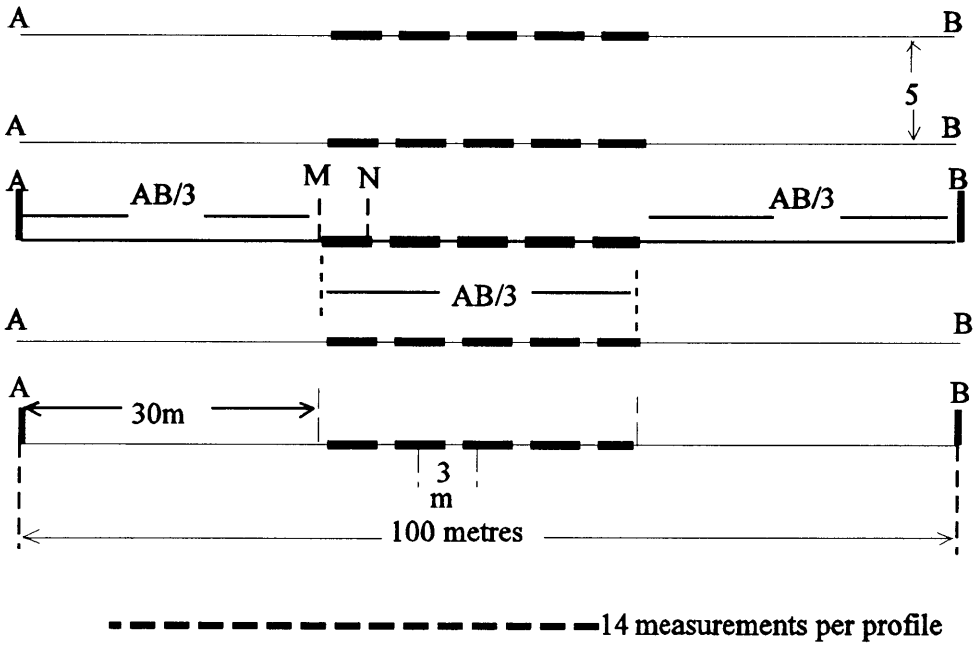
4-3-3 Mapping the Lateral Changes in the Apparent resistivity Using AB Profiles

The technique mentioned in section 4-2-2-1 has been used at College Farm, Aber where five

parallel lines of AB = 100 m were made at 5 m intervals (fig 4.11). A separation of three metres was maintained between the potential electrodes (MN) as they were moved along the profile. Fourteen measurements were made along every line.

Figure 4.11

Equipotential Resistivity survey using the Schlumberger AB Profile



This has resulted in a survey of a rectangular area of about 780m^2 (39m long times 20m width, see fig A4F10, appendix 4). The boreholes BH10/1, BH10/2, BH10/2A, BH10/2B and BH10/2D lie within this area. The geological information from these boreholes can be correlated with the information obtained from this technique to study the lateral variation in the electrical properties of the subsurface in order to map conductive zones.

4-3-4 Pseudosection

Pseudosection surveying was carried out in three places. The first was through the boreholes (fig A4F10), along same line of the geoelectric section, so to delineate the fresh-salt water

interface and then compare with the results from the geoelectric section. The second pseudosection was surveyed near the south west fence. Another two pseudosections were conducted over the same profile about half way between the first and second pseudosections (fig. A4F10). This last survey was intended to investigate the effect of the tide on the movement of the fresh-salt water interface. These pseudosections together can provide valuable information on the resistivity distribution below a large area and hopefully map the saline interface in an areal extent.

4-3-5 Borehole Resistivity Logging

The fluid resistivity logging was carried out as a part of the investigation of the saline water intrusion. The fluid resistivity could help in estimating some of the formation properties like the porosity. Another important use of the fluid resistivity was to calculate the total dissolved solids and observe any changes resulting from tidal effects.

Well BH10/2, which approximately lies in the centre of the field, has been used for all the fluid resistivity logging.

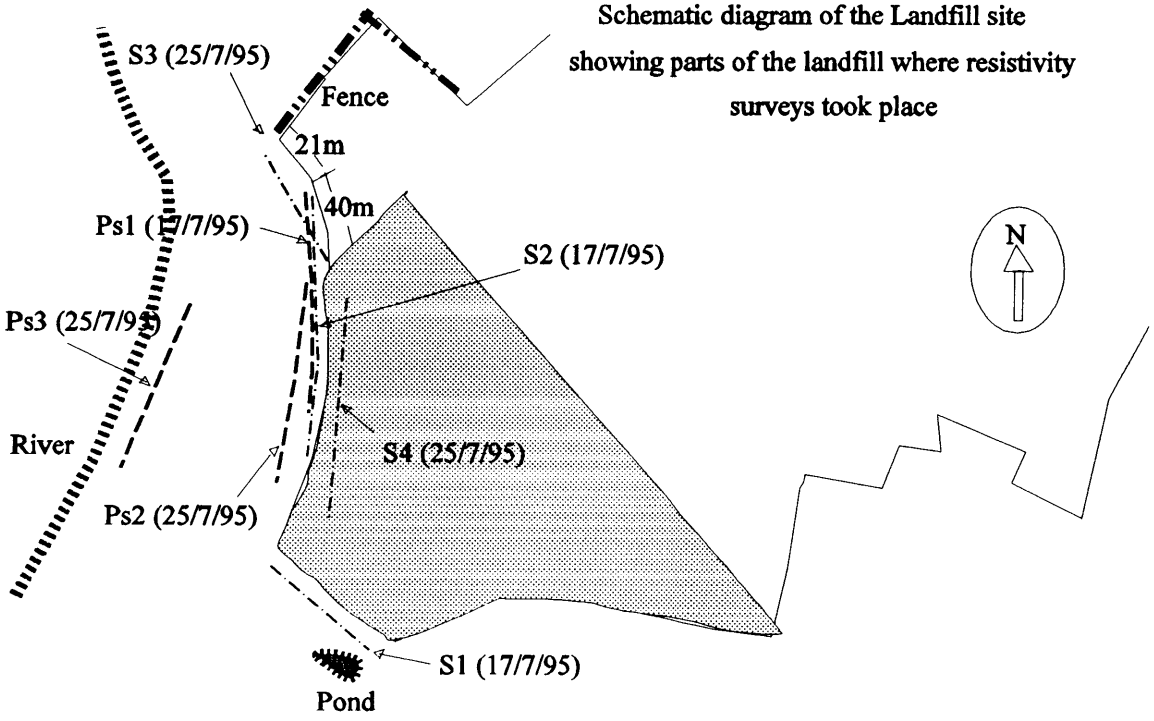
The SAS LOG 200 has been used twice with the Terrameter SAS 300 and once with the Campus Geopulse to make borehole fluid resistivity measurements. Unfortunately the temperature measurement could only be recorded with SAS 300.

4-4 Electrical Surveys Carried Out At the Landfill Site

Four VES surveys and three pseudosections have been conducted on this site. The position and extent of the resistivity work carried out here was limited by several factors. The test area consisted of two parts; a small area, about 60 m in length where no waste has been dumped as yet was chosen to run VES soundings to estimate earth models so to assess the geology which presumably is not affected by any leachate. The second area, about 150 m in length, is a completed tip which is about five metres in height. Fig. 4.12 shows the layout sketch of the test area and all resistivity work; the tipped area, old site, is shaded whereas the small untipped area is left blank.

Figure 4.12

Schematic diagram of the Landfill site showing parts of the landfill where resistivity surveys took place



4-4-1 VES Surveys

Schlumberger soundings S1 and S2 were carried out around the tipped area from two sides. Maximum electrode spacing, AB/2, for S1 was 40m and for S2 was 50m. Soundings S3, was made next to the untipped area with maximum spacing AB/2 of 30m. On the top of the tip one Schlumberger sounding, S4, with maximum spacing AB/2 of 60m was surveyed.

4-4-2 Pseudosection

The first pseudosection, Ps1 was made along a 106 m profile where the first 40m of the profile lies adjacent to the new site, where tipping has only just begun, and about 66m lies adjacent to the old unconfined tip. The start of the pseudosection spread was about 21 m from the fence (to the west of the landfill site) and the spread was approximately parallel to the edge of the tip, within one or two metres of the base of the 3 or 5m high slope.

Pseudosections Ps2 and Ps3, were surveyed along fairly straight lines and with approximate

starting points opposite the northern edge of the tipped area, i.e. about 61m from the fence. The Ps2 spread was deployed about 2m away from the base of the tip. The end of the spread was about 50m from the south western corner of the tip. The Ps3 spread was set up adjacent to the river, about 15m from the tip at the start of the spread and about 26m away from the tip at the end of the spread.

4-5 Errors Involved in Electrical Surveys

The electrical resistivity methods generally involve problems associated with carrying out the surveys. The accuracy of measurement is dependent on many factors. The spread must be laid out in a straight line and the electrodes must be positioned in the ground at accurate spacing distances. In addition the electrodes should not be pushed deeply into the ground especially for short spacings. The possible errors involved in resistivity measurements can be caused by following improper survey procedures.

Another important factor that may lead to considerable error is high contact resistance at the electrodes. This can be reduced by "watering" in the electrodes.

The telluric current, the natural current in the ground generated by the ionospheric tidal effects and the continuous flow of charged particles from the sun which is then trapped by the lines of force of the earth's magnetic field (Zohdy et al., 1974), may affect the resistivity measurements. These are reduced to some extent by averaging the readings over several cycles.

4-5-1 VES Errors

One of the important errors involved in the resistivity measurements is the instrumental error which has been given above. The significant problem connected with the VES resistivity sounding technique is the repeatability. It is related to the accuracy of data if the process of measurement is repeated at the same measurement point where the electrodes will not necessarily be at the previous location, so the measured resistance, R, would be different. The spacing error varies from one electrode arrangement to another. Soomro (1993) used a simple equation to determine errors resulting from any spacing error in the Wenner

configuration system. If there is a difference, Δa, in positioning the electrodes at the right spacing, a, then the resulting difference in R will be ΔR. Therefore the errors in spacing a and resistance R would be $\Delta a/a$ and $\Delta R/R$ respectively, and the maximum error in r.m.s. terms will be:

$$(\delta V/V)^2 = (\Delta a/a)^2 + (\Delta R/R)^2 \qquad 4.13$$

Barker (1981) gave three types of errors that the Offset Wenner sounding system can provide: 1- the spacing error which is called the "Offset error", $e_f(a)$; 2- the near-surface lateral effects which is called the " lateral error", $e_l(a)$; and 3- the observational error, "$e_{obs}(a)$:

1- The "Offset error", $e_f(a)$:

$$e_f(a) = \{[R_{D1}(a)-R_{D2}(A)]/R_D(a)\} \times 100\% \qquad 4.14$$

where a is the spacing and

R_D, R_{D1} and R_{D2} are defined in fig. 4.4b.

The calculation of the Offset errors of the resistivity survey carried out in College Farm, Aber gave high values (see table 4.7) which will be explained in the next chapters.

2- The " lateral error", $e_l(a)$:

$$e_l(a) = [\{R_D(2a)- 2[R_C(a) - R_D(a)]\}/ R_D(2a)]\times 100\% \qquad 4.15$$

3- The observational error, "$e_{obs}(a)$:

$$e_{obs}(a) = [\{R_A(a) - [R_B(a) + R_C(a)]\}/ R_A(a)] \times 100\% \qquad 4.16$$

where the terms in equation 4.15 and 4.16 have already been defined in section 4-2-1-3-1.

The observational error includes all small random effects such as observer errors and instrument errors.

Table 4.7			
Spacing (*a*)	Type of Error		
	Observational error, e_{obs} (%)	Offset error, e_f (%)	Latteral error, e_l (%)
0.5	10	28.6	-14.8
1	11.3	18.2	-8.6
2	19.76	15.6	-19.86
4	10.33	15.9	-11.2
8	10.7	17.5	-8.6
16	21.0	26.2	24
32	5.68	32.7	---

4-5-2 Pseudosection Errors

The pseudosection technique also suffers from the general problems associated with the resistivity surveys, as given in section 4-5. With repeated pseudosections when all the electrodes are left in the ground between measurements the electrode spacings will be the same.

4-6 Positional Site Survey

The method of levelling is very simple. It starts with the positioning of the device at a convenient place, mounting it on the tripod and orientating it horizontally with the help of the levelling bubbles. The height of the levelling telescope above the ground is then measured. The level staff is used to measure any height where the middle point seen in the telescope is the level of that particular point referred to the height of the device itself (fig.4.13).

As many points as desired can be levelled but when moving the device to another position a back sight must be made. The survey must be ended by going back to the reference point.

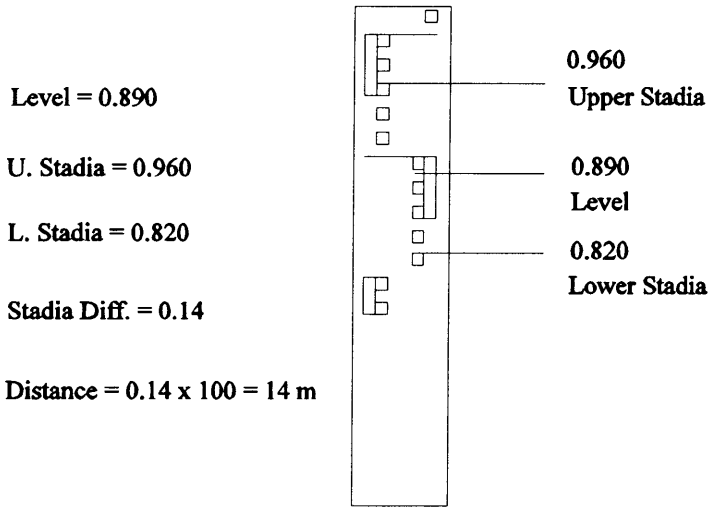
The distance between the position of the device and the measuring point can be calculated by:

Distance in metres = (upper stadia reading - lower stadia reading)× 100 4.17

The levelling device can also indicate the angle, 0 to 360 degrees, of the telescope position that depends on the degree of rotation. For every new measurement when the telescope is

Figure 4.13

Readings from Level Staff as seen in the teloscope



rotated the new angle can be recorded. The angles of rotation for all measurements can be noted and used later to calculate the distances between any two desired points. Principles of plain trigonometry can be applied to calculate the distance between any two points as follows :

$a^2 = b^2 + c^2 - 2\,b\,c\,\mathrm{Cos}A$ 4.18

where a is the desired distance between any two points,

b and c are the distances between the device and the measuring points as calculated in equation 4.17, and

A is the angle between the two desired points.

4-6-1 Positional Surveying Equipment

The level and positioning surveys are both made with a single Level, the Hilger Watts.

4-6-1-1 The Hilger Watts Level

The basic instruments required for levelling are the level itself, and the levelling staff. These and the tripod are shown in photographic plate 4.6. The Level here is a simple robust instrument consisting of two main parts: a telescope and a sensitive bubble; and fitted with a horizontal circle, which enables them to be used in a similar way to a theodolite. The sensitive bubble of the level is read directly. When the bubble is in the centre of its run, it is assumed that the line of sight defined by the telescope cross-wires is horizontal.
The Levelling Staff is made up of four sections which can be extended to a length of 4 metres.

4-6-2 Positioning and Levelling Surveys Carried Out at College Farm, Aber Site

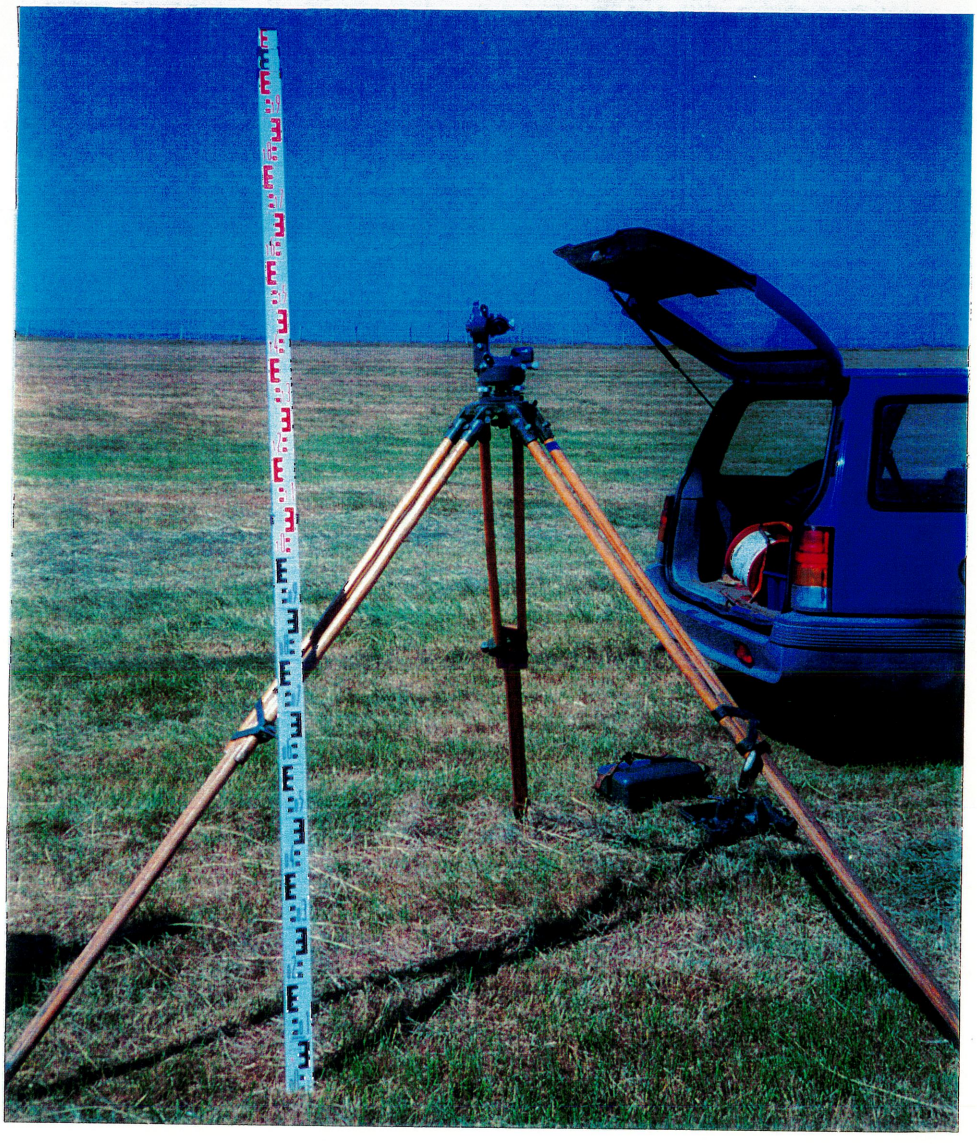
A considerable number of points along the resistivity sounding and pseudosection lines have been levelled at College Farm, Aber using the HILGER WATTS level (Table A4T8, appendix 4.1). The distances from the device at each station to these points are given in fig. A4F14. This was to enable the correlation of all the heights of the ground beneath each resistivity sounding to one single reference point for a better interpretation. The second reason for this survey was to accurately plot positions of all resistivity measurements in relation to the field boundaries. This has enabled an accurate map to be drawn which will be of use in the interpretation stage.

4-6-3 Errors Involved in Positioning and Levelling Surveying

The main errors involved in this survey are essentially observational errors.. The accuracy of the level measurement is ±0.005m which is negligible. An example of such error can be seen in fig. 4.13 as the level reading is 0.890 but in fact it is not quite precise; it could be anything between 0.885 and 0.890, and this is only ± 0.005m.



Photographic plate 4.5. The reference point on College Farm, Aber used for levelling surveys.



Photographic plate 4.6. The Hilger Watts Level, tripod and level staff required to perform level and positioning surveys.

Another similar error is that involved in measuring the height from the ground to the device at each station which depends on the accuracy of the measuring tape and how much it has been stretched when making the measurements. This is within ± 0.01m.

The data collected from this survey (see table A4T8) shows a minor error of 0.035m. This is the overall error involved in the whole survey from start to finish. Theoretically the last reading must give the same value as the first reading.

Measuring the angles also involved a small error which is approximately within ± 1 minutes. However, many problems were encountered when working out the angles at each reading because not enough care was taken, in the field, to actually read the angles from the proper starting value.

5- INTERPRETATION OF ELECTRICAL MEASUREMENTS

In this chapter the techniques of data analysis are explained. Problems of interpretation associated with electrical resistivity methods are also addressed.

5-1 Interpretation of VES Resistivity Curves

The resistivity sounding curves (apparent resistivity/electrode separation curve) have been interpreted by the Resix Plus DC resistivity data interpretation software, which is a product of Interpex Limited. This computer software is an interactive, graphically oriented forward and inverse modelling programme for interpreting resistivity sounding data as a 1-D (one dimensional) layered earth model.

The field data, either Wenner or Schlumberger soundings, are entered as a function of "a" or "AB/2'. Forward modelling allows the calculation of a synthetic resistivity sounding curve for a model with up to ten plane layers. As shown in the RESIX PLUS manual (Interpex Ltd, 1992) the calculation of the resistivity sounding curves is based on using linear filters in the manner described by Davis et al., (1980).

Direct inversion to estimate the layered model directly from the data curve, without having to manually construct the number of layers and layer resistivity and thickness, is primarily used as the first step towards the inversion process for each sounding. This is done, using a method similar to that of Koefoed (1976). Inverse modelling using ridge regression (Inman, 1975) has been subsequently carried out to iteratively adjust the parameters of the estimated model.

During the inversion process the fitting error is calculated as the RMS difference between the measured sounding data and the synthetic sounding data. Several inversions are usually necessary to reduce the fitting error to an acceptable level. This RMS error is one way of determining the quality of the predicted ground model. Another way is to examine the parameter resolution matrix which is a by-product of the ridge regression inverse modelling

algorithm and gives an indication as to how well resolved each of the model parameters is. For perfect resolution the resolution matrix has one's along its diagonal and zero elsewhere. If certain layer parameters are not well resolved, for example when the resistivity and thickness of a thin layer shows equivalence, then the resolved parameters will be logarithmic combinations of the model parameters. The resolvability of all layer parameters may be affected if there are more layers in the model than can be truly resoved by the data.

Equivalence analysis has also been carried out, on all the resistivity curves from both sites, Aber and Landfill, to generate a set of equivalent models that fit the data nearly as well as the best-fit model. This analysis indicates the allowable ranges of each of the model parameters.

5-1-1 Ambiguity of Interpreting the VES Resistivity Curves

VES resistivity surveying suffers from a number of limitations. There are two important cases namely the 'Principle of Equivalence' and the 'Principle of Suppression' that result in ambiguity (Kunetz, 1966). There is also the problem of detecting a thin bed at great depth (the relative thickness).

5-1-1-1 Principle of Equivalence

There are two cases of this type:

1- When the resistivity of intermediate bed is greater than the bed above and below it then this bed manifests itself mostly by it's 'Transverse Resistance'; T = the product of it's resistivity and it's thickness ($T = \rho h$).

2- If this resistivity is less than both beds above and below it then manifests itself by it's Horizontal Conductivity (Kunetz, 1966) or Longitudinal Conductivity in other literature. S is the product of it's conductivity, i.e. the reverse of the resistivity ($1/\rho$), with it's thickness ($S = h/\rho$).

5-1-1-1-1 Examples of Principle of Equivalence

Zohdy et al., (1974) illustrated the principle of equivalence for number of type sections. For example equivalence of K-type curves, $\rho_1 < \rho_2 > \rho_3$, can be illustrated by considering two three-layer sections of K-type. If ρ_1 in one section equals ρ_1' in the other sections, $\rho_3=\rho_3'$, and $T_2=\rho_2 h_2=T'_2=\rho_2' h_2$ ', then the sounding curves for both sections will be practically identical. This type of equivalence is known as equivalence by T and it also applies approximately to Q-type curves, $\rho_1>\rho_2>\rho_3$.

Another example for the equivalence of H-Type curves, $\rho_1>\rho_2<\rho_3$; can be shown by considering two three-layer sections of H-type. If ρ_1 in one section equals ρ_1' in the other section, $\rho_3=\rho_3'$ and $S_2=h_2/\rho_2=S_2'=h_2'/\rho_2'$ then the sounding curves for both sections will be practically identical (equivalence by S).

The equivalence by S also applies to sounding curves of the A type, $\rho_1<\rho_2<\rho_3$. For both equivalence by T and by S, there is a certain range, depending on the ratios ρ_2/ρ_1 and h_2/h_1 , where the two sounding curves coincide very closely. Zohdy et al., (1974) quoted Pilayev (1948), (this reference could not be obtained), who published special nomograms defining this range and these charts were published in the books of Battacharya and Patra (1968), Dakhnov (1953), Golovtsin (1963), and Keller and Frischknecht (1966).

Equivalence is a common problem in many resistivity surveys. Examples of case studies are given by Sandberg, 1993; Overmeern, 1989; Fitterman, 1987; Kosinski and Kelly, 1981; and Frohlich, 1974.

5-1-1-2 Principle of Suppression

The principle of suppression relates to those beds whose resistivities are intermediate between the resistivities of the enclosing beds. Such beds, as long as they do not have a great enough thickness, have practically no influence on the resistivity curve (Kunetz, 1966).

5-1-1-2-1 Examples of Principle of Suppression (Monotonic change in resistivity)

When the resistivity of the subsurface layer increases or decreases monotonically, (A-type ($\rho_1<\rho_2<\rho_3$), AA-type ($\rho_1<\rho_2<\rho_3<\rho_4$), Q-type ($\rho_1>\rho_2>\rho_3$), or QQ-type ($\rho_1>\rho_2>\rho_3>\rho_4$)), the sounding curve may resemble a curve of a simple two-layer Earth model (principle of suppression) unless the thickness of the layers increase significantly with depth (Zohdy et al., 1974).

5-1-1-3 Relative Thickness of a Layer

The detectability of a layer of a given resistivity depends on its relative thickness, which is defined as the ratio of the bed thickness to its depth of burial. The smaller the relative thickness of a given layer, the smaller the chance of its detectability on a sounding curve (Zohdy et al., 1974).

5-2 Interpretation of Resistivity Pseudosections

A pseudosection is a display technique devised by Hallof (1957) which involves plotting resistivity traverse data as a depth section, with each apparent resistivity being plotted as if it were the true resistivity of a point immediately below the centre of the electrode array at a depth proportional to the electrode spacing (Barker, 1992). The contoured data provide an approximate picture of the resistivity distribution in the plane of the section.

The 2-D interpretation techniques are largely based on computer modelling because of the non-linear relationship between the apparent resistivity function and the true ground resistivity. Development of interpretation techniques is described in Turnbull (1986).

In his paper, Barker (1992) showed how an extension of a simple and novel technique published by Zohdy (1989) for the automatic inversion of resistivity sounding curves can be applied to the two-dimensional inversion of Wenner pseudosections. A direct and explicit finite difference technique was employed by Dey and Morrison (1979) so that a single element or block of elements coincides with each point on the pseudosection.

Barker (1992) summarised this technique as follows: the apparent resistivity of a point on the pseudosection is used as the initial resistivity value of the associated element. This initial model is then used to generate a theoretical pseudosection data set. Differences between the model and observed pseudosection apparent resistivities are used to modify the true resistivity of each network element in similar way to Zohdy's (1989) technique in adjusting the amplitudes of the true resistivity of the sounding curves so that the calculated apparent resistivity approachs the observed resistivity according to:

$$\rho_{(i+1)}(j) = \rho_i(j) \frac{\rho_0(j)}{\rho_{ci}(j)} \qquad 5.1$$

where i is the number of iterations already carried out,

j is the number of the layer (or electrode spacing),

$\rho_i(j)$ is the resistivity of layer j after iteration i,

$\rho_o(j)$ is the observed apparent resistivity at the jth spacing on the sounding curve,

$\rho_{ci}(j)$ is the calculated apparent resistivity at the jth spacing for the ith iteration.

Equation 5.1 states that the magnitude of the new iterative layer true resistivity is adjusted as the ratio of the observed to calculated apparent resistivity is multiplied by the corresponding layer true resistivity.

The process of calculating theoretical sounding curves using shifted depths and apparent resistivities without prior knowledge of the true resistivity depth distribution is fully explained by Zohdy (1989). The theoretical pseudosection apparent resistivity is obtained from a starting model in a similar manner to that of the sounding model. The apparent resistivity section for this model is then computed and quantitatively compared with the field section. The model is then modified on the basis of the pattern of the contoured differences between the field and computed data values, following which the section is recomputed. The process is repeated until the RMS value of the differences becomes acceptable (Griffiths et al., 1990). Nawawi and Loke (1995) have used an inversion technique developed by Loke and Barker (1994) to process the data collected in the field immediately after the survey using a notebook computer.

5-2-1 The Inversion Program Used in This Study

In this study an analogous inversion program to that described by Barker, (1992) has been used. This program is able to process 37 first level readings and operate on a maximum of 8 levels. This program requires a large capacity hard disk and considerable RAM (not less than 3M Byte). Therefore, a powerful machine, at least a 386 or preferably a 486SX or DX, IBM compatible computer is required.

This program, however, has a major limitation as far as the number of measurements is concerned. As mentioned earlier, the surveys carried out here with the multicore cable have 51 measurements in the first level. It has therefore been necessary to split the data into two overlapping sections. Each section is inverted separately using this program. The process, consequently, consumes double the time required for a single set of data. The individually inverted parts of the pseudosection must then be joined together, after the inversion process, to produce coloured images of the observed pseudosection and inverted resistivity depth section. If the inversion program was not available, the data as a complete file, could be entered into an appropriate contouring package (eg. Surfer) to produce a contoured pseudosection.

5-2-1-1 Processing Data Using the Inversion Program

The basic resistance values can be entered into a specially prepared spreadsheet to convert them to apparent resistivities (see example data file in table A4T4 appendix 4.1). The parameters are then stored in an ASCII data file suitably for entry in the pseudosection inversion program. The apparent resistivity data for each level is set in a horizontal line and a vertical sequence of the levels are arranged in the following input file format:

1- First line contains the heading title (i.e. short text).

2- Second line contains three space separated figures; where the first figure is the number of levels, the second is the number of measurements at the first level and the third is the spacing distance.

3- From the third line down to line 10; each line contains a set of space separated apparent resistivity data. These sets of data are sequentially arranged, i.e. starting from the first level and ending with level 8.

4- Line 11 must contain this phrase: "Measured Apparent Resistivity in ohm-m".

5- Lines 12 to 15 contain a single zero value.

A sample of a prepared ASCII file with this format is given in table A5T1, appendix 5. This input file must be designated with '.dat' extension. The program can only read files with this extension and the format described above. When the program is correctly directed to read a particular file it will show a summary of the file information which includes: the heading title, the type of array (this program can only deal with Wenner or 2- pole/dipole electrode arrangements), the number of levels, the number of data points in the first level, the electrode spacing, the level that it reads from and the total number of data points.

The second step in processing is to perform the least squares inversion where the program will store the inverted data in an output file that can be used to display the results at any later time. Three types of contour intervals are provided. These are: linear, logarithmic and user defined contour intervals. At this stage the choice of any one is not as important as it is at a later stage where the chosen contours will be presented for inclusion in the report.

After choosing the contour intervals, the program starts sorting the observed data to obtain a starting model by the deconvolution process. Finite difference modelling starts immediately after the deconvolution. Each iteration takes about a minute. The RMS % error is shown on the screen along with the iteration number so far completed. The calculated apparent resistivity contours and the resistivity model are presented at each iteration.

The iteration process continues until the RMS% error reaches a predetermined value. The program provides frequent opportunities to reduce the minimum relative change limit in the RMS% error if the predetermined values are attained. The process then resumes and continues until the RMS% error in the last 2 iterations becomes less than the new minimum relative change limit and then the iteration automatically ends.

Finite difference modelling will also automatically stop when the predetermined number of iterations is completed. When a satisfactory number of iterations is achieved or the RMS% error found to be very slow in reducing the iteration process can be stopped and another activity selected.

In any case the program allows only 12 iterations to be stored in the output file. If any result beyond iteration 12 is desired the screen must be captured by the 'Print Screen' button on the keyboard to pass this selected screen in a bit map image through to any drawing application program. In fact this is the only way of producing a hard copy of the graphic images that this program creates. It is one of the main problems that the program has.

To produce the final display an output file must be first read in. The display data and model section option, within the plotting of resistivity pseudosection menu, can then be selected. A simultaneous display of 2 sections from the following data sets can be made: the measured apparent resistivity values and/or the calculated apparent resistivity values and/or the model resistivity values. The desired iteration number can be displayed, for which the above options were made. The appropriate contour interval can be selected at this stage.

Before displaying the images the apparent resistivity values can be defined as 16 colour boundaries. The program shows the minimum and maximum apparent resistivity values for the chosen images allowing the boundaries to be defined according to these values. Two options of scale, either a logarithmic or a linear contour intervals are available. The latter scale, consists of another two options; a constant and a non constant contour interval. The first can be used when the contour interval value is desired to be a constant increment throughout the defined 16 boundaries. The second is suitable for defining different values for the boundaries. This latter method is very convenient because contours may be designed so that any interesting area can be plotted with a smaller contour interval in order to show more detail. In contrast, large intervals may be chosen for areas where so much detail is not necessary.

In this study all the pseudosections from both test sites have been treated following the strategy described above. In addition each data set was divided into two parts and processed individually. The measured apparent resistivity and the model resistivity of the first iteration of each pseudosection were saved in two files, each half in a separate file. The calculated apparent resistivity and the model resistivity of iteration 12 for each pseudosection were also saved in two separate files. The colour boundaries (contours) of both halves were set with the same values. The Print Screen button on the keyboard was used to capture these images from the screen. Then Paint Brush, a Windows compatible drawing application, was used

to join the two halves of each particular pseudosection. At this stage the black background captured from the images produced by the inversion program was changed to white. The necessary comments, titles and the values of the colour boundaries, were added to the image at this stage before it was sent to a colour printer to produce the final hardcopy image.

5-3 Interpretation Methods of the Surveyed AB Profiles

An ASCII file with data in three columns, x, y and z, were prepared by using the spreadsheet package Quatro Pro. This file contains the apparent resistivity values and the measured x and y coordinates. Table A5T2, appendix 5, shows the ASCII file in this format.

The x-axis contains the distance values at the centre of the MN electrodes, between the successive measurements on the profiles (the middle third of AB). All distances on the x-axis are referred to electrode A as the zero position.

An arbitrary profile can then be chosen to be the reference (zero position) point for the y-axis but care should be taken to represent the actual position of this particular profile in the field with regard to other adjacent profiles. The position of any profile can then be measured from this reference point. The apparent resistivity values of each profile are given in the z-axis

A mapping software programme, UNIMAP, available at the University of Wales, Bangor was used to produce an apparent resistivity contour map of the surveyed rectangular area.

The iso-resistivity map or what can be termed as equipotential map (strictly a map showing lines of equal potential) gives the lateral variation of the bulk apparent resistivity down to the explored depth. It cannot show changes in true resistivity as the pseudosection can (more information about this problem will be discussed in chapter seven). The explored depth with the current electrode separation, AB, equal 100m is assumed to be between 30 and 50m. This assumption is based on the idea that depth of investigation is approximately half the maximum electrode spacing, as in the VES technique (Keary and Brooks, 1991).

The resistivity data of this survey can also be correlated with other information collected

from depth probes, pseudosections and borehole logging to resolve the difficulties in locating the saline interface on the site.

6- RESULTS OF SURVEYS

The interpretation methods explained in chapter 5 have been applied to the various resistivity data collected for this project. This has led to the production of results that can now be presented, explained and compared. The results from each site are dealt with separately here.

6-1 Data from College Farm, Aber

6-1-1 The VES Resistivity Surveys

As mentioned in section 4-3-2, the objective of conducting VES surveys was to compare the three electrode configuration techniques namely Wenner, Schlumberger, and Offset Wenner. The results of this comparison are given in section 6-1-1-1 below. The second objective for using the VES technique was to delineate the fresh-salt water interface by constructing a geoelectric section. The interpretation of these curves is given in section 6-1-1-2. Finally the VES technique was used to study temporal changes in the groundwater conductivity. The results of this process are given in section 6-1-1-3.

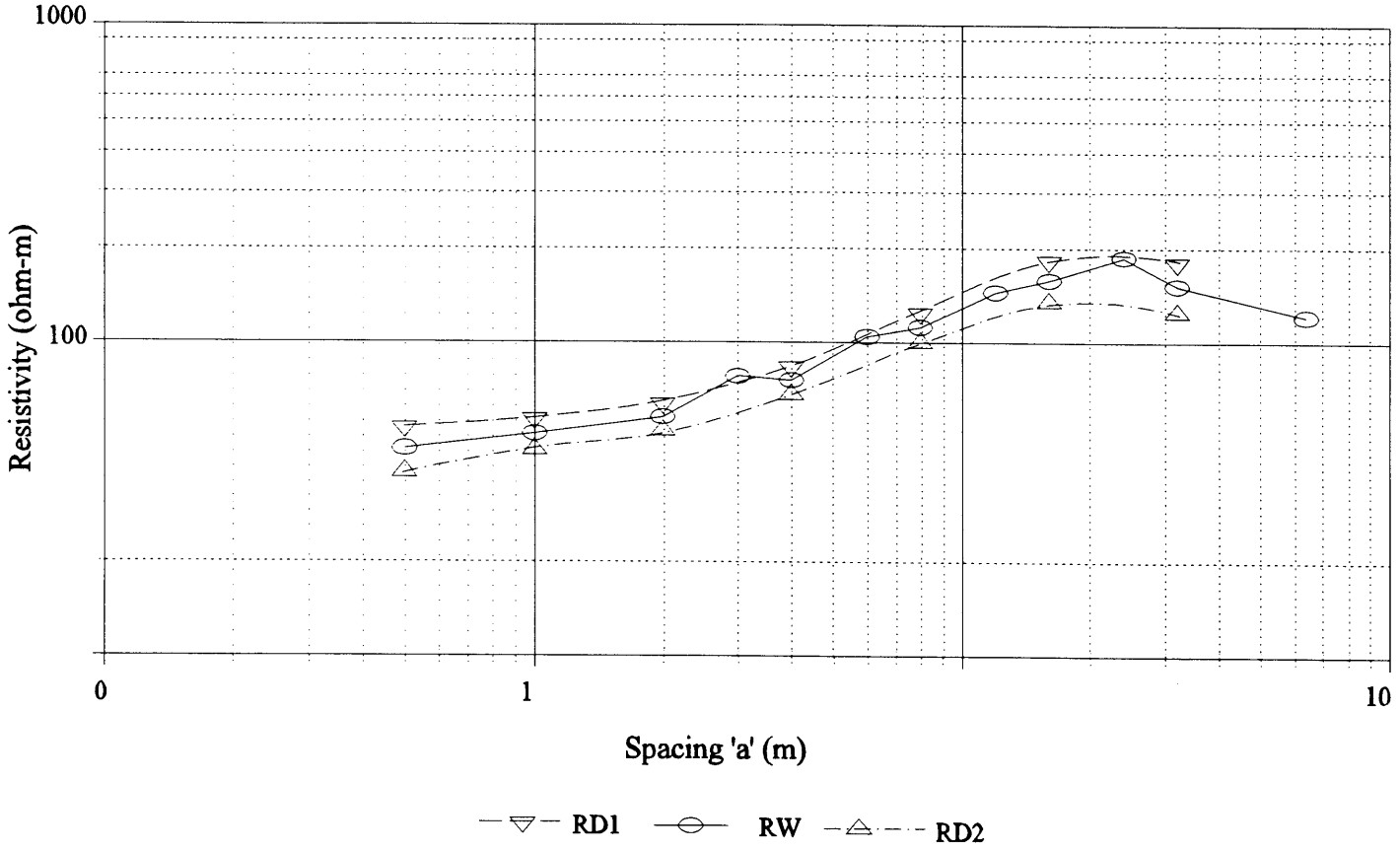
6-1-1-1 Comparison of Different VES Configurations

The resistivity sounding data collected at the same location, at a position close to BH10/2, have been analysed using the methods described in chapter 5.

Fig. 6.1 shows the raw and the interpolated data from the Offset Wenner Sounding. It shows the large difference in apparent resistivity for the adjacent resistance measurements R_{D1} and R_{D2} indicating that the site suffers from considerable lateral variation. These parameters have been assessed in terms of the Offset errors, the lateral errors and the observational errors described in section 4.5.1 and presented in table 4.7. The Offset error was significant, of the order of 15 to 32% which is greater than the 10% suggested by Barker (1981) as the threshold between a good and poor interpretation of an apparent resistivity curve.

Figure 6.1

Offset Wenner Resistivity curve



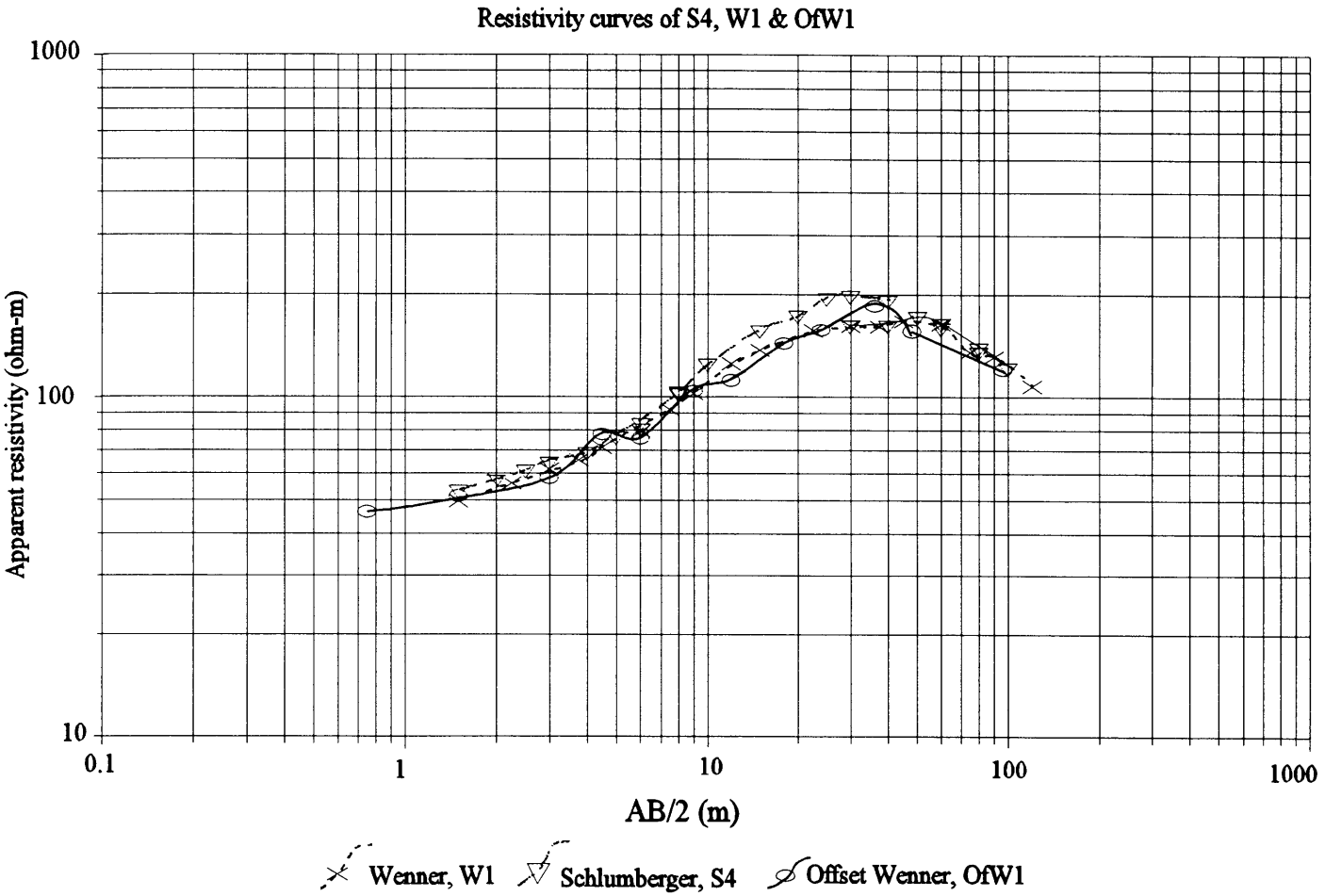
A possible reason for this could be the presence of lenses of anomalous resistivity material within the sediment sequence. Barker (1981) mentioned that the Offset averaging technique substantially reduces near-surface lateral variations, but that the deeper, larger-scale lateral resistivity variations such as dipping beds and faults, are likely to seriously distort the sounding curve. The offset error is an indication of these deeper effects. The lateral error, expected to be three times the offset error (Barker, 1981), was found to be negative presumably because R_{D1} was always greater than R_{D2}. Finally the observational error was outside the expected range of ±5% quoted by Barker (1981). This might be a problem with high electrode contact resistances because of the dry surface material on the site.

The average Offset Wenner data are presented together with the Schlumberger and conventional Wenner sounding data in fig. 6.2. Both the Offset Wenner and Wenner apparent resistivities have been plotted against equivalent AB/2 values to facilitate a direct comparison with the Schlumberger sounding curve.

The Schlumberger data , having been obtained as overlapping segments each time the spacing of the potential electrodes (MN) was increased, also has the potential for determining the lateral variability in apparent resistivity. The Wenner sounding, however, where all the electrodes are moved for each reading, tends to average out the lateral variations and consequently cannot determine the magnitude of lateral resistivity variability. In fact it is possible to derive Wenner sounding curves from lateral changes in resistivity which are similar to the sounding curves for a vertical layered resistivity sequence.

The sounding data shown in fig. 6.2 generally shows good agreement between the various techniques. The general shape of the sounding curves indicates that a 3-layer K-type ($\rho_1<\rho_2>\rho_3$) model is suitable for the initial interpretation. In general the Schlumberger data have higher values of apparent resistivity than the other arrays except at the largest electrode spacing where the agreement is very good. The Schlumberger curve shows a steeper rise in apparent resistivity with increasing AB/2 than the other curves. In addition the peak value is at an AB/2 of 30m compared to 45m for the Wenner array. Generally the overlapping segments of the Schlumberger data show close agreement, except for the AB/2 spacings of 30 & 40m, indicating that perhaps the lateral variation is not as significant as predicted by the Offset Wenner sounding data.

Figure 6.2


Resistivity curves of S4, W1 & OfW1
1000
100
10
Apparent resistivity (ohm-m)
0.1
1
10
100
1000
AB/2 (m)
Wenner, W1
Schlumberger, S4
Offset Wenner, OfW1

Both Wenner and Schlumberger soundings were analysed initially using the direct inversion facility of Resix Plus to derive an approximate starting model. The Schlumberger data predicted a three layer K-type model whilst the Wenner model predicted a four layer AK-type ($\rho_1<\rho_2<\rho_3>\rho_4$) model. The extra layer predicted by the Wenner data might be a function of the lateral variability but this is not clearly evident. However, the site variability and the fact that both techniques investigate different volumes of the ground could explain these conflicting models.

In order to compare the models derived from the three soundings the following strategy was adopted. First each data set was inverted using the same three layer starting model derived from the Schlumberger direct inversion. Secondly each data set was inverted using the same four layer starting model derived from the Wenner direct inversion. Finally a six layer model, based on the layering present in BH10/2, was used in the inversion process. The thicknesses of the first four layers were constrained to the actual values recorded in the borehole whilst all the other parameters were left "free" to change to achieve the best fit model. The results of all these inversions are summarised in table 6.1.

Sandberg (1993) states:

> *"A model can fit a data set well, but individual parameters of that model may not be well determined by the data values. For a layered-earth model the thin-layer-equivalence problem exemplifies a whole range of linear combinations of layer resistivity and thickness that can fit a data set equally well".*

Thus in addition to the inversion of the data, equivalence analyses were carried out for all the above models. This data is presented in full in appendix A6.1.

Fig. 6.3 shows a comparison of the 3-layer models derived from each of the sounding curves. The agreement between the models derived from Wenner and Offset Wenner soundings is very good. All three data sets agree on the first layer resistivity value of about 50 ohm-m. The Schlumberger data, however, gives a thicker first layer but a thinner second layer of higher resistivity than the Wenner data sets. The final layer resistivities again tend to agree quite well. The low resistivity first layer obvious relates to the alluvial silty soil found in the borehole log of BH10/2. The higher resistivity second layer correlates with the coarser gravelly material found in the borehole. The boundary between these layers,

however, does not really correlate with the depths shown in the borehole log.

A comparison of the four layer models, suggested by the direct inversion of the Wenner data, is given in fig. 6.4. Once again the first layer resistivity from each of the data sets is in very good agreement. The Wenner data sets, also show good agreement for the third and fourth layers. The Schlumberger model has a third layer of slightly less thickness and greater resistivity. The predictions for the intermediate resistivity second layer are at odds with one another indicating perhaps the tenuous nature of this particular interpretation of the data.

Finally fig. 6.5 shows the predicted models for the six layer interpretation in which the thickness of the first layers have been fixed with respect to the borehole log of BH10/2. Again the resistivity of the first layer (45 ohm-m) is very similar for all the three data sets. The rest of the predictions seem to be at odds with each other for each of the soundings. The six layer model in general has the best fit to the sounding data in terms of the RMS fitting error. Perhaps this should be expected since more layers can induce subtle changes in the predicted sounding curve which could match small inflections in the measured sounding curve.

Figure 6.3

Three layer model of S4, W1 and OfsetW1

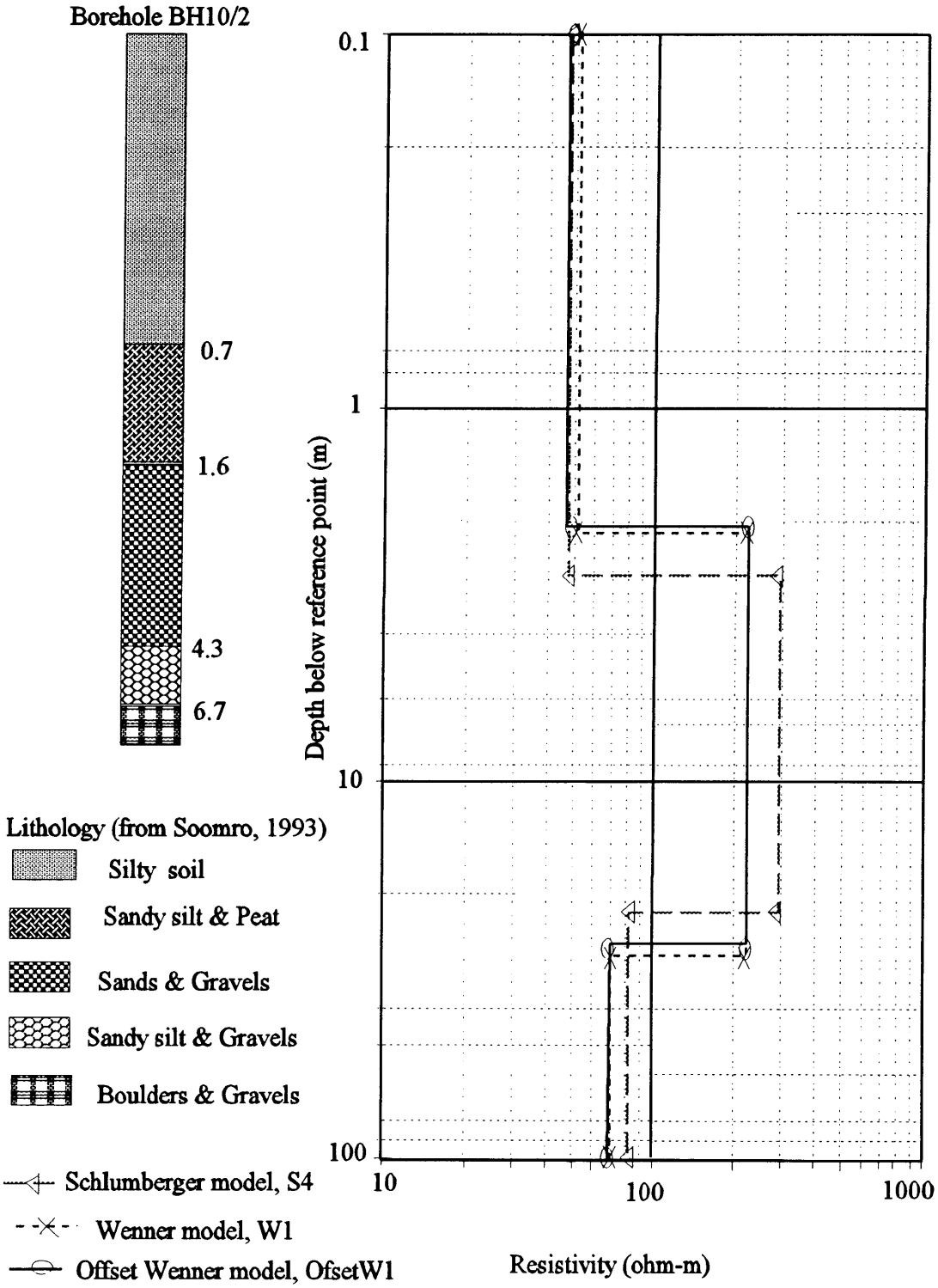


Figure 6.4
Four layer model of S4, W1 and OfsetW1

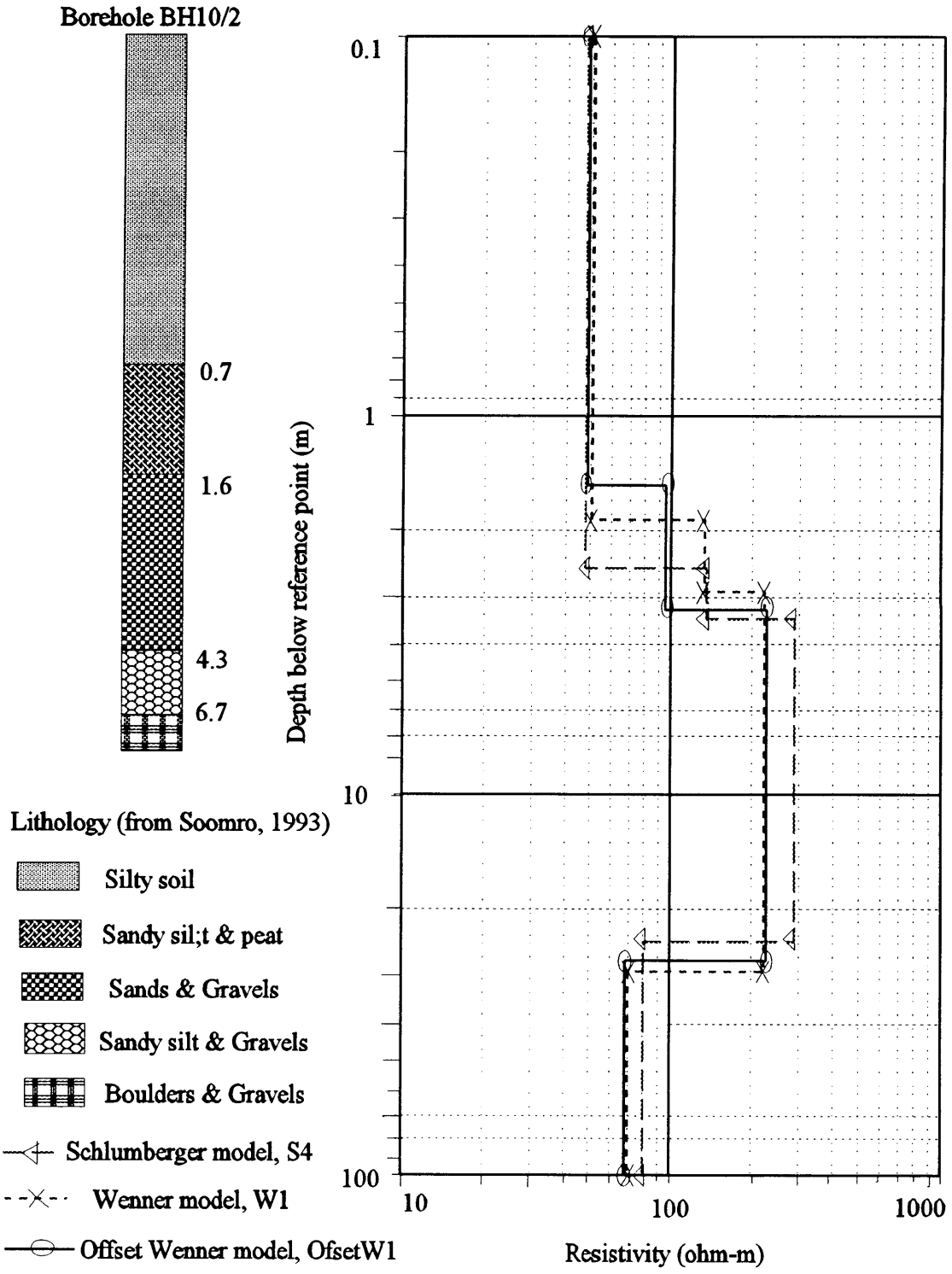
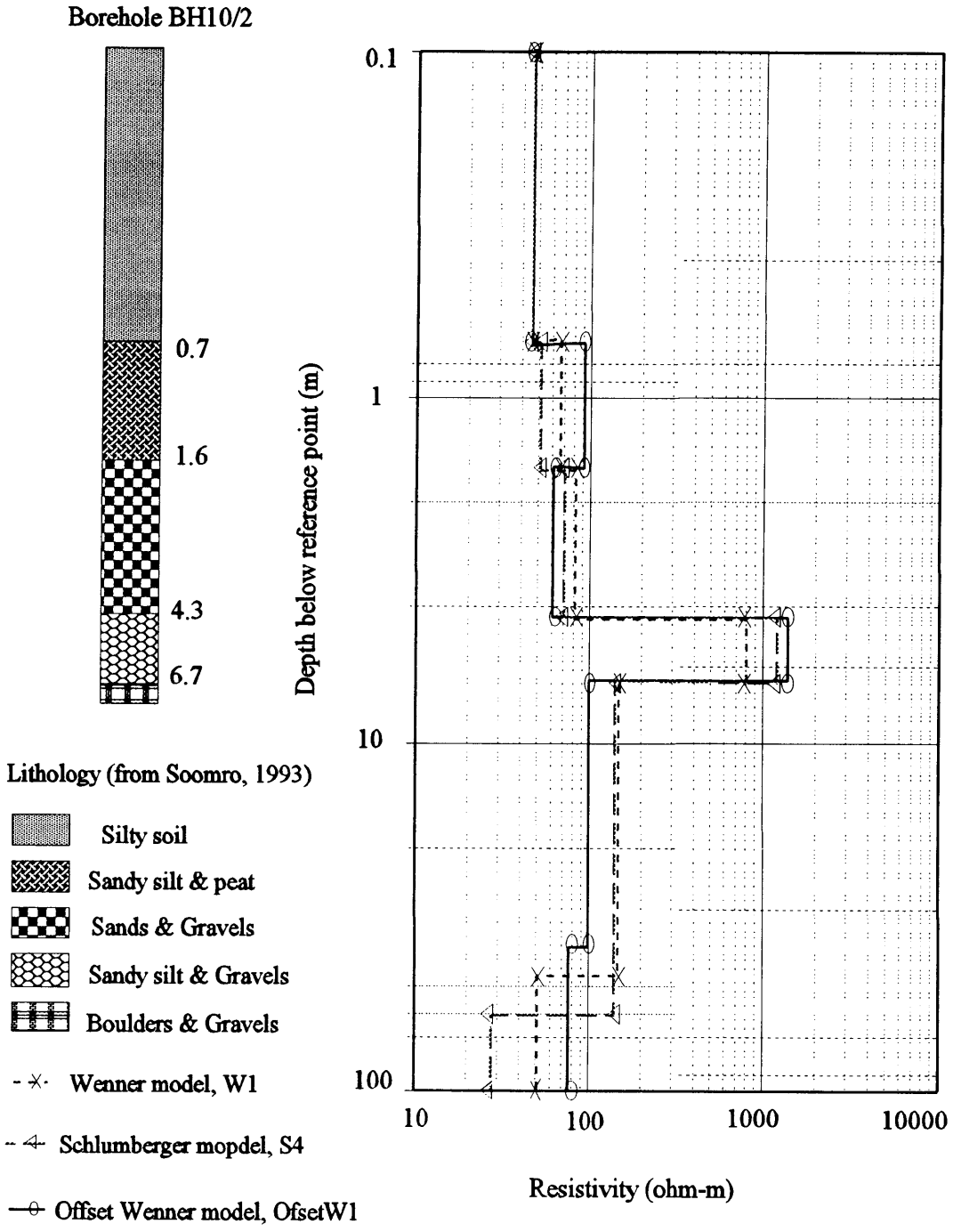


Figure 6.5

Six layer model of S4, W1 and OfsetW1



In any case the disagreement between the models below layer one indicate that the six layer interpretation is perhaps not the best representation of the situation at this particular position.

Table 6.1

Comparison between the layer model of S4, W1 and OfsetW1 for 3-4-6 layer model

Lay. #	Schlumberger sounding S4			Wenner sounding W1			Offset Wenner sounding OfsetW1		
	Thick. (m)	Depth (m) *	Rsistv. (Ω-m)	Thick. (m)	Depth (m) *	Rsistv. (Ω-m)	Thick. (m)	Depth (m) *	Rsistv. (Ω-m)
Three layer model									
	3.12	2.81	47.39	2.46	2.15	50.55	2.39	2.08	48.44
1	19.42	22.24	282.7	27.22	29.37	219.2	25.77	27.85	221.1
2	------	------	81.10	------	-----	69.96	-----	----	68.28
3	RMS error 3.128%			RMS error 2.969%			RMS error 6.415%		
Four layer model									
1	2.83	2.52	47.16	2.20	1.89	50.11	1.82	1.51	47.91
2	0.925	3.445	131.2	1.04	2.93	131.4	1.68	3.20	97.06
3	20.45	23.895	275.8	26.36	29.29	220.5	24.29	27.49	226.8
4	------	------	77.37	------	------	70.01	------	------	68.03
	RMS error 3.152%			RMS error 2.939%			RMS error 6.209%		
Six layer model									
1	1.00	0.690	45.06	1.00	0.690	46.26	1	0.690	44.94
2	0.900	1.59	50.87	0.900	1.59	67.78	0.900	1.59	91.90
3	2.70	4.29	68.64	2.70	4.29	83.30	2.70	4.29	62.87
4	2.40	6.69	1163	2.40	6.69	782.5	2.40	6.69	1383
5	53.27	59.96	141.5	40.12	46.81	151.3	31.13	37.82	100.8
6	------	-----	26.41	------	------	51.36	------	------	80.18
6	RMS error 2.905%			RMS error 2.537%			RMS error 5.545%		

*Depth is measured below ground level which is 0.31m above the reference point

6-1-1-2 Geoelectric Section Derived from the VES Data

The resistivity curves of the three Schlumberger soundings, S1, S2 and S3 referred to in section 4-3-1 have been processed in the same way as described in chapter 5 and the resulting ground models have been used to plot a geoelectric section (fig. 6.6a).

The first sounding, S1, was located 3m southeast of borehole BH10/2 (approximately in the same position as the soundings described in section 6-2-1-1). This sounding produced a K-type ($\rho_1<\rho_2>\rho_3$) 3-layer model similar to the Schlumberger S4 sounding but with a significantly different set of parameters.

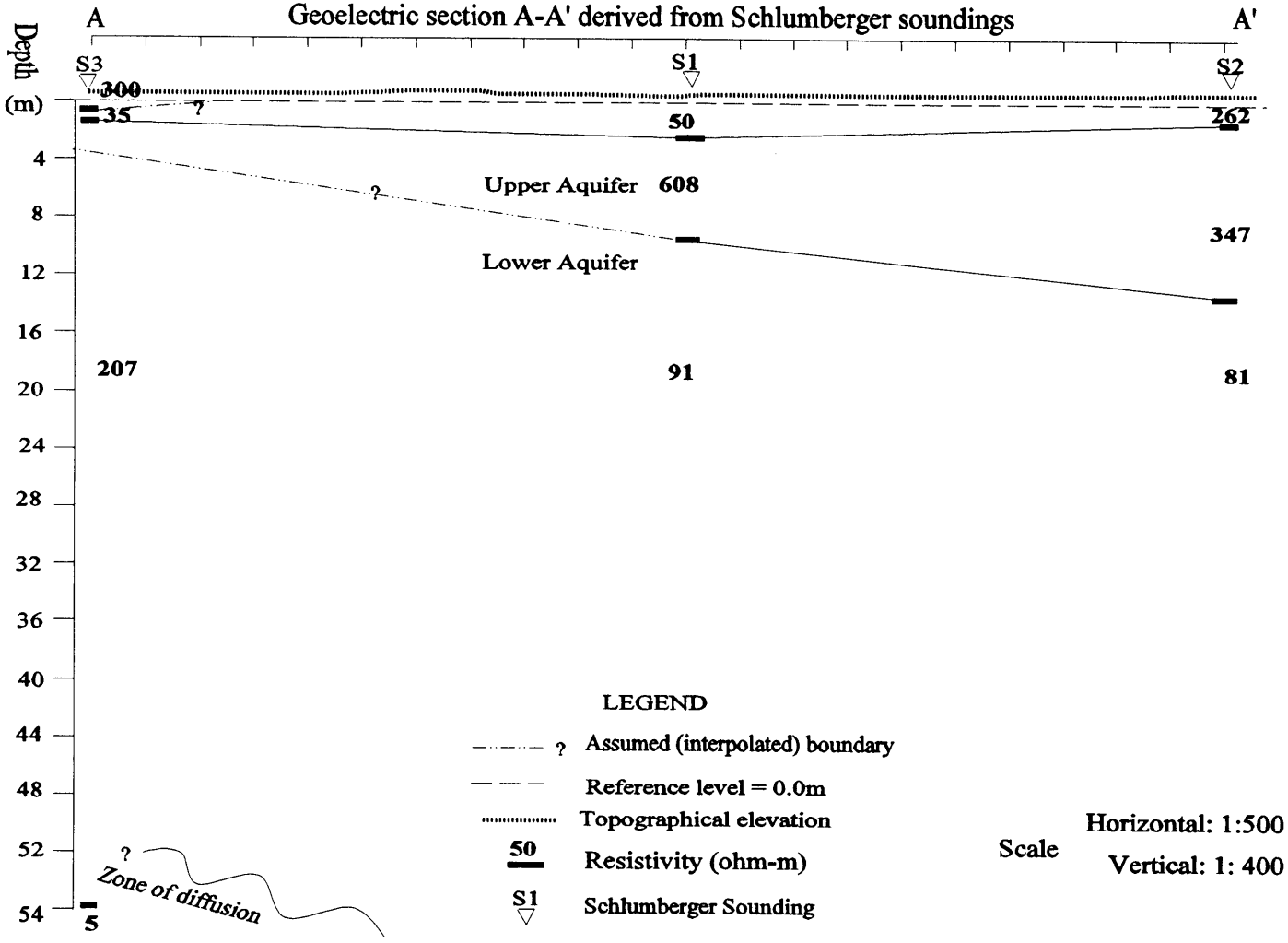
The second sounding, S2, was located about 50m south east of S1 about 5m from the field boundary hedge. The inverted data also produced a K-type model.

The third sounding, S3, was located about 55 m north west of S1, approximately 30 m from the coast. The inverted model is of the HK-type ($\rho_1>\rho_2<\rho_3>\rho_4$)having four layers. The first layer, about 1m in thickness, is a very resistive layer. This indicates that the surface layer is very dry and composed of sands and gravels. This area is slightly elevated compared to the rest of the site. All the data and models for these soundings are presented in appendix A6.2 while the summary of the inverted data of the three sounding is given in table 6.2.

The resistivity/thickness models from these three soundings were used to plot a geoelectric section that extends for about 107m through the boreholes towards the coast (fig. 6.6a). This geoelectric section can be compared with fig. 6.6b taken from Soomro (1993). In addition the top six metres can be directly compared with Pseudosection Ps1. To the west of the section there is a thin, highly resistive layer of dry gravely material which is slightly elevated with respect to borehole BH10/2 close to S1. Below this is a low resistivity layer which outcrops at the surface at S1 and which correlates to the silty alluvial material found in borehole BH10/2. The resistivity of this layer tends to increase eastward. Below this is a highly resistive layer corresponding to the underlying gravelly material.

Figure 6.6a

Geoelectric section A-A' derived from Schlumberger soundings



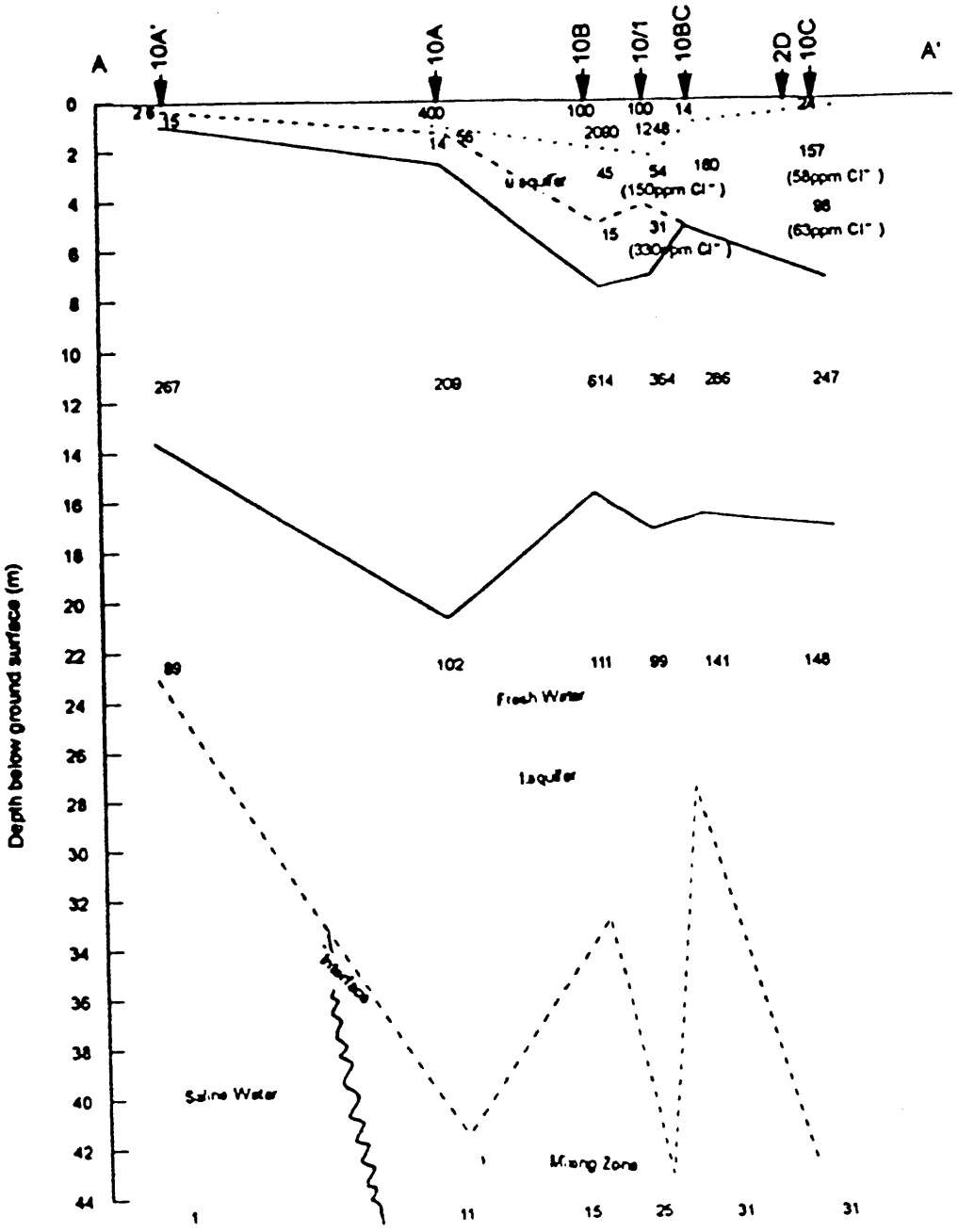


Fig. 6.6b. Geoelectric section A-A' derived from vertical electric and electromagnetic soundings.
Resistivities in ohm-m.
Scale: Hor. 1:1000, Vert. 1:200.

(From Soomro, 1993)

Finally at greater depth there is low resistivity which might correspond to the intrusion of slightly saline water into the lower aquifer. In the far west closest to the coast, this is particularly evident with the prediction of a very low resistivity of 5.2 ohm-m.

Table 6.2
Comparison between the layer model of S1, S2 and S3 used to construct AA' Geoelectric section

Layer #	Schlumberger sounding S3 (close to the shore). RMS error 4.788%			Schlumberger sounding S1 (nearly at the centre of the field). RMS error 2.952%			Schlumberger sounding S2 (near the fence in the landward direction). RMS 3.154%		
	Thick. (m)	Depth (m)	Rsistv. (Ω-m)	Thick. (m)	Depth (m)	Rsistv. (Ω-m)	Thick. (m)	Depth (m)	Rsistv. (Ω-m)
1	0.957	0.507	299.8	3.90	3.59	50.52	2.33	1.63	261.8
2	1.24	1.75	34.57	6.85	10.45	607.8	11.96	13.59	347.5
3	52.3	54.05	207	------	-------	91.44	------	------	80.55
4	------	------	5.23			-------			------

6-1-1-3 Temporal Changes in Groundwater Conductivity

Resistivity soundings S5, S6, and S7, were surveyed at the same location over a time period of about 3 hours during the approach of high tide on 31/7/95. This location was about 2 m south east of borehole BH10/2 (i.e. about 1m closer to the borehole than the soundings described in sections 6.1.1.1 and 6.1.1.2).

Some problems were encountered during the collection of data. Most problems were due to the dry surface sediments where some electrodes required slight repositioning to improve their electrical contact with the ground. Some readings in each of the data sets, however, were still found to be inconsistent with the overall pattern of apparent resistivity change with increasing electrode spacing. In these cases direct inversion of the data would lead to erroneous models with layers being due to a single measurement point or even having a

negative thickness. To avoid this situation the problem data points were "masked" so they were not used in the inversion process. Once a suitable curve fit had been achieved the masked data points were adjusted to fit the curve. The original data, sounding curves, models and equivalence models from the analyses of these three soundings are given in Appendix A6.3.

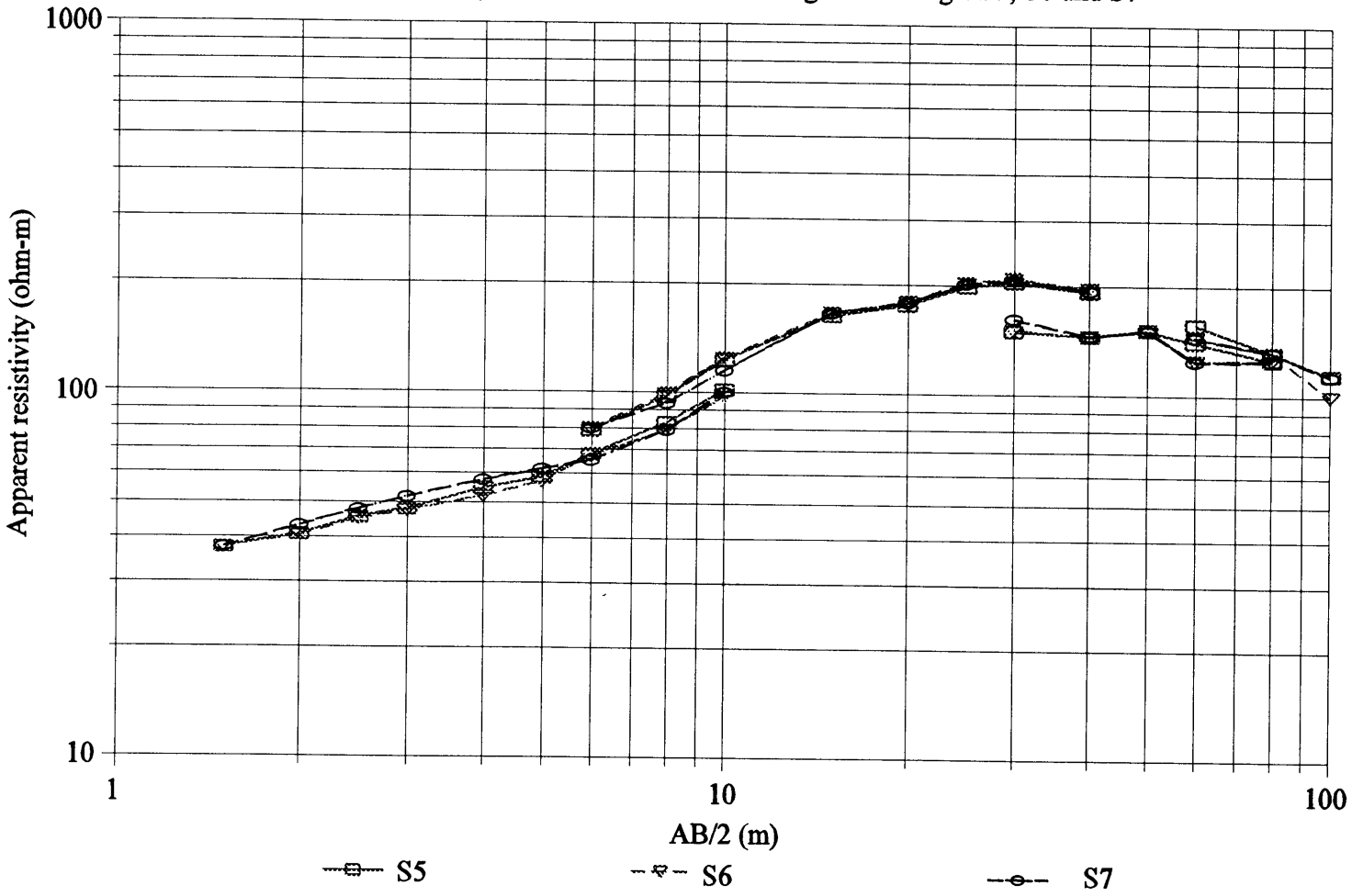
The first sounding was conducted at 11.15 hours, about two and half hours before high tide (tidal information was taken from Chart Datum, Beaumaris and is given in Appendix A6.4. The second sounding was started at about 12.00 hours whilst the third sounding was made at 13.45 hours when the tide was at its peak. Fig. 6.7 illustrates the corrected VES curves for each of the soundings measured at these times. Each of the segments have been displaced from each other indicating the lateral variability of the site. The second segment shows exceptionally good agreement between the soundings. The last two segments show some random variability in the sounding data. The first segment shows more systematic variation with the latest sounding having the highest apparent resistivities out to an AB/2 electrode spacing of 6m.

Fig. 6.8 shows the different models obtained from the three sounding curves at these times. As can be observed the models seem to change with time as the tide rises to its peak. Unfortunately the variations do not seem to be systematic as the tide rises. The main problem is that sounding S6 has had to be interpreted as a 3-layer model whilst the other soundings have required a four layer interpretation. The final sounding, however, does show the lowest resistivities for both the shallowest and deepest layers

6-1-2 Pseudosections and Inverted Resistivity Depth Profiles

The pseudosections measurements on this site can be categorised into three groups on the basis of the following aims. Firstly a pseudosection, (Ps1) was made extending through the borehole positions towards the sea for a distance of 106m, in order to compare the results of this technique with the geoelectric section constructed over a similar profile from the three soundings described in section 6-1-1-2. Secondly another two pseudosections, Ps2, Ps3, were surveyed at adjacent locations in order to map the spacial resistivity variation across the site.

Figure 6.7
The apparent resistivity curves of VES Schlumberger soundings: S5, S6 and S7



Finally an additional pseudosection, Ps4, was carried out at the same position as Ps3, without moving the electrodes, in order to monitor any changes in groundwater conductivity due to the influence of the rising tide

6-1-2-1 Pseudosection 'Ps1' for The Delineation of Saline interface

This pseudosection was carried out along a straight line that approximately occupied the same position as the geoelectric section presented in section 6-1-1-2. In this survey only the first six levels, of electrode separation, were utilized in the interpretation. (Level eight was surveyed but level seven was omitted since the requisite stripboard connector had not been made by the time of the survey. The complete data set is illustrated in fig.6.9.

The top illustration shows the measured pseudosection where the values of apparent resistivity are plotted along the section at the levels representing the increasing electrode separation. The location of BH10/2 is included for reference. The pseudosection data confirm that there is considerable lateral resistivity variation across the site. The pseudosection can be conveniently divided into four zones which are segregated by nearly vertical apparent resistivity contours. First the region, between 62 to 94m, shows the highest apparent resistivities which decrease rapidly with increasing N level or depth. This area corresponds to the slightly elevated area in the centre of the site which comprises dry sands and gravels. Beneath this thin surface layer is presumably a layer of silty alluvium and saturated gravel.

The area close to BH10/2, between 30 to 56m along the profile, has the lowest resistivity along with the far north of the profile beyond 99m. This corresponds to the silty alluvium which is underlain by sand and gravels of higher resistivity. The apparent resistivity contours in the region close to BH10/2 are, however, by no means horizontal. Finally the zone south of the 30m point on the profile shows an increase in apparent resistivity landwards which can be related to either the coarsening of the sediments southwards or the groundwater becoming less saline or a combination of both.

Figure 6.8

Resistivity earth models obtained from

the inversion process of the resistivity curves of S5, S6 and S7

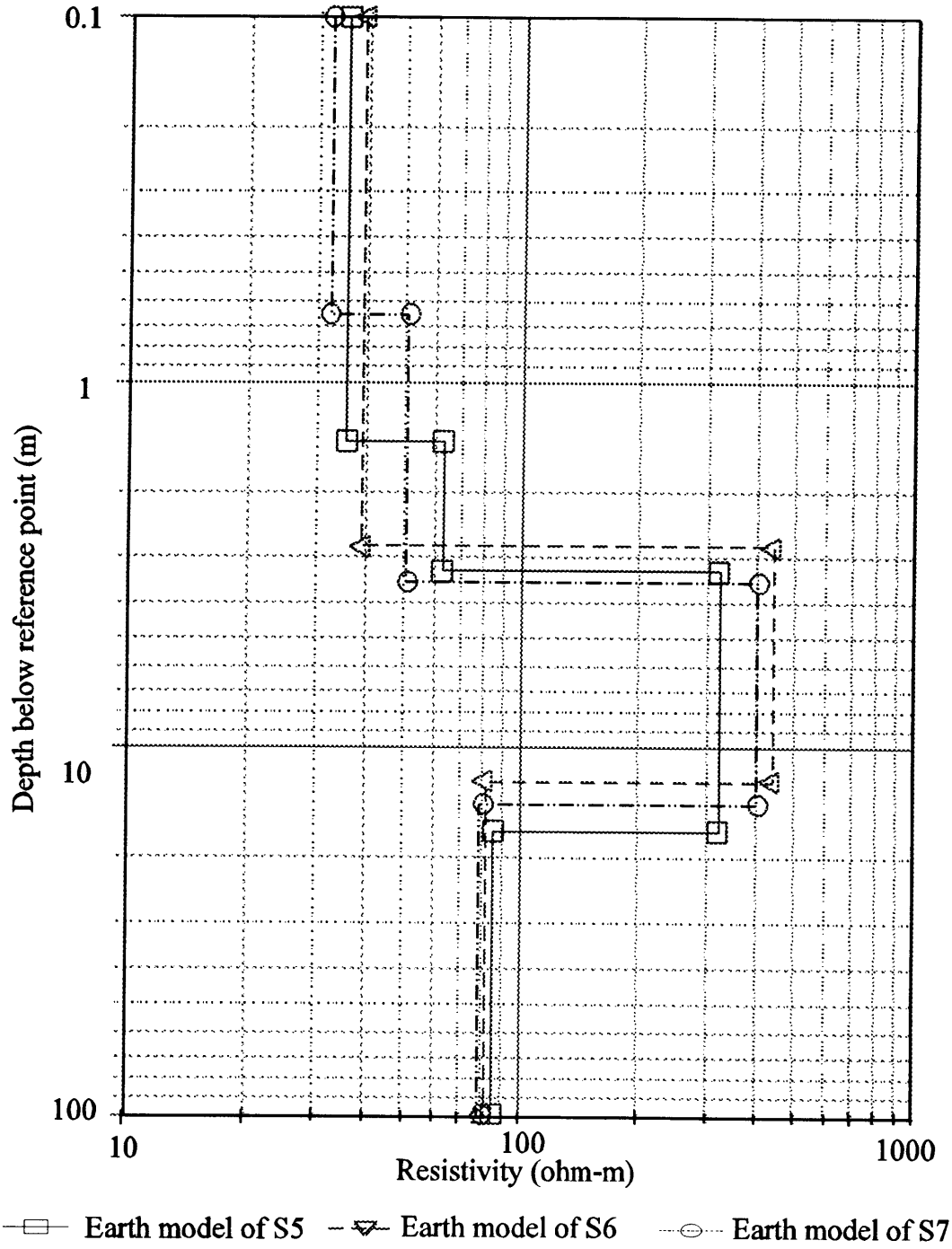
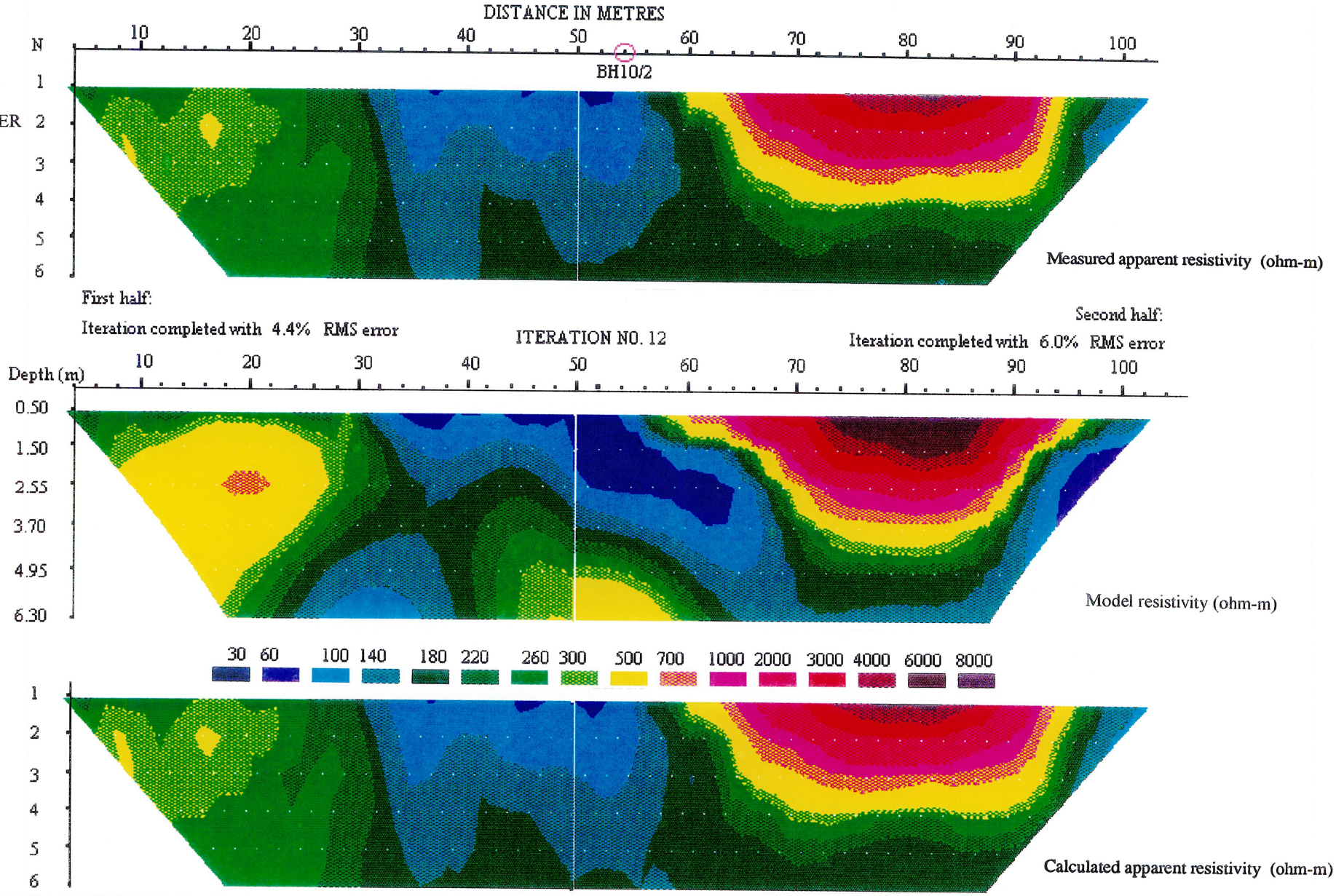


FIGURE NO. 6.9

PSEUDOSECTION 1

COLLEGE FARM, ABER



The inverted resistivity section corresponding to this pseudosection data is illustrated below the pseudosection in fig. 6.9 for iteration 12. This section extends down to 6.3m and can be directly compared to the upper parts of the geoelectric section presented in section 6-1-1-2. The true resistivity section has been slightly altered from the pseudosection in terms of the pattern of lateral variations. The high resistivity zone between 60 to 96m is still present but the low resistivity region close to BH10/2 is shown to extend below the high resistivity layer towards the coast. It is suspected that the depth of high resistivity zone is exaggerated and the low resistivity zone continues towards the coast to join up with the low resistivity zone in the far north of the section.

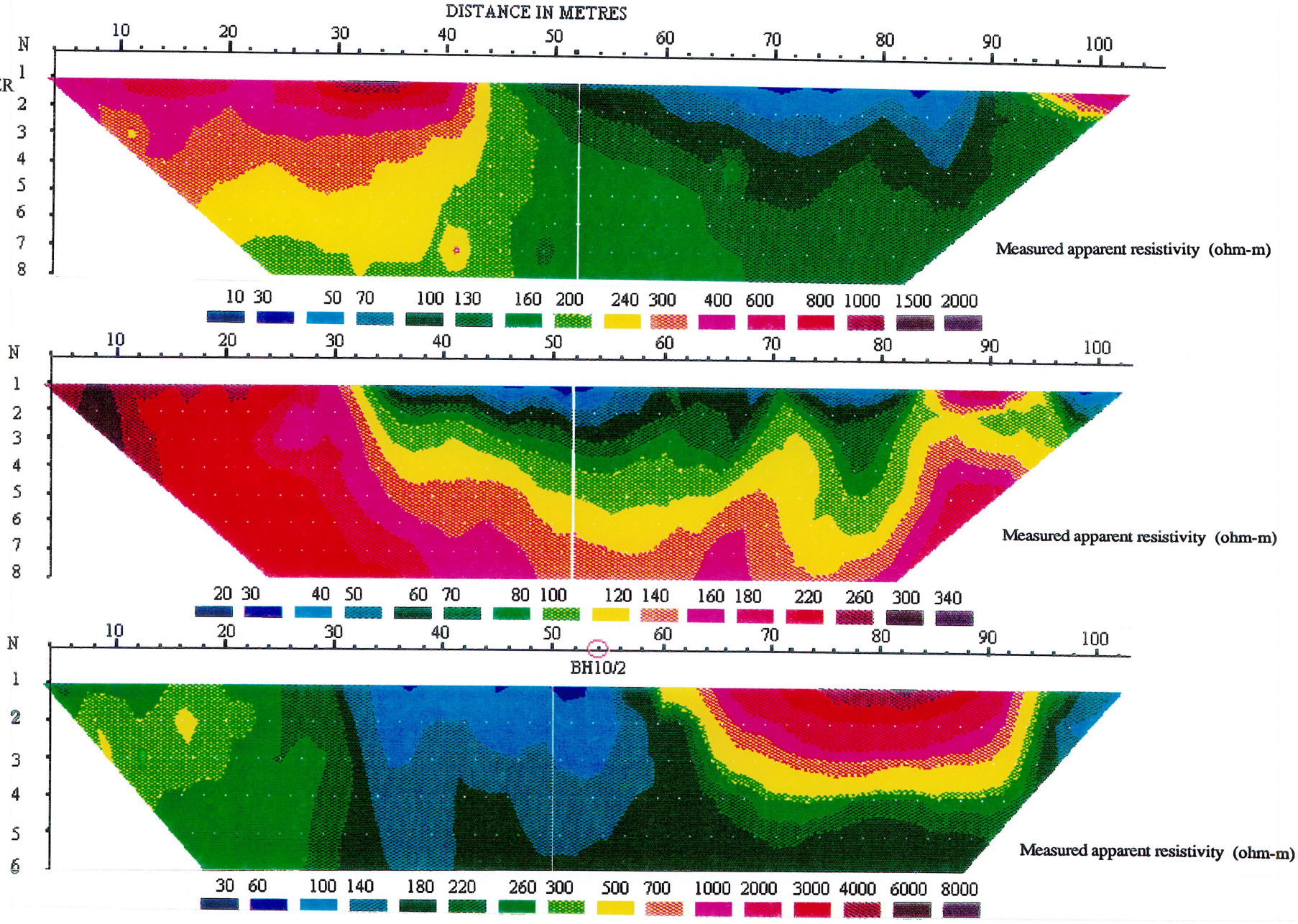
6-1-2-2 Spatial Variations in Resistivity

In order to determine how the resistivity varies across the site a further two pseudosections, Ps2 and Ps3, were carried out. The locations of the three pseudosections are shown on the site map in fig. A4F10. The three pseudosections are presented in fig. 6.10 with the top section being furtherest to the west and the right hand side being closest to the sea in the north. Care should be taken when comparing these pseudosections since the ranges of apparent resistivity in each section have been contoured with different colours. The main reason for this is that the middle section has the smallest range of apparent resistivities. Each of the sections contain zones of low apparent resistivity (<100 ohm-m) which correspond to the presence of the silty alluvium which may or may not be contaminated with saline water. The highest resistivities occur in conjunction with the areas which are slightly elevated compared to the rest of the site and which are composed of dry sands and gravels. These occur to the south and far north of Ps2 and the zone from 62 to 94m in Ps1.

All three sections show an almost vertical apparent resistivity contour which segregates the low apparent resistivity zone from the higher apparent resistivities to the south away from the coast. This might represent the extent of the landward limit of the saline contamination of the groundwater.

FIGURE NO. 6.10

COLLEGE FARM, ABER



Each of the pseudosections were inverted as described in section 5.2 and are presented in fig. 6.11 in terms of true resistivity depth sections. The sections have been artificially joined at about 50m along the profiles. Although there are some mismatches in resistivity the pattern of resistivity variation is still maintained across this artificial boundary.

Although the pattern of resistivity variation appears to be quite complex there are some generalisations that can be made about the sections. Firstly the low resistivity zones seem to link together, even beneath the high resistivity surface zones to eventually meet the coastal zone to the north. Secondly towards the southern boundary of the site the resistivity values tend to increase. Finally resistivity values tend to increase with depth although there are some major anomalies which disrupt the zones of almost horizontal layering shown in the pseudosections of fig. 6.10. These generalisations are reinforced by the contour plot of fig. 6.12 which shows the variation of surficial resistivity across the area of the site covered by the pseudosections. The 50 ohm-m contour tends to isolate the lower resistivity slightly lower lying areas of the site from the slightly elevated, higher resistivity, drier areas. It also possibly marks the southern extent of the saline groundwater contamination within the upper aquifer.

FIGURE NO. 6.11

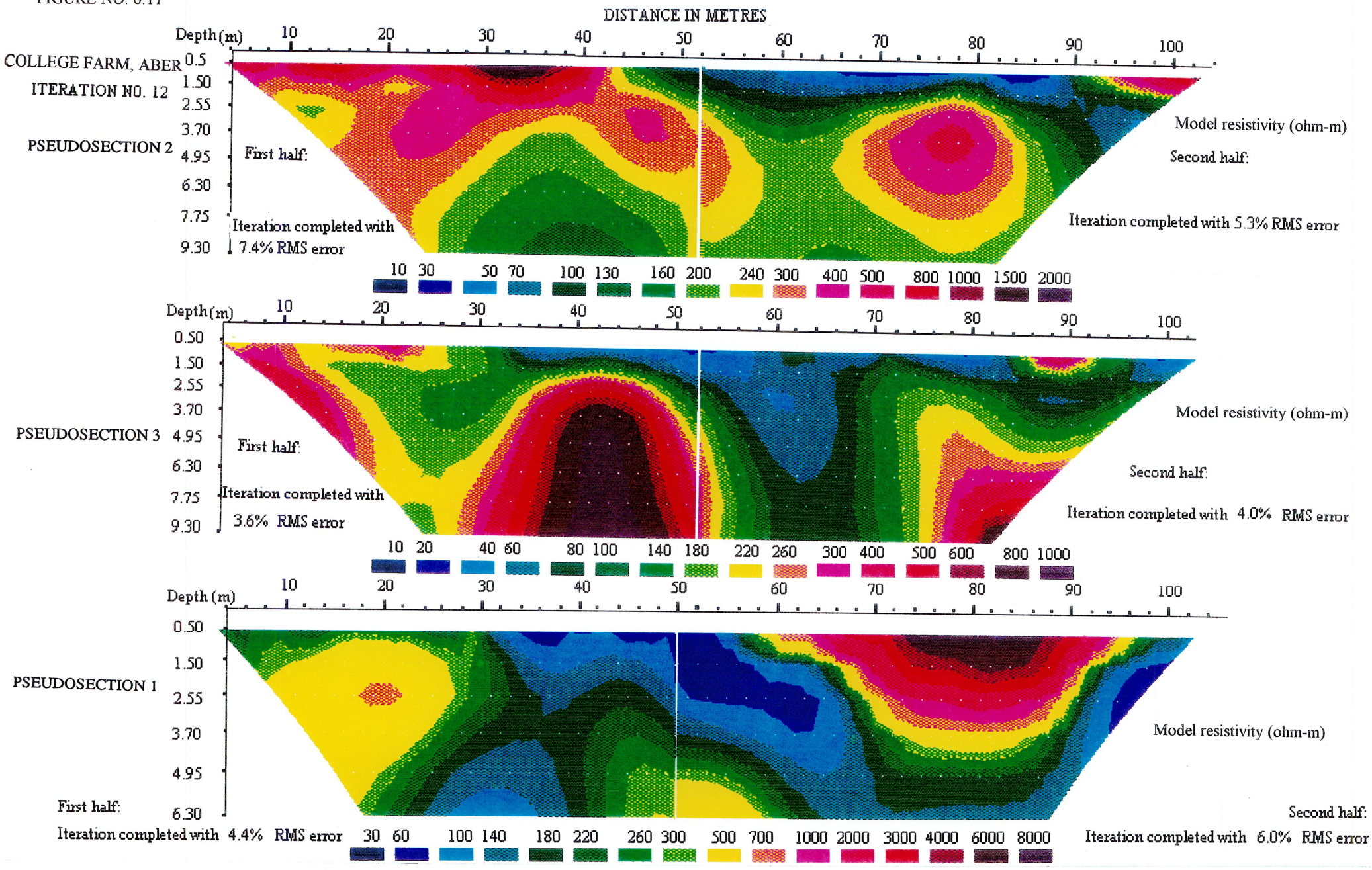
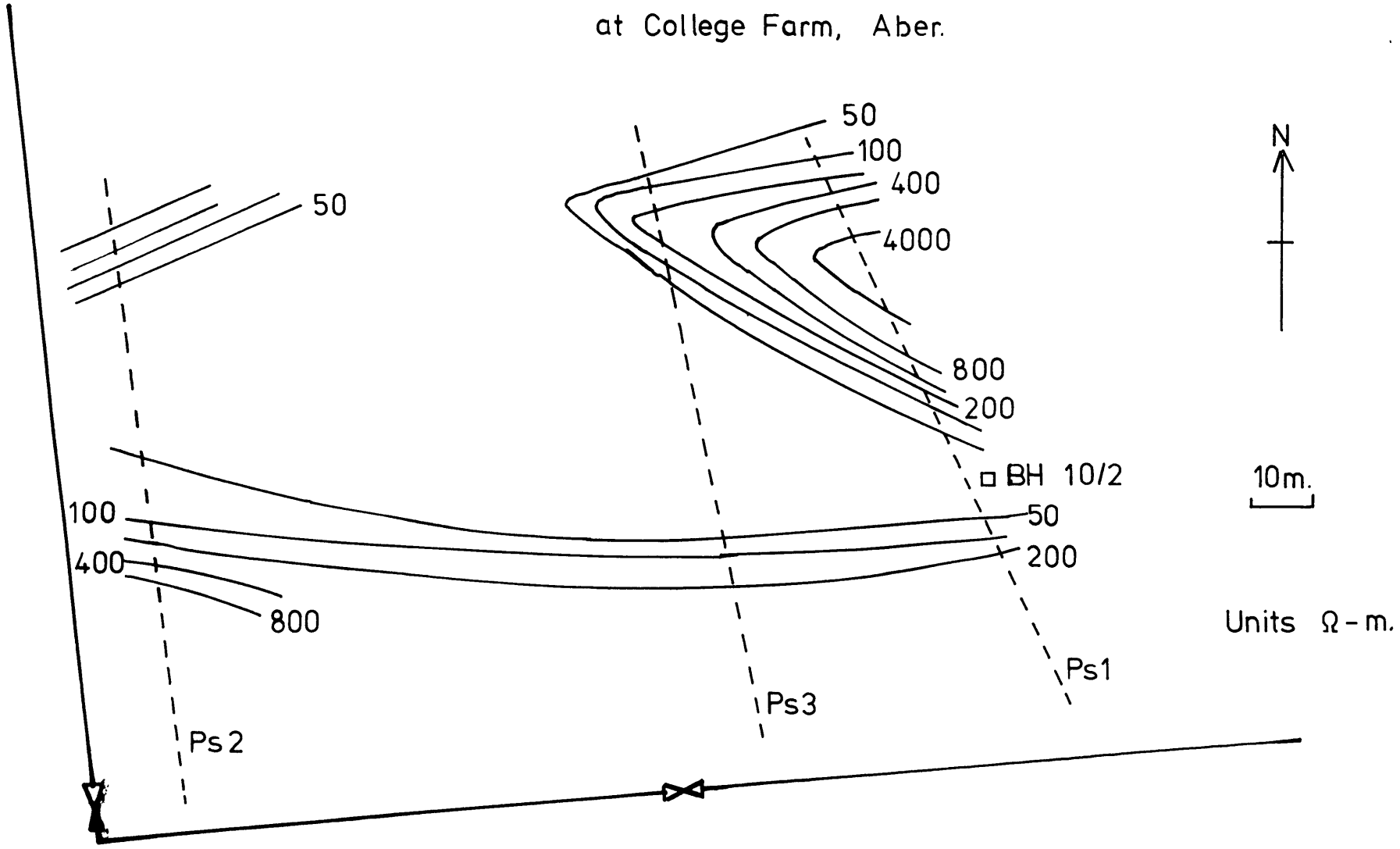


Fig. 6.12 Surface resistivity contours taken from inverted pseudosections at College Farm, Aber.



6-1-2-3 Monitoring Tidal Effect on the Groundwater Conductivity

Pseudosection Ps3 was measured on 31/7/95 about two hours before high water. The complete survey took about two hours. In order to see if the rising tide would change the groundwater conductivity a further set of measurements, Pseudosection Ps4, was carried out without changing the electrode positions, over the high water period. Fig.6.13 shows a comparison of these two pseudosections which tend to be remarkably similar. Both of these images have been inverted and the model resistivity depth sections are plotted in fig. 6.14. Again the difference between the sections is minimal. This seems to indicate that the effect of the rising tide has very little influence on the groundwater conductivity in the upper aquifer.

6-1-3 Schlumberger AB Profiles

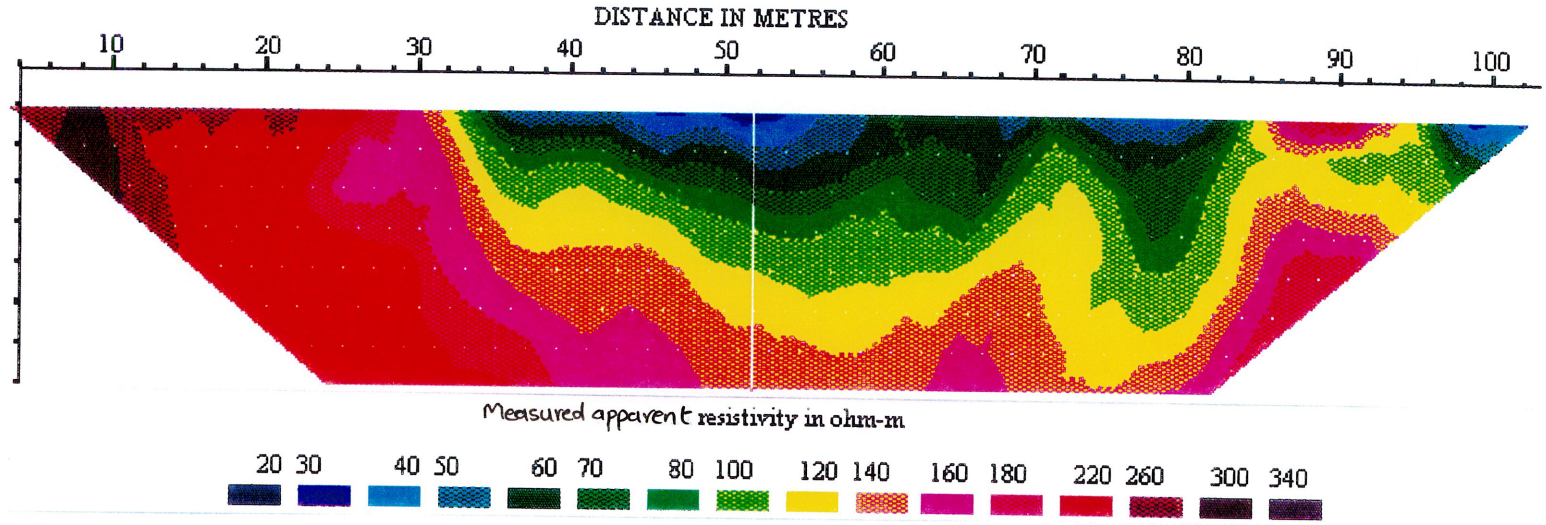
The results of this survey has led to the construction of an apparent resistivity image of a $780m^2$ rectangular area the location of which is shown on the site map in fig. A4F10. This apparent resistivity map is shown in fig. 6.15. The image shows the distribution of the apparent resistivity averaged over a depth of several tens of metres. The lateral variability of resistivity is clearly illustrated with this type of display. This image can be directly compared to the middle of pseudosection Ps1 which passes through the 5m coordinate. The apparent resistivity tends to increase towards the north of the survey region towards the coast even though the effect of any saline intrusion should reduce the apparent resistivity. This region corresponds to the slightly elevated region of high resistivity, dry gravelly, sand deposits previously identified by the pseudosection. The lower apparent resistivity area, around BH10/2, tends to correspond to the silty alluvial deposits which are outcropping in the lower areas of the site. The ridge of higher apparent resistivity south west of BH10/2 is probably a result of lateral variations, some depth below the surface.

FIGURE NO. 6.13

COLLEGE FARM, ABER

PSEUDOSECTION 3

AT 10.45 HRS ON 31/7/95

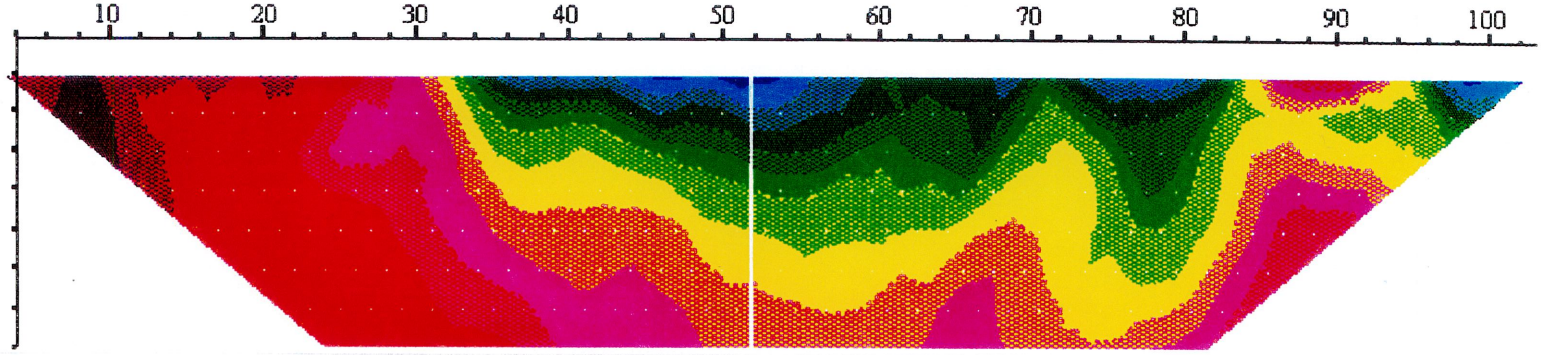


Measured apparent resistivity in ohm-m

20 30 40 50 60 70 80 100 120 140 160 180 220 260 300 340

PSEUDOSECTION 3

AT 13.30 HRS ON 31/7/95



Measured apparent resistivity (ohm-m)

FIGURE NO. 6.14

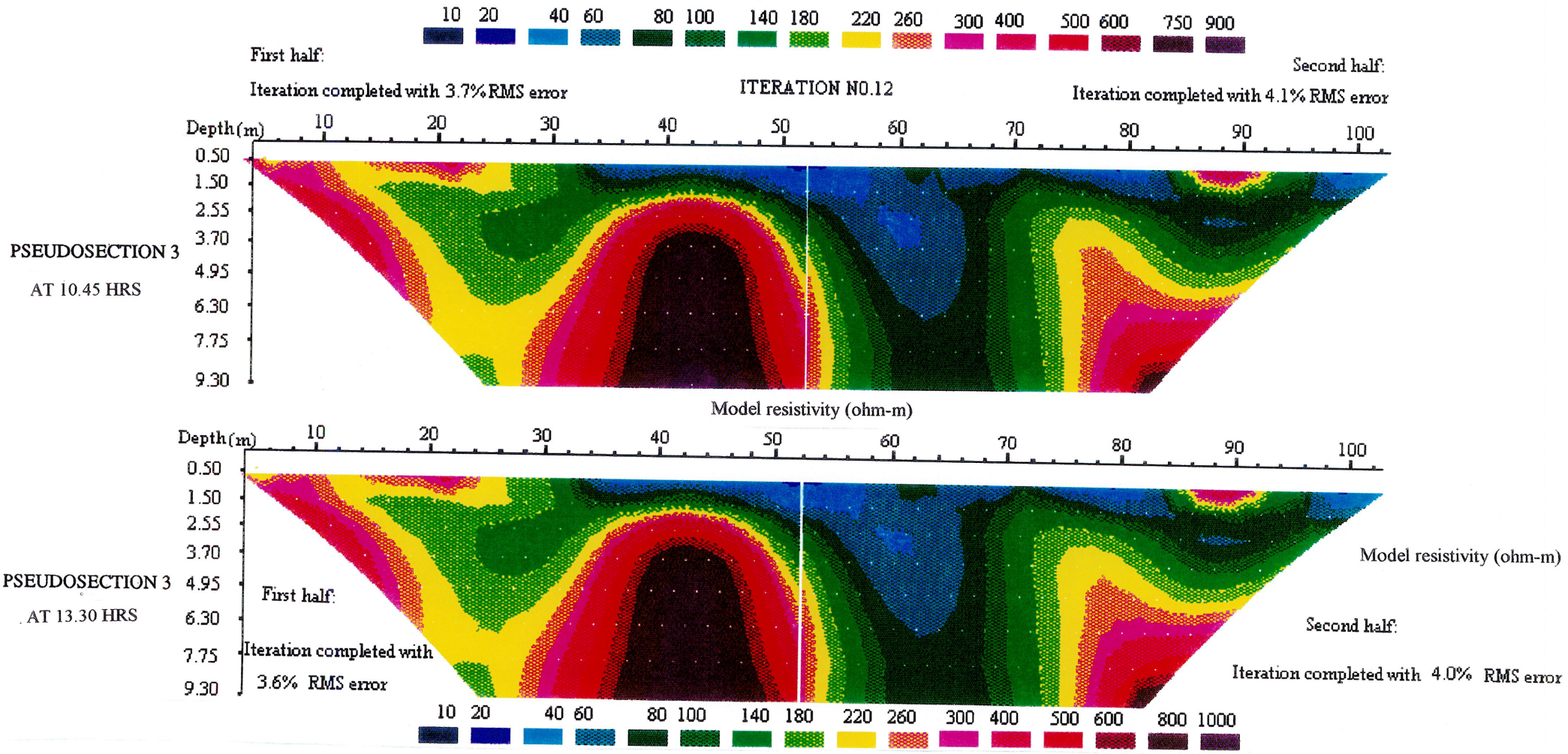
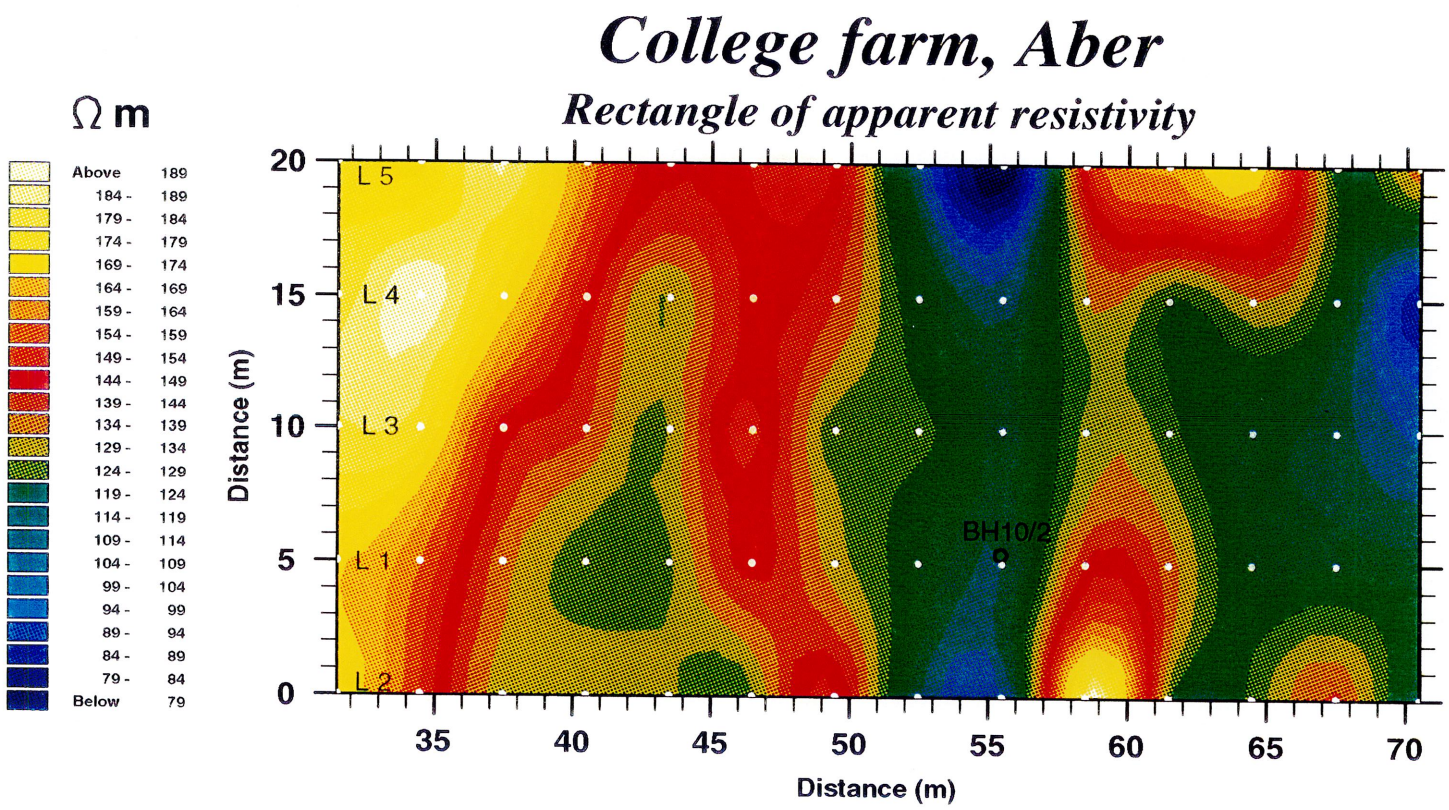


FIGURE NO. 6.15



6-2 Data From the Landfill Site

6-2-1 VES Resistivity Curves

In general it was difficult to carry out VES surveys on the landfill site due to the limited unobstructed space available to expand the electrode arrays. This was compounded by the fact that the underlying groundwater conductivity was affected by the presence of the waste material. Consequently the electrode expansions that were used for the four Schlumberger soundings were limited in their extent and hence their depth of penetration.

The positions of the VES surveys are shown in fig. 4.12. Sounding S1 was located adjacent to the south west corner of the tipped area over a relatively marshy area between the tip and the river. Sounding S2 was carried out to the west of the landfill, at the foot of the waste tip which was about 5 to 6m above the original ground level. The expansion of the electrodes for this sounding resulted in some of the electrode positions being beyond the influence of the tip, and so some lateral variability should be expected for this data set. Sounding S3 was located in the north west and was entirely carried out away from the influence of the tip and thus should represent the resistivity of the original ground conditions. Finally sounding S4 was carried out on top of the tip itself. This data set should provide an idea of the resistivity of the leachate as well as its depth of influence. The inversion of the sounding data followed the methods described in section 5.1. The raw data, models and sounding curves together with equivalence analysis, for each of the Schlumberger sounding curves carried out on the landfill site are presented in appendix A6.5. A summary of the models for each VES is provided in table 6.3 for comparison.

In general terms each of these VES data sets has its own particular problem associated with its interpretation. Consequently each sounding interpretation will be dealt with separately here.

6-2-1-1 VES S1

This sounding curve shows a gradual increase in apparent resistivity with increasing AB/2 spacing. The curve shows some slight inflexions which might be due to thin layers of

intermediate resistivity or to variable surface conditions which have been observed at this location. The direct inversion of this data resulted in a 3-layer A-type model ($\rho_1 < \rho_2 < \rho_3$) but the parameters resolution matrix for this model showed that the thickness of layer 2 and the resistivity of layer 3 was not well resolved. A simpler two layer interpretation, with data segments adjusted to correspond with the smaller MN spacing and the last data point masked led to a less ambiguous model of a low resistivity, 14 ohm-m, upper layer of thickness 3.2m overlying a higher resistivity, 66 ohm-m substratum. The final data point is perhaps indicative of a further higher resistivity layer at greater depth but more sounding data at AB/2 ranges greater than 40m are required to substantiate this. Unfortunately there was insufficient space to obtain measurements at these greater electrode separations.

6-2-1-2- VES S2

This sounding curve shows some very spurious data, probably as a result of the survey being conducted across the boundary between the tipped and untipped areas of the site. This data is really not suitable to interpret further. However, a very simple two layer interpretation has been attempted by selectively picking suitable data points. The tentative model shows a low resistivity upper layer (38 ohm-m) of thickness 11m overlying a higher resistivity layer (224 ohm-m).

6-2-1-3 VES S3

This is the best of the four VES data sets from this site which is perhaps not surprising as it was performed in an area of the site that was not influenced by the waste tip. The sounding curve does exhibit one or two inflections but the direct inversion of the data suggested a 2-layer starting model. Further inversion produced a best fit model of a low resistivity upper layer (38 ohm-m) of thickness 2.9m overlying a higher resistivity substratum (261 ohm-m). The upper layer probably corresponds to the surficial alluvial clay which is underlain by more resistive sandy, gravelly material which forms a minor aquifer. The sounding was not able to resolve the depth to the expected highly resistive, schist bedrock since there was insufficient space to expand the electrodes beyond the maximum achievable AB/2 spacing of 30m.

Table 6.3

Comparison between the layer model of S1, S2, S3 and S4 at the Landfill

Layer #	Schlumberger sounding S3			Schlumberger sounding S4				Schlumberger sounding S2			Schlumberger sounding S1		
	Thick. (m)	Depth (m)	Rsistv. (Ω-m)		Thick. (m)	Depth (m)	Rsistv. (Ω-m)	Thick(m)	Depth (m)	Rsistv. (Ω-m)	Thick (m)	Depth (m)	Rsistv. (Ω-m)
1	2.85	2.85	38.22	1	0.898	0.898	24.62	1.14	1.14	25.6	2.66	2.66	13.3
				2	8.14	9.04	8.84						
2	------	------	261.1	11.45		20.50	80.12	10.8	11.9	50.2	11.6	14.3	42.1
3	------	------	------	-------		-----	25079	-------	-------	271	------	------	158
	RMS error 2.108			RMS error 5.338				RMS error 3.765			RMS error 2.299		

6-2-1-4 VES S4

This is the most complicated of the sounding curves obtained from this site and considering the fact that it was performed on the levelled top of the old, unconfined waste tip the quality of the data is surprisingly good. An initial direct inversion of the data indicated that a four layer starting model might be suitable. The resulting parameter resolution matrix, however, indicated that layers 3 and 4 were poorly resolved in terms of their resistivity and thicknesses. Consequently a simplified 3-layer model was attempted on the basis that it would be a more suitable interpretation of the shape of the sounding curve which is indicative of a H-type ($\rho1>\rho2<\rho3$) model (see fig. 6.16). The inversion of this starting model resulted in a thin, about 0.8m, surficial layer of resistivity 23 ohm-m and an underlying layer of very low resistivity (8 ohm-m) of thickness 9.8m. The final layer resistivity is not well resolved being anything between 350 to 44,000 ohm-m. To resolve the resistivity of this layer additional measurements at AB/2 spacings greater than 60m are required. The upper layer corresponds to the dry surficial covering material. The very low resistivity layer probably corresponds to the contaminated leachate within the waste material itself. This leachate also extends further down into underlying alluvium and sandy, gravels.

6-2-2 Pseudosections Sections and Resistivity-Depth Profiles

The three pseudosections measured on this site are interpreted using the methods described in section 5-2. The positions of each of the pseudosections are illustrated in fig. 4.12. They have been allocated the names Ps1, Ps2 and Ps3 in relation to the order in which they were surveyed.

6-2-2-1 Pseudosection Ps1

This pseudosection was located adjacent to the western edge of the waste tip overlapping the region between the old unconfined waste and the newer confined area which is only just beginning to be filled with waste. The pseudosection is displayed in fig. 6.17 in terms of the measured apparent resistivity plotted down to 8 levels corresponding to the successive increase in electrode separation.

Fig. 6.16

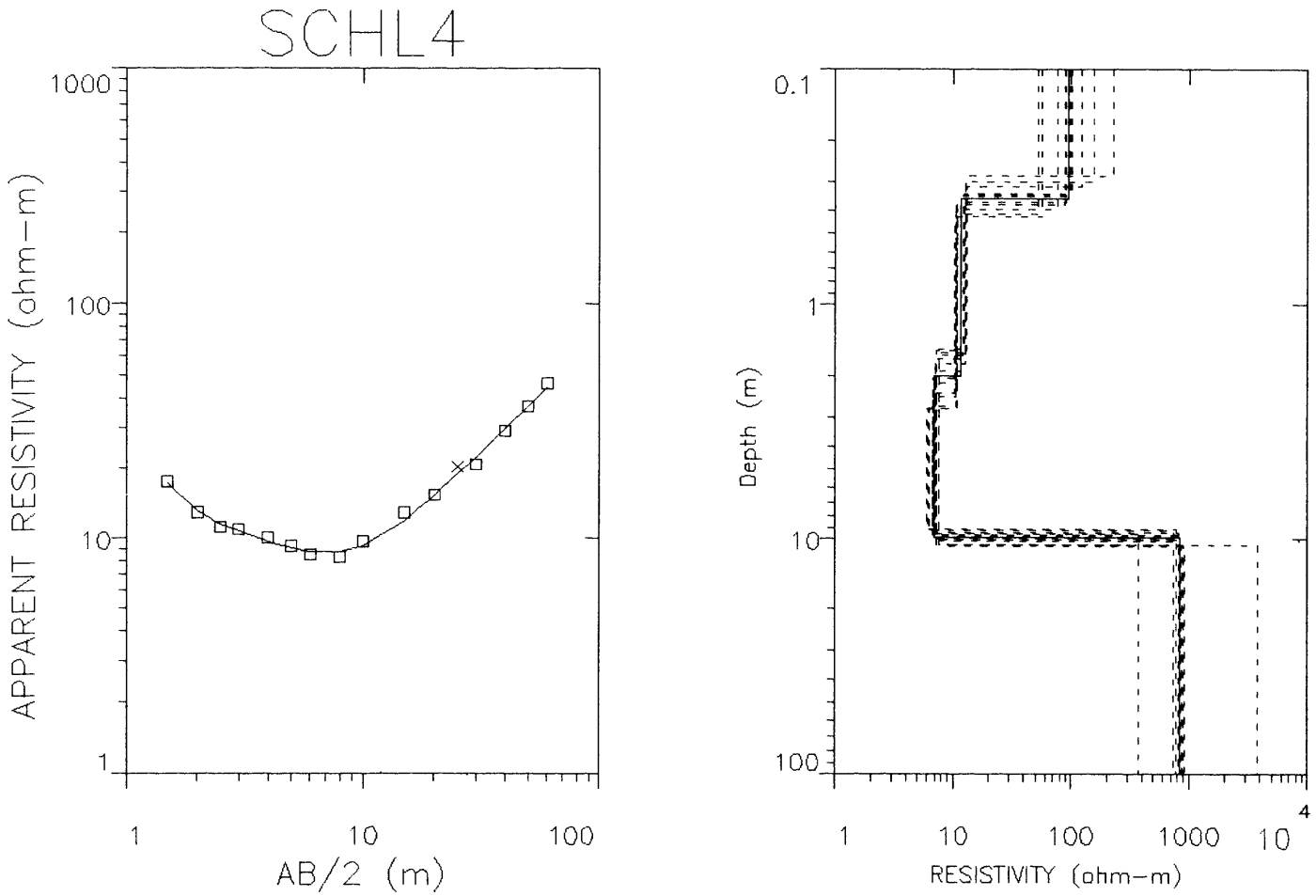
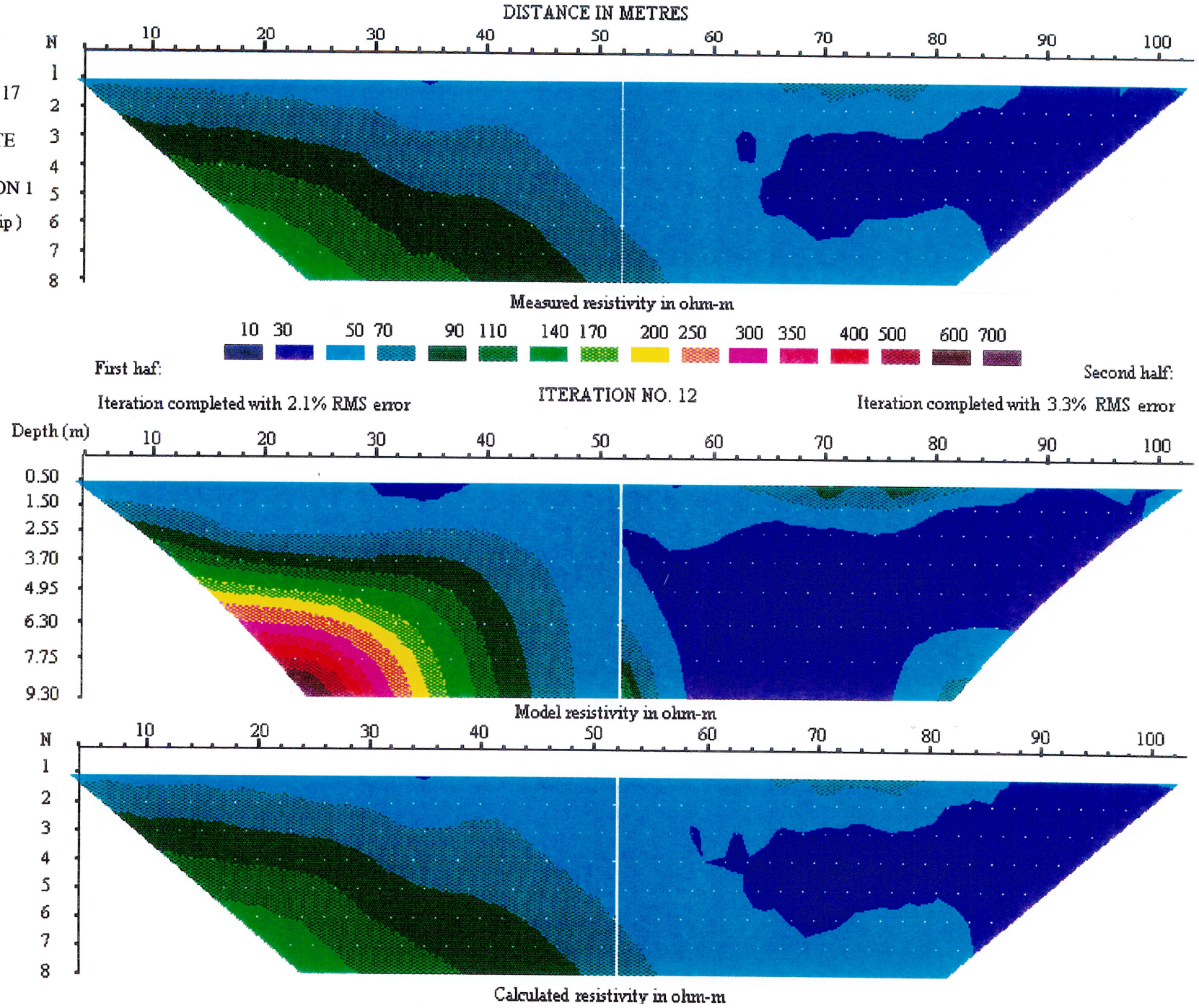

SCHL4
APPARENT RESISTIVITY (ohm-m)
1000
100
10
1
1
10
100
AB/2 (m)
Depth (m)
0.1
1
10
100
1
10
100
1000
10^4
RESISTIVITY (ohm-m)

FIGURE NO. 6.17

LANDFILL SITE

PSEUDOSECTION 1

(adjacent to the tip)



The section, starting from the left hand side, is some 40m from the edge of the old, unconfined waste tip. This can be immediately recognised in the pseudosection data where the apparent resistivities adjacent to the tipped area are significantly lower than those adjacent to the untipped area. This demarcation in even more clearly see in the inverted true resistivity-depth section plotted below the pseudosection. At 40m along the profile the resistivity contours are nearly vertical segregating the original, uncontaminated ground resistivity profile from the zone of leachate contaminated groundwater.

The near surface layer of alluvium is characterised by resistivities between 30 to 50 ohm-m across the section, in agreement to the results of VES S3. On the left of the section resistivities increase with depth to values approaching 600 ohm-m which might be indicating the presence of the schist bedrock. On the right hand side of the section the low resistivities persist with depth reaching values as low as 10 to 30 ohm-m. In fact near the end of the section this very low resistivity region outcrops on the ground surface. This region corresponds to a major leak of leachate observed on the surface at about 93m along the section. There were also minor leachate seeps at 62m and 73m but these do not seem to be connected to the contaminated groundwater at a depth of 2m shown on the resistivity-depth section.

The last section presented in fig. 6.17 is the calculated apparent resistivity pseudosection derived from the model true resistivity-depth section. The agreement between the measured and calculated pseudosections gives some confidence in terms of the inverted resistivity-depth model.

The pseudosection was surveyed within a metre or two of the base of the tip. It is therefore quite feasible, especially for the larger electrode spacings, that the current flow between the electrodes is preferentially flowing in the highly conductive leachate material within the tipped area, thus giving a slightly distorted picture of the resistivity distribution directly below the section. The pseudosection technique, has however, successfully detected the presence of leachate within the vicinity of the electrode array.

6-2-2-2 Comparison of Pseudosections Ps2 and Ps3

To shed more light on the problem of surveying close to the base of the waste tip two further pseudosections were carried out. The first, Ps2, occupied a similar position to Ps1 but started at the edge of the old, unconfined tip (i.e. at the 40m position of Ps1). The second, Ps3, was surveyed near to the river, about 15m away from Ps2 at its northern end and 26m from its southern end. The area between the river and the tip is a reed bed, through which it was extremely difficult to set up a perfectly straight profile parallel to Ps2. In addition to the presence of the reeds resulted in extremely variable couping of the electrodes to the ground. This was most noticeable for the near surface, small electrode separation, readings which were very erratic and sometimes even negative. (These spurious readings were removed in the processing stage of Ps3 before the pseudosection was finally inverted).

The two pseudosections are presented in fig. 6.18 with the top section, Ps2, being immediately adjacent to the base of the tip. Most of Ps2 shows apparent resistivities below 60 ohm-m. The main exception is a small near-surface zone between 70 to 82m which has an apparent resistivity of about 100 ohm-m. In the middle of the section is a zone of low apparent resistivity (>20 ohm-m) which seems to outcrop at the surface. This coincides with the large surficial leak identified for Ps1 at a location of 93m. Ps3 is characterised by much higher apparent resistivities especially in the lower levels of the section and towards the end of the section which is further away from the base of the tip. The apparent resistivity contours are almost horizontal for this section with the values increasing with depth. If the section had been located parallel to the edge of the tip the contours would probably be more nearly horizontal. The near surface apparent resistivity values, for level 1 and 2, show considerable variability due to the variable electrode contacts with the ground along the section.

Fig. 6.19 shows the true resistivity depth sections derived from the pseudosections shown in fig. 6.18. The upper section adjacent to the tip still shows evidence for the leak observed on the surface at 52m with the lowest resistivity value of between 5 to 10 ohm-m. Another minor surface leak of leachate was observed at 22m along the section. Two surficial zones of high resistivity occur between 26 and 40m and 70 and 84m. Low resistivity zones (>30 ohm-m) occur in isolated zones which form the middle part of the section. This is likely to

be a diluted solution of leachate in the groundwater. Generally the resistivity values increase with depth indicating the presence of freshwater in the underlying sands and gravels.

The lower section corresponds to the true resistivity-depth section carried out close to the river. It is evident that the low resistivity zones (>30 ohm-m) are still present although more limited in thickness (about 2m). These low resistivity zones are bounded above and below by higher resistive zones. In fact very high resistivities are encountered to the right of the section below 6.3m which probably indicates the proximity of the schist bedrock.

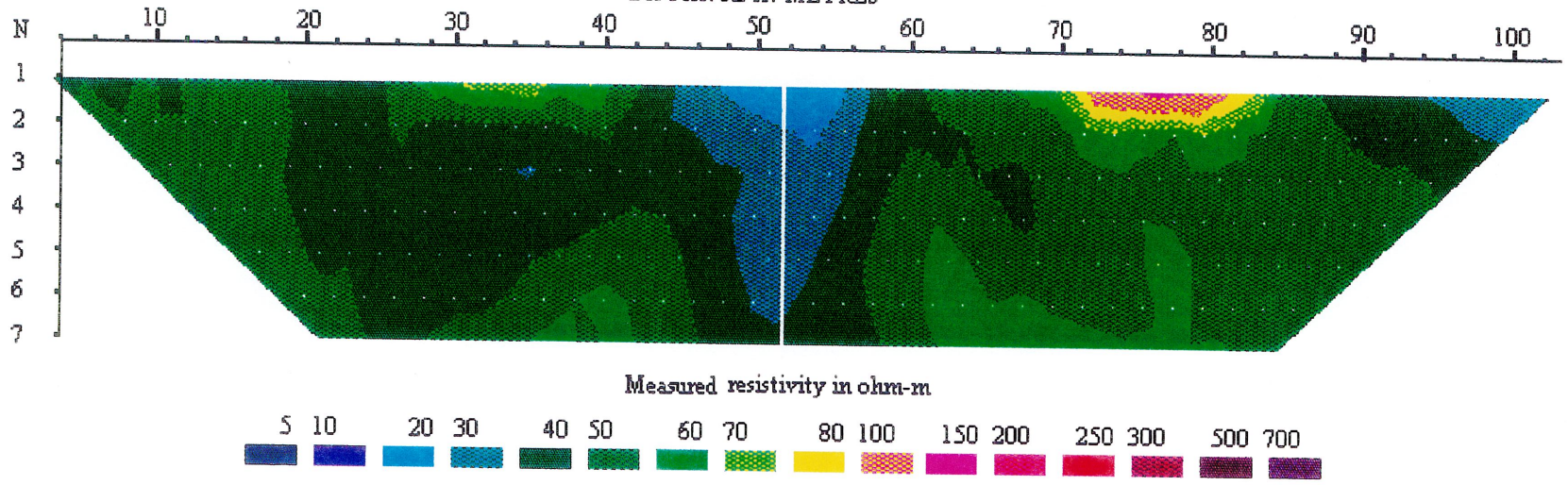
The evidence seems to indicate that leachate is indeed leaking from the tip and forming a wedge shaped zone of groundwater contamination within the sands and gravels, below the surface alluvium. This wedge becomes thinner further away from the tip. The low resistivities seen in these sections are not as low as the resistivity measured within the waste tip by VES S4 indicating that the volume of leachate within the pores of the sediment is less than that in the waste material or that the leachate is somewhat diluted.

FIGURE NO. 6.18

LANDFILL SITE

DISTANCE IN METRES

PSEUDOSECTION 2



PSEUDOSECTION 3

(adjacent to the river)

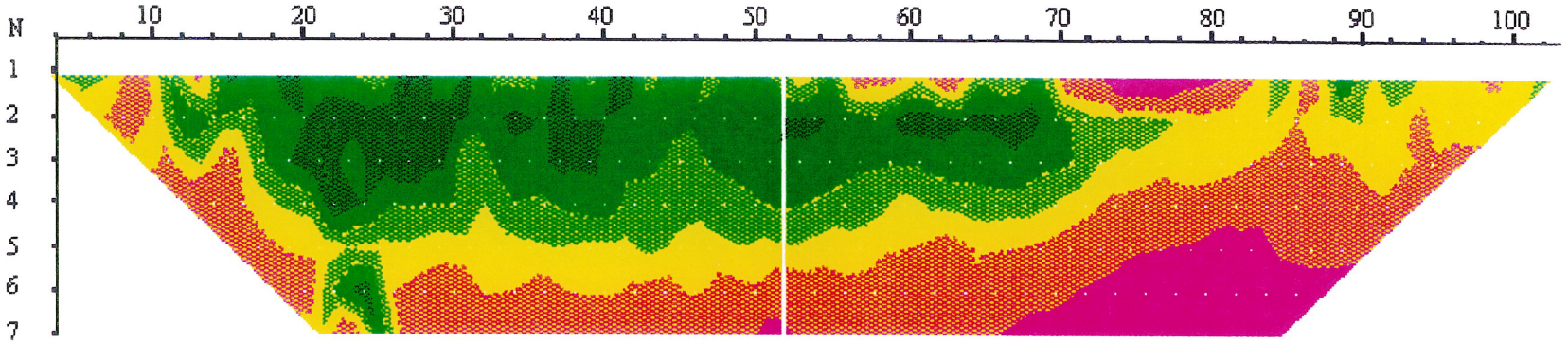
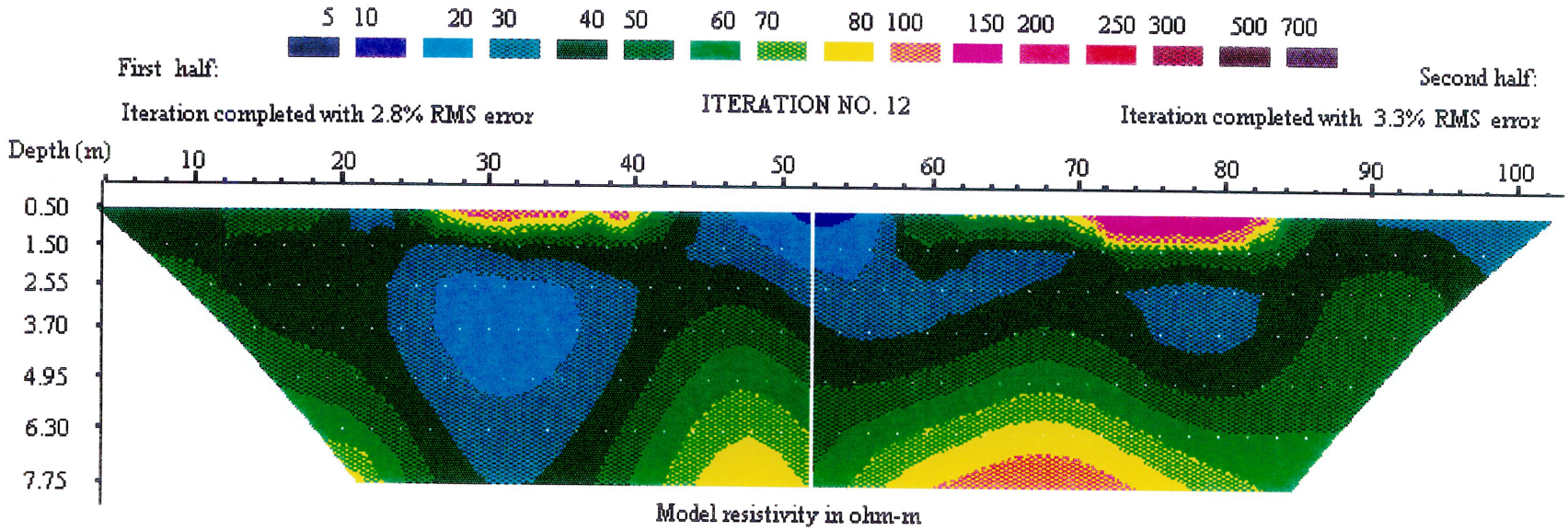
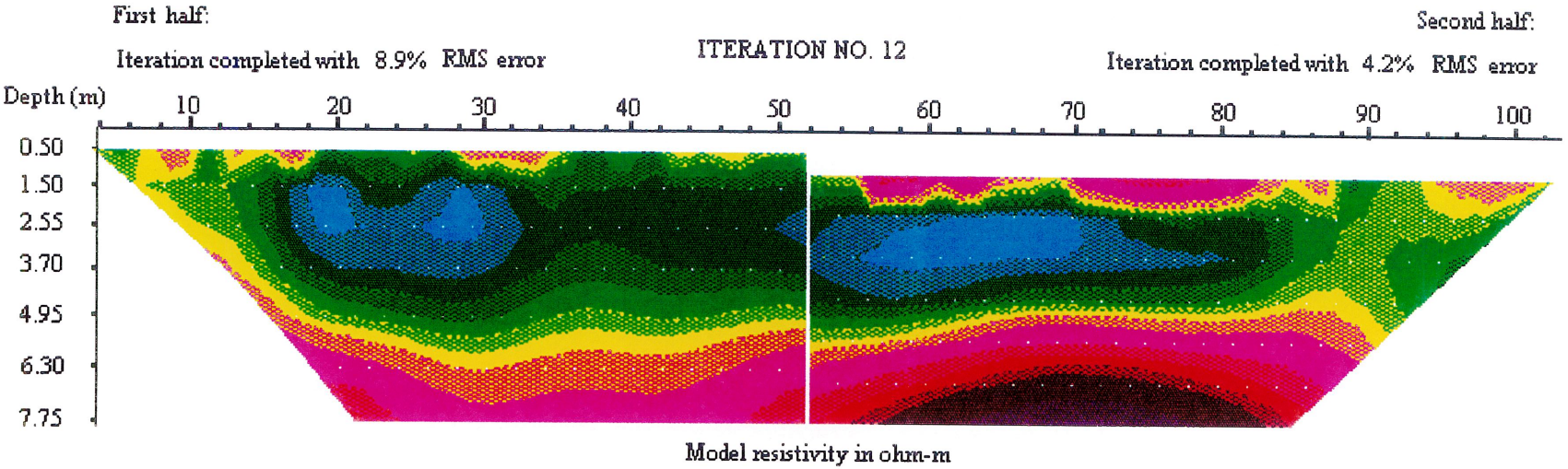


FIGURE NO. 6.19



LANDFILL SITE: PSEUDOSECTION 2 (adjacent to the tip) ON 25/7/95



LANDFILL SITE: PSEUDOSECTION 3 (adjacent to the river)

7- DISCUSSION

The results from both of the sites investigated will first be considered separately before a general comparison is attempted.

7-1 College Farm, Aber

7-1-1 Comparison of VES Array Configurations

The fact that each of the VES arrays employed furnished significantly different sounding curves and ground models was not too suprising considering that the arrays were measuring the properties of different volumes of the ground and that considerable lateral variation in resistivity had been detected in the pseudosection measurements. Even if the ground had been homogeneous with horizontal layering, resulting in identical sounding curves for the different VES arrays, the inverted ground models would still be slightly different due to the difference in linear filter coefficients used for Wenner and Schlumberger interpretation in the Resix Plus resistivity programme (Bennell, pers. com.).

The greatest problem with the interpretation of sounding curves from this site is the ambiguity caused by "equivalence" and " suppresion" effects. This together with the uncertainty in choosing the number of layers that should be used in the final earth models makes it very difficult to be certain about the interpretations. To some extent these problems can be assessed by how well the layer parameters are resolved. The earth models can also be related to the adjacent borehole logs. The extreme lateral variability, however, still makes VES interpretation problematic.

Section 6-1-1-1illustrates some of these problems. Three different layered models have been used to represent the sounding data. Even though the most complicated (the one with 6 layers) has the least RMS fitting error it is the most ambigous in terms of the different arrays used. It is therefore difficult to justify the use of a six layer interpretation unless there is more geological and hydrogeological control information available. Soomro (1993) constrained his models on the basis of the geological borehole logs, the conductivity of the

borehole fluids and the geology shown in nearby civil engineering excavations. Without this knowledge, however, a simple three layer model should be used to represent the sounding data with least ambiguity. This will be discussed further in section 7-1-2.

Both Schlumberger and Offset Wenner array techniques can detect problems in electrical soundings due to lateral variations in resistivity and are thus preferable to the ordinary Wenner array wich will tend to average out any lateral changes. The Wenner array also requires more effort to carry out a survey in that all the electrodes need to be moved for each measurement. The only real adventage it has is its conceptual simplicity. The Offset Wenner technique has the advantage that any sounding error and the lateral resistivity variations can be readily assessed. The use of the Barker Cable and switch box also makes the collection of sounding data less time consuming and labour intensive (the electrodes only have to be laid out once per sounding).

The Schlumberger technique is a good compromise between the Offset Wenner and normal Wenner techniques. Its main disadventage is that potential measurements are not well resolved when the potential electrode spacing, MN, is small. In addition when there is considerable lateral resistivity variation each of the data segments, relating to the different MN values, will show large offsets. A certain amount of skill and experience is required in order to correct the data to get a continuous sounding curve. This of course is generally true of all resistivity investigations!

On balance, therefore, it would seem that the Offset Wenner array would be the best technique to use for VES surveys providing that the special cables and switch boxes were available.

7-1-2 Comparison of Geoelectric Section and Pseudosection Ps1

For the section through the boreholes towards the coast it is possible to compare Soomro's geoelectric section (fig. 6.6b) and the geoelectric section presented here (fig. 6.6a) with pseudosection Ps1 (fig. 6.9). The VES data give a fairly accurate depth model at a few locations to give the geoelectric profile. On the other hand pseudosections provide higher horizontal resolution, with measurements every 2 metres, but is limited in its vertical extent.

In addition even though the pseudosection data has been inverted to provide a true resistivity depth section the absolute depths are not clear cut as the resistivity changes are shown as being continuous with depth rather than as discrete layers. Nevertheless both data sets can be considered complementary in the overall interpretation of the pattern of resistivity variation over the site.

The geoelectric section in figs. 6.6a and b are in reasonable agreement bearing in mind that 6.6a only contains data from 3 VES's. The main difference in interpretation of the VES data is that a simpler 3 or 4 layer model has been used in this interpretation. Soomro (1993) uses 5 or 6 layers dividing both the upper and lower aquifers into freshwater and saline water zones. The evidence for this, however, seems very tenuous. Fig. 6.6a therefore represents a simpler alternative. On reflection the section could be adjusted to reflect equivalence problems, i.e. for VES S1 layer 2 resistivity could be reduced to 300 ohm-m for a layer thickness of about 16 to 18m. Similarly for S3 layer 3 could have a higher resistivity of 400 ohm-m for a reduced thickness of 25m. Both geoelectric sections show evidence of a highly resistive surface layer in some locations.

Pseudosection Ps1 shows the extent of these surface variations with much greater resolution. The depth of penetration is limited to about 6m which covers the upper aquifer. The true resistivity section illustrates the presence of several of the zones shown in the upper levels of the geoelectric sections. Firstly the lower resistivity areas, perhaps representing alluvium, which outcrops in the topographically lower areas of the site is shown to extend seawards beneath a thin, highly resistive, dry gravelly layer which is topographically elevated. Because of the extreme contrast in resistivity the dry gravelly layer is probably shown as a thicker layer than it actually is. Away from the coast the resistivity values increase from 30 ohm-m to 500 ohm-m which probably corresponds to a change to gravelly material saturated with freshwater. Below the borehole position resistivities increase to 300 to 400 ohm-m where these gravels again occur, at a depth of about 5m. This is about the depth in borehole BH10/2 that corresponds to the position where sandy silt and gravels grade into boulders and gravels. Either side of this zone there are lower resistivity, 60 to 140 ohm-m areas which might be more saline zones.

The pseudosection data provides a shallow highly resolved resistivity image across the site

which serves to illustrate the large lateral resistivity variations that exist. The time involved in carrying out measurements to provide a pseudosection is considered well worthwhile in the context of the high quality extra information that can be obtained when compared to VES data. To obtain an image at even greater depths would require a cable with large electrode separations. This would reduce the horizontal resolution and also increase the logistic problems associated with the deployment of longer and heavier cables. The MRT system described by Griffiths and Turnbull (1985) and Griffiths et al (1990) should be an ideal system for providing deeper penetration and allowing direct computer data acquisition and interpretation.

7-1-3 Spatial Variation in Resistivity Across the Site

The variation of resistivity across the site is best considered by comparing the pseudosection data in figs. 6.9 and 6.10 with the rectangle of apparent resistivity in fig. 6.15. Both data sets show considerable lateral variation in the measured apparent resistivity . The small rectangle that was surveyed using the Schlumberger technique had good spacial resolution but required considerable effort to organise the electrode movements between measurements. Thus to cover an appreciable area of the field would have taken many man hours. The apparent resistivities illustrated in the rectangle effectively represent an average resistivity down to a depth equal to half the AB spacing. Thus the displayed lateral apparent resistivity variation is a combination of "shallow", "medium" and "deep" fluctuations in true resistivity. Unfortunately with this technique it is very difficult to separate out "deep" and shallow" effects in a quantitative manner.

The pseudosection data had excellent horizontal resolution in one direction. In the other horizontal direction only three profiles had been carried out. The depth of penetration was limited to between 6 and 8m but it was possible to provide a true resistivity depth section for this shallow region. Although the pseudosections take some time to perform, about 2 hours each, once the electrodes are positioned and connected to the cable only one person is required to acquire the data. Areal surveys are acomplished by carrying out adjacent pseudosections, and although time consuming they can provide a great insight into the variation of near surface resistivity.

At the College Farm site 3 pseudosections were carried out aligned almost perpendicular to the coast. By comparing and correllating the features of each of these sections it is possible to achieve a greater understanding of the electrical properties of the site in general.

1- High surficial resistivity values occur at both ends of the pseudosections as well as in the middle of Ps1. These can be correlated to the higher or slightly elevated parts of the site in which dry, sandy, gravelly materials are present above the water table.

2- The lowest resistivity values occur in the depressions on the site and correlate with the presence of the alluvium. These depressions are often flooded, especially in winter, and the remnants of these ponds were observed during the dry summer when the study was made. The depression close to the boreholes had a direct connection to the sea via a land drain. At periods of very high spring tides this depression is flooded with saline water.

3- In the area of the field away from the coast the resistivity contours appear to be almost vertical with resistivity increasing away from the coast. This could represent a coarsening of the sediments from alluviual silts to sands and gravels coupled with the groundwater becoming less conductive and hence less contaminated with sea water.

4- Resistivity values generally tend to increase with depth, apart from the thin surficial dry layer present in the elevated parts of the site. This corresponds to the boundary between the holocene and pleistocene sediments which occurs at a depth of about five metres near the boreholes.

The pseudosection data is thus less ambiguous than the Schlumberger AB rectangle data. The depth of pentration could be improved by using larger electrode spacings in the pseudosection cable and the spatial resolution improved by surveying extra intermediate position sections.

7-1-4 Temporal Variation in Groundwater Conductivity

Changes in groundwater conductivity should be related to the saline intrusion of seawater and its daily variability due to tidal pumping effects. The extent of the intrusion will also be

affected by the supply of freshwater in the form of rainfall percolating down through the ground surface and flowing down from the adjacent Carneddau Mountains which will induce some variability over longer time scales.

To examine any variability over short time scales related to tidal effects, repeated VES and pseudosection surveys were carried out at the same place over a short period of time; about 4 hours, up to and over the high spring tide on 31/7/95. The interpretation of the pseudosection data showed that there was very little resistivity variation in the upper six metres of the profile (Ps3 & Ps4) due to the tidal effect. The VES surveys penetrated to greater depths and showed some variability with time. It is not clear, however, if this variability was induced by the tidal action or was a result of random errors caused by repeating the surveys. The fact that the variability was not systematic and that identical electrode positions would not have been used for each VES survey indicates that the latter explanation is most likely.

It is suggested that to observe the variation in groundwater conductivity due to the effect of the tide, measurements should be made much closer to the sea. Great care should also be taken to minimise the electrode positional errors possible in VES surveys, perhaps by installing a permanent array of electrodes in which the spacings can be guaranteed to remain constant over several surveys.

None of the data collected on the site was suitable to infer anything about longer term groundwater conductivity variability, due to variations in freshwater supply. Again permanent arrays would have to be installed to ensure that repeated surveys were carried out in exactly the same position and with the same electrode separations.

7-2 Landfill Site

7-2-1 Comparison of the VES and Pseudosection Surveys

The vertical electrical sounding, VES, data generally give a good representation of the variation of resistivity with depth at a few isolated positions. The pseudosection data gives a highly resolved, horizontal image of the variation in resistivity that is limited in its vertical

extent. The two techniques can therefore be seen as complementary when trying to interpret the variation of groundwater conductivity across the landfill site. On this site it was difficult to produce a geoelectric section from the VES models since each of the soundings were carried out in significantly differing environments which are difficult to correlate. The data from the psudosections, however, gives a good indication of the horizontal resistivity variation in relation to the waste tip.

Sounding S1, carried out to the southwest of area 2 well away from any of the pseudosections, gave a 2 layer model with a very low surface resistivity overlying a slightly higher resistivity substratum at depth of 3m. This area is generally very wet and has been found to be quite markely contaminated with leachate. This has been attributed to the emergence of leachate at the toe of the tip where the underlying alluvial clay acts as an aquiclude.

Sounding S2 was carried out in the middle of pseudosection Ps1. The curve was poorly defined mainly because the expanding electrode spread straddled the boundary between tipped and untipped areas. The interpretation of the amended sounding curve data provided a model that was in general agreement with the pseudosection interpretation. In this case the low resistivity upper layer 38 ohm-m with thickness 11m correlates with the true resistivity section values of 10 to 50 ohm-m to depths in excess of 9.3m. Pseudosections Ps1 and Ps2 have been able to detect a leachate plume which reaches to the ground surface. This was observed to correspond with a surficial stain of leachate material which had originated from halfway up the steep face of the tip.

Sounding S3 was located in the untipped northwest area of the site, at the extreme northern end of Ps1. The model of a low surface resistivity layer overlying a higher resistivity substratum at a depth of 3m agrees very well with the pseudosection-true resistivity section at this location. The upper layer corresponds to the alluvial clay, whilst the lower material is the sand and gravel freshwater aquifer. The pseudosection shows that this lower sand gravel layer becomes contaminated with leachate when the section is adjacent to the toe of the waste tip.

Finally sounding S4 carried out on the top of the tip showed that the leachate was more

highly conductive than the uncontaminated groundwater having a resistivity of less than 10 ohm-m. The thickness of this layer of about 10m indicates that the leachate has penetrated the alluvial clay and contaminated the underlying sand and gravel as had already been confirmed by borehole evidence (taken from a previous study of the site). This observation indicates that resistivity techniques should be capable of detecting and mapping plumes of leachate that might be leaking from the tip.

A comparison of pseudosections 2 and 3 indicates that there are plumes of leachate moving away from the tip westwards towards the river. The size of the plume has, however, been greatly reduced as the river is approached and seems to be confined to the sand-gravel, alluvium boundary. The resistivity of the plumes in Ps3 adjacent to the river (10 to 30ohm-m) are only slightly lower than the resistivity of the alluvium in Ps1 (30 to 50ohm-m) but are comparable to the contaminated zone of Ps1 (10-30ohm-m). This indicates that the contamination although more confined is probably of the same concentration at a distance of about 20m from the toe of the tip compared to the section adjacent to the tip.

The results of this pilot investigation are extremly encouraging. Although there was insufficient time to carry out further survys to monitor temporal groundwater conductivity changes the pseudosection technique should be ideally suited for a regular monitoring scheme especially if a permanent electrode array could be installed. This would make repeated surveys, carried out at regular intervals, relatively easy especially if the computor acquisition software was available.

7-3 Comparison of the Results from Both Sites

The results from both sites indicate that electrical techniques in general and VES and pseudosection techniques in particular are useful means of locating and mapping groundwater contamination. The presence of impurities, salts and leachate, serve to increase the conductivity of the natural groundwater. The electrical techniques are very good at detecting zones of highly contrasting resistivity. The main problem is in deciphering whether the resistivity contrasts are due to lithological or hydrochemical changes in the hydrogeological model. If the results are seen to fluctuate with time then it is possible to delineate the contaminated zones of groundwater from a saline intrusion or a plume of

leachate without consulting the geological log from a nearby borehole. Of course geological control for any resistivity survey is highly desirable in that the final interpretation will be less ambiguous.

Temporal fluctuations in groundwater properties were not really observed in either site survey. Consequently most of the interpretations have relied on the prior knowledge of the site geology from borehole information. This was by no means complete, the boreholes being widely spaced and relatively shallow. The results from both surveys indicate that both the geological and hydrochemical properties of the groundwater vary widely across both sites.

8- CONCLUSIONS

This study was designed to investigate the feasibility of different electrical resistivity techniques to define areas of contamination in groundwater. To achieve this spatial and temporal, surface electrical resistivity surveys were conducted at two different, contrasting sites. The first site was a coastal aquifer at College Farm, Aber in which the groundwater contamination was caused by a saline intrusion. The second site was a landfill area in which the contamination of the groundwater was suspected to be from leachate leaking from the waste tip.

The main conclusions from the investigations can be summarised as follows:

1- A comparison of VES arrays indicated that the Offset Wenner system would be the easiest to use. It also provides the most reliable data in terms of error assessement. If the special equipment required to perform this survey was not available, however, then the Schlumberger array technique provided the best alternative.

2- The pseudosection technique was shown to have good horizontal resolution, but limited in its vertical extent, and was prefered to the Schlumberger AB rectangle method for showing lateral changes in resistivity.

3- Temporal changes in groundwater resistivity were not conclusivly observed on either site even though carefully controlled experiments were undertaken at College Farm. To determine these hydrogeological changes with time the following suggestions are made:

a) to detect the change in saline intrusion with tidal pumping the surveys need to be conducted closer to the coast over an extremely high spring tide cycle.

b) permanent electrode arrays should be installed so as to avoid moving electrodes between surveys, and

c) surveys should be carried out regularly over longer periods of time to correlate changes with rainfall and waste disposal rates.

4- The College Farm site at Aber was shown to have a complicated geological and a hydrogeological structure which was difficult to interpret. The main problems were the lateral variations in apparent resistivity. In many instances these could equally well be explained by changes in the lithology as well as changes in the groundwater hydrochemistry. In the top 5 or 6 metres the areas of highest resistivity were correlated to the slightly elevated parts of the site which had a surficial layer of dry sand and gravel. The lowest resistivities corresponded to the lower areas of the site in which alluvial silts were present. These silts were presumed to underlie the dry surface gravels. Finally the areas of intermediate resistivity were assumed to be saturated gravels and Till of Pleistocene age.

The VES data showed a further low resistivity layer at depth which Soomro (1993) called the lower aquifer. This showed a gradual decrease in resistivity towards the coast which probably points to increased saline contamination of the groundwater. The saline intrusion into Soomro's upper aquifer was not so clear cut. It was tentatively suggested, however, that there was a direct hydraulic connection of the low resistivity layer to the sea and that the landward extent of this layer was marked by the 50ohm-m contour of fig. 6.12. The actual geological situation is likely to be much more complicated than this as shown in the borehole logs of fig. 3.2. It is suggested that seismic measurements could perhaps help resolve some of this ambiguity in relation to the lithology.

5- The landfill site demonstrated that resistivity techniques could identify areas contaminated by leachate. The pseudosection technique was particularly succesful in delineating the horizontal extent of the leachate contamination. A general lack of suitable terrain for carrying out electrical surveys hampered a more complete investigation of the site. The results were encouraging, however, in that leachate plumes were identified and shown to extend at least 20 m away from the waste tip. It would be interesting to install a permanent electrode array in order to correlate the movement, if any, of these plumes with changes in rainfall and waste disposal.

The experience gained from both these site investigations will be invaluable for solving water resources problems back home in Bahrain using surface resistivity techniques.

Although the depths of investigation in Bahrain are somwhat greater than achieved here there are numerous deep boreholes to provide greater borehole control. VES techniques could be used to determine the fresh-salt water interface. The pseudosection technique, with larger electrode separations than used here, would be useful for monitoring the movement of the saline front in conjuction with water abstraction from adjacent wells. This would form part of the overall monitoring programme which already involves regular sampling and downhole resistivity measurement in the existing network of boreholes.

APPENDICES

Appendix 4.1

Appendix 4.2

Appendix 4.3

Appendix 5

Appendix 6.1

Appendix 6.2

Appendix 6.3

Appendix 6.4

Appendix 6.5

Appendix 4.1

This appendix contains the following tables:

1- Table A4T1: Field work carried out in the College Farm, Aber and the Landfill site.

2- Table A4T2: The resistance increment of the SAS 300, single reading.

3- Table A4T3: Detailed information for buiding up a pseudosection survey.

4- Table A4T4: Example file of a collected data set of pseudosection survey.

5- Table A4T5: Measured fluid resistivity data and the converted TDS values.

6- Table A4T6: Offset Wenner measured and calculated data.

7- Table A4T8: Data collected from levelling surveys at College Farm, Aber.

8- Figure A4F10: A map showing the location of boreholes and resistivity surveys.

9- Figure A4F14: Locations of points and stations used for positioning and levelling surveys.

Table A4T1

Field work carried out in College Farm, Aber and the Landfill site

DATE	LOCATION	TYPE OF WORK	PURPOSE OF WORK
22-6-95	College Farm, Aber	Schlumberger sounding 1 (S1)	To construct a Geoelectric section perpendicular to the coast.
		Schlumberger sounding 2 (S2)	
		Schlumberger sounding 3 (S3)	
		Schlumberger AB profile	To compare with pseudosection techniques
11-7-95	College Farm, Aber	Pseudosection (Ps1)	To delineate the fresh-salt water interface so to compare with the geoelectric section results
12-7-95	College Farm, Aber	Schlumberger sounding 4 (S4)	Used for making a comparison between them.
		Wenner sounding 1	
		Offset Wenner Sounding	
		Pseudosection (Ps2)	Made at distance from pseudosection 1 to study the spatial variation in groundwater.
		Borehole resistivity logging	Data may help the interpretation of the surface resistivity methods
17-7-95	Landfill site	Schlumberger 1 (LS1)	To determine earth layer models along two sides of the tip.
		Schlumberger 2 (LS2)	
		Pseudosection 1	Carried out along fairly straight line adjacent to the tip to map leachate
25-7-95	Landfill site	Schlumberger sounding 3 (LS3)	LS3 carried out on the same position of Pseudosection 1 and LS4 on the top of the tip to explore depths to different layers.
		Schlumberger sounding 4 (LS4)	

		Wenner sounding 1 (W1)	Made on the same position as LS3 and LS4 respectively to compare the two techniques
		Wenner sounding 2 (W2)	
		Pseudosection 2	Made, nearly, along the same line of pseudosection 1 but with better alignment.
		Pseudosection 3	Carried out near the river so to construct a spatial resistivity image along with pseudosection 1 & 2
31-7-95	College Farm, Aber	Schlumberger sounding 5 (S5)	To monitor tidal effect on the advancement of the saline interface.
		Schlumberger sounding 6 (S6)	
		Schlumberger sounding 7 (S7)	
		Pseudosection (Ps3)	Used for the same purpose as above so to compare with the sounding techniques
		Pseudosection (Ps4)	
		Borehole resistivity logging	To compare with the results from S5, S6&S7
8-8-95	College Farm, Aber	Positioning and Level surveying	To plot the position of all resistivity surveys

Table A4T2

The resistance increments of the SAS 300, single reading.

Current in mA	Range setting			
	1Ω	100Ω	10 kiloΩ	1 mega Ω
0.2	25 mΩ	25 mΩ	200 mΩ	25Ω
0.5	10 mΩ	10 mΩ	100 mΩ	10Ω
1	5 mΩ	5 mΩ	50 mΩ	5Ω
2	2.5 mΩ	2.5 mΩ	250 mΩ	205Ω
5	1 mΩ	1 mΩ	100 mΩ	1Ω
10	500 μΩ	500 μΩ	50 mΩ	500 mΩ
20	250 μΩ	2.5 mΩ	250 mΩ	250 mΩ
50	100 μΩ	1 mΩ	100 mΩ	100 mΩ
100	50 μΩ	500 μΩ	50 mΩ	50 mΩ
200	25 μΩ	2.5 mΩ	25 mΩ	25 mΩ
500	10 μΩ	1 mΩ	10 mΩ	10 mΩ

Table A4T3

Details of buiding up of a pseudosection survey.

Level number (n)	Distance, metres, between adjacent electrodes (x)	Depth, metres (x/2)	Number of measurements	
1	a	a/2	51	
2	2a	a	48	
3	3a	3a/2	45	
4	4a	2a	42	
5	5a	5a/2	39	
6	6a	3a	36	
7	7a	7a/2	33	
8	8a	4a	30	Total 324 points

a = spacing of initial electrodes separation = 2 metres.

Table A4T4

An example of data set recovered from a pseudosection survey along with the calculated apparent resistivity values.

Surveying with 2m spacing				Surveying with 4m spacing				Surveying with 6m spacing				Surveying with 8m spacing			
Distance from starting position, m	Z (m)	Measured Resistance Ω	Apparent Resistivity Ω-m	Distance from starting position, m	Z (m)	Measured Resistance Ω	Apparent Resistivity Ω-m	Distance from starting position, m	Z (m)	Measured Resistance Ω	Apparent Resistivity Ω-m	Distance from starting position, m	Z (m)	Measured Resistance Ω	Apparent Resistivity Ω-m
3	-1	20.3	255.097	6	-2	10.32	259.36	9	-3	7.23	272.56	12	-4	4.89	245.79
5	-1	17.41	218.78	8	-2	11.22	281.98	11	-3	6.71	252.96	14	-4	4.32	217.14
7	-1	20.6	258.867	10	-2	10.37	260.62	13	-3	5.9	222.42	16	-4	4.32	217.14
9	-1	20.6	258.867	12	-2	8.61	216.39	15	-3	5.6	211.11	18	-4	4.13	207.59
11	-1	17.63	221.545	14	-2	8.46	212.62	17	-3	5.54	208.85	20	-4	3.85	193.52
13	-1	18.12	227.702	16	-2	8.51	213.87	19	-3	5.66	213.37	22	-4	3.76	188.99
15	-1	17.57	220.791	18	-2	7.56	190	21	-3	5.11	192.64	24	-4	3.6	180.95
17	-1	18.65	234.362	20	-2	8.27	207.84	23	-3	4.56	171.9	26	-4	3.47	174.42
19	-1	16.69	209.732	22	-2	8.06	202.56	25	-3	3.97	149.66	28	-4	3.4	170.9
21	-1	19.58	246.049	24	-2	7.15	179.69	27	-3	4	150.79	30	-4	3.21	161.35
23	-1	16.16	203.072	26	-2	6.01	151.04	29	-3	4.2	158.33	32	-4	2.92	146.77
25	-1	16.37	205.711	28	-2	6.27	157.58	31	-3	4.21	158.71	34	-4	2.69	135.21
27	-1	14.17	178.065	30	-2	6.3	158.33	33	-3	3.54	133.45	36	-4	2.28	114.6
29	-1	12.37	155.446	32	-2	5.16	129.68	35	-3	2.6	98.017	38	-4	2.18	109.57
31	-1	9.7	121.893	34	-2	3.52	88.467	37	-3	2.38	89.723	40	-4	2.27	114.1
33	-1	6.14	77.157	36	-2	2.76	69.366	39	-3	2.61	98.394	42	-4	2.3	115.61
35	-1	3.79	47.626	38	-2	2.64	66.35	41	-3	2.69	101.41	44	-4	2.26	113.59
37	-1	2.91	36.568	40	-2	2.77	69.617	43	-3	2.42	91.231	46	-4	2.14	107.56
39	-1	3.02	37.95	42	-2	2.76	69.366	45	-3	2.15	81.053	48	-4	1.811	91.03
41	-1	2.92	36.693	44	-2	2.25	56.548	47	-3	1.939	73.098	50	-4	1.69	84.948
43	-1	3.04	38.201	46	-2	1.889	47.475	49	-3	1.891	71.289	52	-4	1.616	81.229
45	-1	2.33	29.279	48	-2	2.18	54.789	51	-3	1.801	67.896	54	-4	1.53	76.906

47	-1	2.18	27.394	50	-2	2.07	52.024	53	-3	1.581	59.602	56	-4	1.545	77.66
49	-1	2.45	30.787	52	-2	1.678	42.172	55	-3	1.596	60.167	58	-4	1.715	86.205
51	-1	1.916	24.077	54	-2	1.681	42.248	57	-3	1.655	62.392	60	-4	1.682	84.546
53	-1	2.09	26.263	56	-2	1.974	49.612	59	-3	1.861	70.158	62	-4	1.583	79.57
55	-1	2.51	31.541	58	-2	1.986	49.913	61	-3	2.03	76.529	64	-4	1.652	83.038
57	-1	3.6	45.238	60	-2	2.26	56.799	63	-3	1.782	67.179	66	-4	1.489	74.845
59	-1	3.76	47.249	62	-2	2.4	60.318	65	-3	1.677	63.221	68	-4	1.916	96.308
61	-1	4.85	60.946	64	-2	2.54	63.837	67	-3	1.571	59.225	70	-4	2.22	111.58
63	-1	4.39	55.166	66	-2	2.38	59.815	69	-3	2.16	81.43	72	-4	2.1	105.55
65	-1	3.88	48.757	68	-2	2.15	54.035	71	-3	2.56	96.509	74	-4	2.16	108.57
67	-1	4.63	58.182	70	-2	2.89	72.633	73	-3	2.82	106.31	76	-4	1.657	83.289
69	-1	2.93	36.819	72	-2	3.5	87.964	75	-3	2.25	84.823	78	-4	1.349	67.808
71	-1	4.63	58.182	74	-2	2.77	69.617	77	-3	1.744	65.747	80	-4	1.451	72.935
73	-1	3.88	48.757	76	-2	2.19	55.04	79	-3	1.654	62.354	82	-4	1.78	89.472
75	-1	3	37.699	78	-2	2.33	58.559	81	-3	1.928	72.683	84	-4	2.3	115.61
77	-1	2.9	36.442	80	-2	2.38	59.815	83	-3	2.55	96.132	86	-4	2.83	142.25
79	-1	2.32	29.153	82	-2	2.78	69.869	85	-3	3.14	118.37	88	-4	3.05	153.3
81	-1	3.2	40.212	84	-2	3.67	92.237	87	-3	3.31	124.78	90	-4	2.9	145.76
83	-1	4.65	58.433	86	-2	4.01	100.78	89	-3	3.08	116.11	92	-4	2.85	143.25
85	-1	8.61	108.196	88	-2	4.45	111.84	91	-3	2.88	108.57	94	-4	2.43	122.14
87	-1	13.24	166.378	90	-2	3.68	92.488	93	-3	2.86	107.81				
89	-1	15.16	190.506	92	-2	3.33	83.692	95	-3	2.68	101.03				
91	-1	15.57	195.658	94	-2	3.74	93.996	97	-3	2.57	96.886				
93	-1	10.71	134.585	96	-2	3.83	96.258								
95	-1	8.31	104.426	98	-2	2.28	57.302								
97	-1	3.6	45.2389	100	-2	2.01	50.516								
99	-1	2.04	25.635												
101	-1	2.38	29.907												
103	-1	2.17	27.269												

Surveying with 10m spacing				Surveying with 12m spacing				Surveying with 14m spacing				Surveying with 16m spacing			
Distance from starting position, m	Z (m)	Measured Resistance Ω	Apparent Resistivity Ω-m	Distance from starting position, m	Z (m)	Measured Resistance Ω	Apparent Resistivity Ω-m	Distance from starting position, m	Z (m)	Measured Resistance Ω	Apparent Resistivity Ω-m	Distance from starting position, m	Z (m)	Measured Resistance Ω	Apparent Resistivity Ω-m
15	-5	3.32	208.6	18	-6	2.64	199.05	21	-7	2.23	196.16	24	-8	1.967	197.74
17	-5	3.17	199.17	20	-6	2.63	198.29	23	-7	2.21	194.4	26	-8	1.931	194.12
19	-5	3.16	198.54	22	-6	2.65	199.8	25	-7	2.33	204.95	28	-8	1.931	194.12
21	-5	3.05	191.63	24	-6	2.67	201.31	27	-7	2.29	201.43	30	-8	1.836	184.57
23	-5	3.16	198.54	26	-6	2.75	207.34	29	-7	2.16	190	32	-8	1.821	183.06
25	-5	3.28	206.08	28	-6	2.61	196.78	31	-7	2.07	182.08	34	-8	1.837	184.67
27	-5	3.06	192.26	30	-6	2.38	179.44	33	-7	1.979	174.08	36	-8	1.812	182.16
29	-5	3.06	192.26	32	-6	2.19	165.12	35	-7	1.943	170.91	38	-8	1.661	166.98
31	-5	2.57	161.47	34	-6	2.1	158.33	37	-7	1.862	163.79	40	-8	1.528	153.61
33	-5	2.43	152.68	36	-6	2	150.79	39	-7	1.683	148.04	42	-8	1.527	153.51
35	-5	2.19	137.6	38	-6	1.863	140.46	41	-7	1.61	141.62	44	-8	1.475	148.28
37	-5	2.04	128.17	40	-6	1.808	136.31	43	-7	1.665	146.46	46	-8	1.497	150.49
39	-5	2.04	128.17	42	-6	1.815	136.84	45	-7	1.672	147.07	48	-8	1.41	141.74
41	-5	2	125.66	44	-6	1.868	140.84	47	-7	1.595	140.3	50	-8	1.333	134
43	-5	2.02	126.92	46	-6	1.792	135.11	49	-7	1.525	134.14	52	-8	1.265	127.17
45	-5	2.08	130.69	48	-6	1.704	128.47	51	-7	1.399	123.06	54	-8	1.332	133.9
47	-5	1.927	121.07	50	-6	1.564	117.92	53	-7	1.407	123.76	56	-8	1.389	139.63
49	-5	1.659	104.23	52	-6	1.563	117.84	55	-7	1.43	125.78	58	-8	1.318	132.49
51	-5	1.608	101.03	54	-6	1.463	110.3	57	-7	1.344	118.22	60	-8	1.365	137.22
53	-5	1.549	97.326	56	-6	1.37	103.29	59	-7	1.353	119.01	62	-8	1.315	132.19
55	-5	1.478	92.865	58	-6	1.409	106.23	61	-7	1.435	126.22	64	-8	1.445	145.26
57	-5	1.508	94.75	60	-6	1.446	109.02	63	-7	1.434	126.14	66	-8	1.457	146.47
59	-5	1.536	96.509	62	-6	1.579	119.05	65	-7	1.647	144.87	68	-8	1.416	142.35

61	-5	1.515	95.19	64	-6	1.53	115.35	67	-7	1.602	140.91	70	-8	1.333	134
63	-5	1.585	99.588	66	-6	1.779	134.13	69	-7	1.539	135.37	72	-8	1.209	121.54
65	-5	1.589	99.839	68	-6	1.848	139.33	71	-7	1.437	126.4	74	-8	1.212	121.84
67	-5	1.871	117.55	70	-6	1.671	125.99	73	-7	1.331	117.08	76	-8	1.226	123.25
69	-5	1.985	124.72	72	-6	1.512	114	75	-7	1.203	105.82	78	-8	1.383	139.03
71	-5	1.874	117.74	74	-6	1.328	100.12	77	-7	1.267	111.45	80	-8	1.429	143.65
73	-5	1.647	103.48	76	-6	1.354	102.08	79	-7	1.31	115.23	82	-8	1.59	159.84
75	-5	1.539	96.698	78	-6	1.195	90.1	81	-7	1.443	126.93				
77	-5	1.308	82.184	80	-6	1.282	96.66	83	-7	1.736	152.7				
79	-5	1.282	80.55	82	-6	1.589	119.8	85	-7	1.938	170.47				
81	-5	1.441	90.54	84	-6	1.918	144.61								
83	-5	1.75	109.95	86	-6	2.22	167.38								
85	-5	2.22	139.48	88	-6	2.32	174.92								
87	-5	2.66	167.13												
89	-5	2.81	176.55												
91	-5	2.89	181.58												

Table A4T5

Measured fluid resistivity data and the converted TDS values.

Depth (m)	Measured Resistivity (ohm-m)	Corrected Resistivity (ohm)	Temperature °C	Resistivity at 25 °C	TDS (ppm)
Date of Survey 12-7-95					
1	37.2	37.57	9.7	25.69	249.14
2	56.5	57.07	9.7	39.02	164.04
3	51.4	51.91	9.7	35.49	180.31
4	45.1	45.55	9.8	31.24	204.87
5	48	48.48	9.6	33.04	193.68
6	53.3	53.83	9.5	36.58	174.96
7	51.1	51.61	9.5	35.07	182.49
Date of Survey 31-7-95 at 12.05 hours					
1	32.4	32.72			
2	53.2	53.73			
3	49.1	49.59			
4	47.7	48.18			
5	48.2	48.68			
6	53.1	53.63			
7	51.4	51.91			
Date of Survey 31-7-95 at 14.08 hours					
1	33.7	34.04			
2	54	54.54			
3	51.3	51.81			
4	44.4	44.84			
5	46.7	47.17			
6	51.5	52.02			
7	50.3	50.80			

Table A4T6

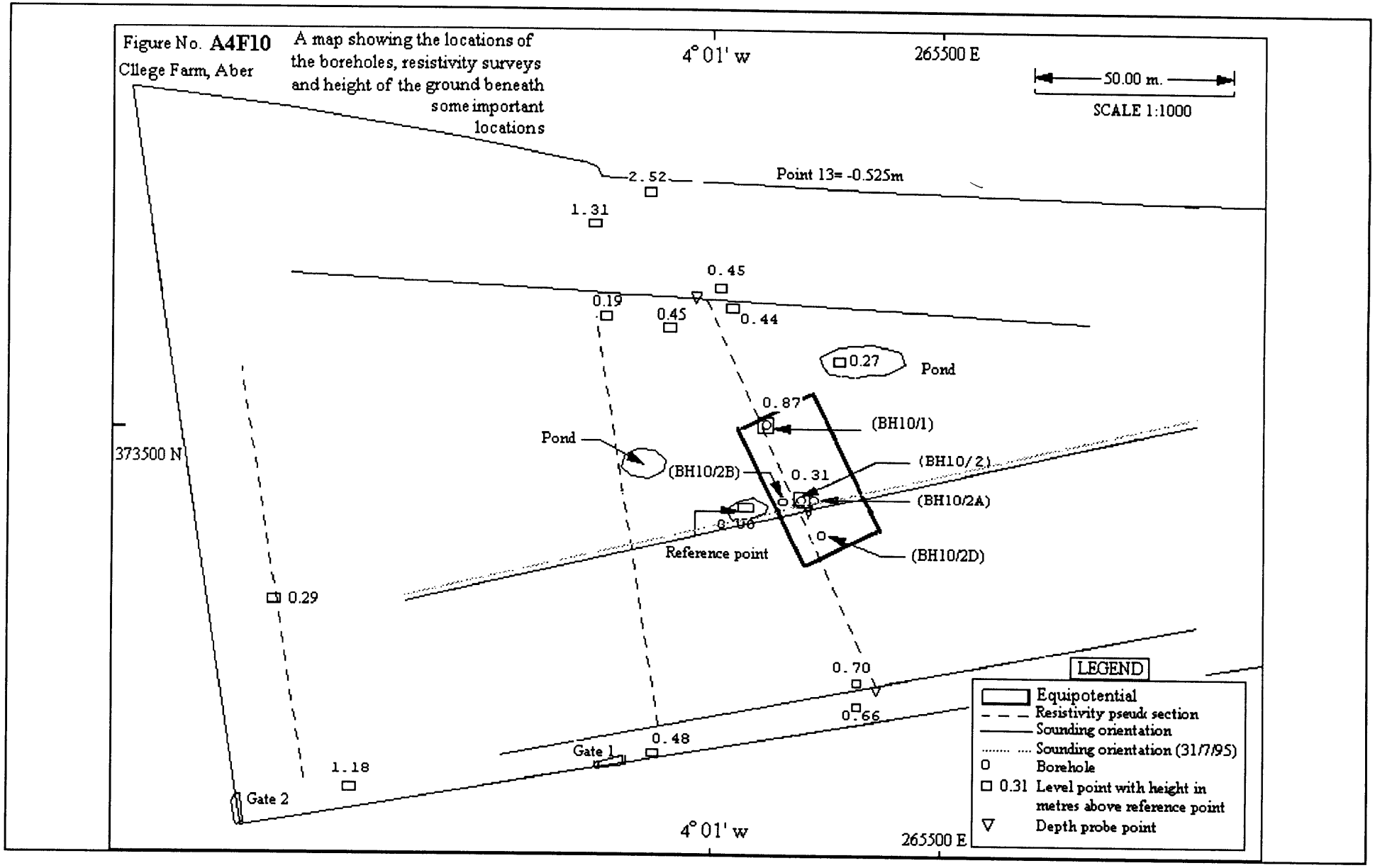
Measured and calculated Offset Wenner resistance data and the calculated apparent resistivity values.

RDG	SPC a	MF $2\pi a$	Configuration Resistances					Average R_W (Ω)	ρ_a (Ω-m)
			R_A (Ω)	R_C (Ω)	R_{D1} (Ω)	R_{D2} (Ω)	R_B (Ω)	$(R_{D1}+R_{D2})/2$	MF×R
1	0.5	3.14	20.4	19.4	16.8	12.6	-1.16	14.70	46.16
2	1	6.28	11.3	10.7	8.93	7.44	-0.683	8.19	51.40
3	2	12.57	5.07	6.44	4.99	4.27	-0.368	4.63	58.20
4	3	18.85						4.14	78.04
5	4	25.13	4.50	4.26	3.26	2.78	-0.225	3.02	75.89
6	6	37.70						2.77	104.35
7	8	50.27	3.21	3.08	2.42	2.03	-0.213	2.23	111.85
8	12	75.40						1.91	143.98
9	16	100.5	2.17	1.85	1.77	1.36	-0.136	1.56	157.33
10	24	150.8						1.04	156.83
11	32	201.1	0.897	0.902	0.873	0.628	-0.056	0.75	150.90
12	64	402.1						0.3	122.24

TABEL A4T8

RESULTS OF LEVEL SURVEYING
COLLEGE FARM, ABER

STATION	Hieght, m	Point no.	Reading, m	Level ref. to relavent station, m	Remarks	Hieght ref. to A	Level ref. to A	Reference point(1)	Level ref. to point 1
A	1.530	1	1.820	-0.290		1.530	-0.290	-0.290	-0.000
	1.530	2	1.510	0.020		1.530	0.020	-0.290	0.310
	1.530	3	0.950	0.580		1.530	0.580	-0.290	0.870
	1.530	4	1.380	0.150		1.530	0.150	-0.290	0.440
	1.530	5	1.160	0.370		1.530	0.370	-0.290	0.660
	1.530	6	1.340	0.190		1.530	0.190	-0.290	0.480
	1.530	7	1.630	-0.100		1.530	-0.100	-0.290	0.190
	1.530	8	0.510	1.020		1.530	1.020	-0.290	1.310
	1.530	9	0.640	0.890		1.530	0.890	-0.290	1.180
	1.530	10	1.530	0.000		1.530	0.000	-0.290	0.290
	1.530	11	1.120	0.410	Hieght of B ref. to A	1.530	0.410	-0.290	0.700
	1.530	12	1.370	0.160	0.16+1.75=1.91m(above A)	1.530	0.160	-0.290	0.450
B	1.235	12	2.985	-1.750		1.910	0.160	-0.290	0.450
	1.235	13	3.960	-2.725		1.910	-0.815	-0.290	-0.525
	1.235	14	0.915	0.320		1.910	2.230	-0.290	2.520
	1.235	15	3.160	-1.925	Hieght of C ref. to B	1.910	-0.015	-0.290	0.275
	1.235	16	2.985	-1.750	1.75-0.535=1.215m(below	1.910	0.160	-0.290	0.450
C	1.430	16	1.965	-0.535	Hieght of C ref. to A	0.695	0.160	-0.290	0.450
	1.430	17(ie 1)	2.380	-0.950	1.91-1.215=0.695m(above	0.695	-0.255	-0.290	0.035


Figure No. A4F10
Cllege Farm, Aber
A map showing the locations of the boreholes, resistivity surveys and height of the ground beneath some important locations
4° 01' w
265500 E
50.00 m.
SCALE 1:1000
2.52
Point 13= -0.525m
1.31
0.45
0.19
0.45
0.44
0.27
Pond
0.87
(BH10/1)
Pond
373500 N
(BH10/2B)
0.31
(BH10/2)
(BH10/2A)
0.16
Reference point
(BH10/2D)
0.29
0.70
0.66
0.48
Gate 1
1.18
Gate 2
4° 01' w
265500 E
LEGEND
Equipotential
Resistivity pseudo section
Sounding orientation
Sounding orientation (31/7/95)
Borehole
0.31 Level point with height in metres above reference point
Depth probe point

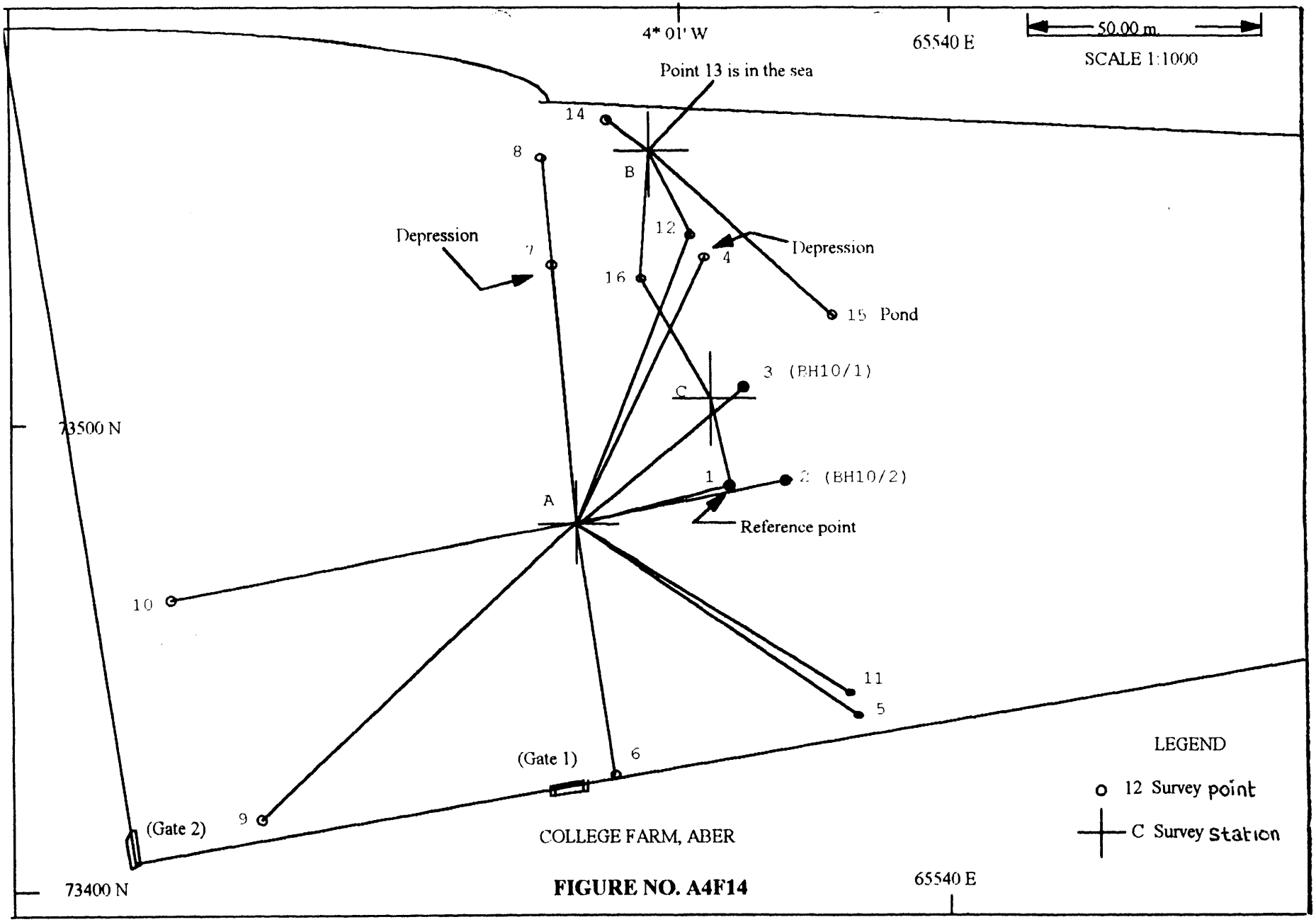


FIGURE NO. A4F14

The Campus Geopulse resistivity meter

The Automatic Processing of the Signal to Produce A Single Resistance Measurement

The transmitter uses mechanically reversed DC to produce the signal shown in fig. A4.2F1. An internal three position switch on the microprocessor board provides three sampling rates. These are given below:

Sampling rate no.	On (seconds)	Off (seconds)	On (seconds)	Off (seconds)	Repetition time (seconds)
1	0.75	0.3	0.75	0.3	2.1
2	1.5	0.6	1.5	0.6	2.4
3	3.0	1.2	3.0	1.2	4.8

The standard setting with which the instrument leaves the manufacturer laboratories is the first of these. The on period is sampled for only the last 4/5 of the on time e.g. 0.6s in 0.75s. An example of the received signal in the presence of electrical ground noise is shown in figure A4.2F1b. This figure also illustrates the processing technique used to extract a value of the required potential difference from the received signal, here shown superimposed on a slowly varying earth current.

The signal is digitally sampled over times A, B, and C and the amplitude calculated as (Va+Vc-2Vb)/4). The on/off ratio is 2.5:1 and the sample/ unsampled ratio during any period is 4:1. This is to allow any coupling and IP effects to die away before sampling takes place.

When a number of cycles are averaged the microprocessor calculates the potential difference from successive sets of three 'on' periods ABC, BCD, DEF giving values (Va+Vc-2Vb)/4, (Vb+Vd-2Vc)/4, etc.

When conditions are adverse, e.g. a low signal/ground noise ratio, apparent as a lack of consistency in the readings, the highest current setting must be used that does not cause a gain error in the instrument. In this instance the operator must average over 16 cycles. Gain errors are usually due to sudden increases in ground noise saturating the system. If the area

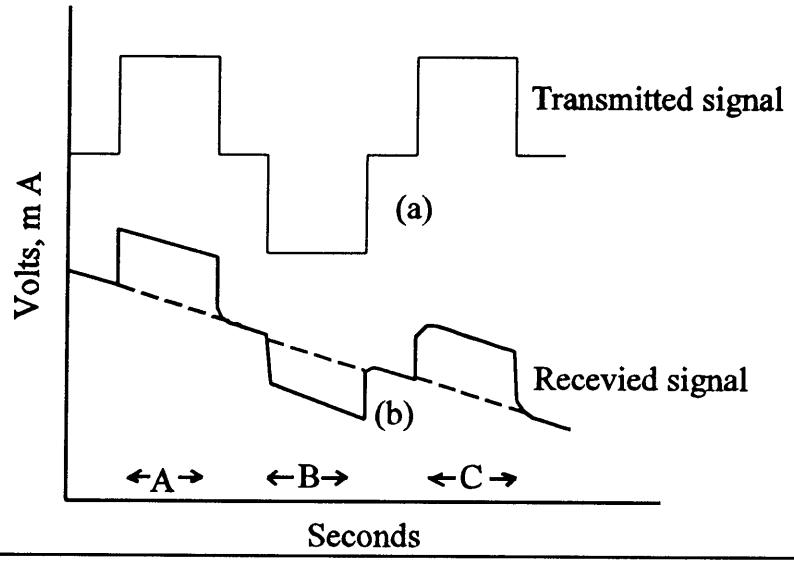
is generally very noisy it may be necessary to operate at the longest cycling time.

In extreme conditions, i.e. measuring very low resistances against a background of large amplitude and varying SP, highly inconsistent readings may be obtained. In this case it is necessary to put the instrument into the computer command mode and vary the sampling parameters until satisfactory results are obtaine

Figure A4.2F1

The Geopulse signal (From the instrument's manual, CGIL, 1992)

The attenuated and modified signal is superimposed on slowly varying earth currents. It is sampled over time A, B and C.



Procedures for conducting the fluid resistivity and temperature logging as per the ABEM instruction manual.

1- FLUID RESISTIVITY LOGGING :

Set the MODE selector to the FLUID position and press the MEASURE button on the SAS 300. Current (200 mA) is injected via the ring electrode (E), while the potential is measured between the upper probe electrode (D) and the centre electrode (F). The SAS LOG 200 needs no conversion factor here.

$\rho_{fluid} = R_{display}$ (ohn-m)

The following corrections should be made for small-diameter wells:

Well diameter in mm	Multiply $R_{display}$ by
50 - 60	1.08
60 - 70	1.06
70 - 80	1.04
80 - 90	1.03
90 -100	1.01

2- TEMPERATURE LOGGING:

Temperature is measured while the SAS 300 is in the resistivity surveying mode and the MODE selector on the SAS 200 is at the TEMP °C position. the 1 ohm scale and 0.5 m a current are used, and 1 °C is equivalence to 1 ohm. If the current selector is not at the 0.5 mA position, the SAS 300 issues an alarm (beeper signal) and error code 1 appears. Temperature is measured to an accuracy of ± 1°C within the 0°... +50 °C range. The usable precision is 0.01°C within the 0° ...+ 20 °C range and 0.1 °C within the +20 °C...+ 50 °C range, thus permitting local temperature gradients to be studied in detail.

When using the high precision for temperature gradient studies, ample time must be allowed to permit the probe to reach thermal equilibrium vis-a-vis the fluid. Move the probe slightly up and down a few times while waiting for equilibrium to be established.

Table A5T1

An ASCII file, containing data collected from a pseudosection survey, in the format suitable to be read by the inversion program.

Aber Farm through boreholes 1st half

6 37 2

233.86 192.27 245.67 244.04 237.38 232.73 261.38 272.69 263.89 245.92 242.03 220.54 181.58 220.04 117.5 101.54 69.24 52.15 68.86
61.07 76.78 56.8 60.82 67.61 50.27 53.28 77.66 163.87 182.97 385.79 433.54 697.43 1142.28 1585.88 2014.39 2902.83 3053.63
256.1 298.07 288.02 258.87 277.72 311.9 294.3 271.94 274.2 234.24 204.58 208.6 207.35 129.43 95 92.49 94 102.54 102.29 77.41
71.88 90.48 92.24 73.64 73.89 90.73 120.64 157.33 162.36 274.2 510.19 771.58 819.33 1105.84
305.74 276.71 271.06 272.19 292.55 288.4 244.67 222.8 217.9 234.11 222.42 193.4 125.92 95.38 98.02 123.28 132.7 116.49 105.93 103.3
107.07 96.89 90.1 96.13 126.67 136.47 145.52 170.4 258.99 336.65 359.27
278.97 260.38 256.35 239.26 243.28 237.76 228.71 240.77 221.67 199.55 171.41 121.14 114.1 113.6 128.18 147.78 143.76 142.75 115.11
106.06 113.6 109.58 134.71 140.24 141.75 162.86 167.89 187.49
234.36 224.31 235.62 218.03 237.5 249.44 228.71 194.78 175.93 158.96 124.66 124.03 135.09 139.49 150.17 158.96 146.4 129.43 130.06
128.18 138.23 144.51 150.8 152.05 163.99
236 241.27 236 236 225.44 211.87 183.22 156.07 150.8 133.83 137 138.51 141.37 155.32 153.06 153.81 148.23 148.61 161.35 148.01
145.29 153.06

Apparent Resistivity in ohm-m

0

0

0

Table A5T2

An ASCII file containing data recovered from AB profile surveys suitable to be read by the Unimap Software.

Distance on x-axis (m)	Distance on y-axis (m)	Apparent resistivity (ohm-m)
31.5	0	176.34
34.5	0	154.5
37.5	0	127.64
40.5	0	134.84
43.5	0	132.98
46.5	0	116.24
49.5	0	164.47
52.5	0	102.8
55.5	0	93.82
58.5	0	223.39
61.5	0	106.03
64.5	0	128.24
67.5	0	148.43
70.5	0	111.27
31.5	5	170.52
34.5	5	160.35
37.5	5	133.87
40.5	5	124.28
43.5	5	120.8
46.5	5	154.64
49.5	5	131.0
52.5	5	119.68
55.5	5	97.6
58.5	5	155.56
61.5	5	136.99
64.5	5	113.27
67.5	5	119.92
70.5	5	105.85

31.5	10	183.19
34.5	10	191.13
37.5	10	137.12
40.5	10	146.33
43.5	10	117.08
46.5	10	167.27
49.5	10	119.24
52.5	10	131.1
55.5	10	104.92
58.5	10	137.82
61.5	10	123.63
64.5	10	113.27
67.5	10	110.96
70.5	10	95.79
31.5	15	176.34
34.5	15	204.58
37.5	15	175.83
40.5	15	151.02
43.5	15	118.32
46.5	15	148.19
49.5	15	143.82
52.5	15	115.78
55.5	15	101.13
58.5	15	145.01
61.5	15	109.37
64.5	15	137.35
67.5	15	122.61
70.5	15	78.93
31.5	20	178.05
34.5	20	165.03
37.5	20	198.32
40.5	20	163.91
43.5	20	145.51
46.5	20	148.19
49.5	20	159.51
52.5	20	97.87
55.5	20	61.28
58.5	20	171.14
61.5	20	166.62
64.5	20	190.54
67.5	20	108.45
70.5	20	145.01

DATA SET: SH4-3LYR

CLIENT: UWB
LOCATION: ABER, COLLEGE FARM
COUNTY: GWYNEDD, UK
PROJECT: MSc THESIS, AMEER
ELEVATION: 0.31
SOUNDING COORDINATES: X: 0.0000 Y: 0.0000

DATE: 12-7-95
SOUNDING: 4
AZIMUTH: NE-SW
EQUIPMENT: GEOPULSE

Schlumberger Configuration

FITTING ERROR: 3.128 PERCENT

L #	RESISTIVITY (ohm-m)	THICKNESS (meters)	ELEVATION (meters)	LONG. COND. (Siemens)	TRANS. RES. (Ohm-m^2)
			0.310		
1	47.39	3.12	-2.81	0.0659	148.2
2	282.7	19.42	-22.24	0.0687	5492.7
3	81.10				

ALL PARAMETERS ARE FREE

PARAMETER BOUNDS FROM EQUIVALENCE ANALYSIS

	LAYER	MINIMUM	BEST	MAXIMUM
RHO	1	44.336	47.396	50.451
	2	228.744	282.707	362.427
	3	58.983	81.101	107.380
THICK	1	2.747	3.128	3.590
	2	11.169	19.429	31.498
DEPTH	1	2.747	3.128	3.590
	2	14.634	22.557	34.408

No.	SPACING (m)	RHO-A (ohm-m) DATA	RHO-A (ohm-m) SYNTHETIC	DIFFERENCE (percent)
1	1.50	52.88	55.24	-4.46
2	2.00	56.66	56.58	0.130
3	2.50	60.69	58.58	3.47
4	3.00	63.78	61.21	4.02
5	4.00	68.28	68.06	0.308
6	5.00	75.96	76.35	-0.520

No.	SPACING (m)	RHO-A (ohm-m) DATA	RHO-A (ohm-m) SYNTHETIC	DIFFERENCE (percent)
7	6.00	82.99	85.28	-2.76
8	8.00	102.9	103.0	-0.120
9	10.00	124.4	119.3	4.09
10	6.00	79.98	85.28	-6.62
11	8.00	101.3	103.0	-1.73
12	10.00	124.4	119.3	4.09
13	15.00	155.6	151.5	2.63
14	20.00	172.1	173.6	-0.880
15	25.00	193.6	187.8	2.98
16	30.00	197.0	196.0	0.501
17	40.00	190.5	199.9	-4.93
18	30.00	160.8	166.0	-3.25
19	40.00	161.3	169.3	-4.93
20	50.00	171.5	164.1	4.27
21	60.00	158.3	155.1	2.00
22	80.00	134.5	135.0	-0.349
23	60.00	163.3	160.2	1.89
24	80.00	139.0	139.5	-0.349
25	100.0	121.3	122.2	-0.701

PARAMETER RESOLUTION MATRIX:
"F" INDICATES FIXED PARAMETER

P 1	1.00				
P 2	0.00	1.00			
P 3	0.00	0.00	0.99		
T 1	0.00	0.00	0.00	1.00	
T 2	0.00	0.01	0.01	0.00	0.98
	P 1	P 2	P 3	T 1	T 2

Appendix A6.1

DATA SET: WEN3-LYR

CLIENT: UWB
LOCATION: ABER, COLLEGE FARM
COUNTY: GWYNEDD, UK
PROJECT: MSc THESIS, AMEER
ELEVATION: 0.31
DATE: 12-7-95
SOUNDING: 5
AZIMUTH: NE-SW
EQUIPMENT: GEOPULSE
SOUNDING COORDINATES: X: 0.0000 Y: 0.0000

Wenner Configuration

FITTING ERROR: 2.969 PERCENT

L f	RESISTIVITY (ohm-m)	THICKNESS (meters)	ELEVATION (meters)	LONG. COND. (Siemens)	TRANS. RES. (Ohm-m^2)
			0.310		
1	50.55	2.46	-2.15	0.0487	124.6
2	219.2	27.22	-29.38	0.124	5968.4
3	69.96				

ALL PARAMETERS ARE FREE

PARAMETER BOUNDS FROM EQUIVALENCE ANALYSIS

	LAYER	MINIMUM	BEST	MAXIMUM
RHO	1	46.667	50.550	53.945
	2	194.961	219.213	252.079
	3	52.359	69.961	92.675
THICK	1	2.099	2.466	2.904
	2	17.651	27.227	38.457
DEPTH	1	2.099	2.466	2.904
	2	20.408	29.692	40.808

No.	SPACING (m)	RHO-A (ohm-m) DATA	SYNTHETIC	DIFFERENCE (percent)
1	1.00	49.80	52.05	-4.53
2	1.50	56.05	54.96	1.94
3	2.00	61.72	59.31	3.89
4	2.50	65.67	64.68	1.50
5	3.00	71.25	70.59	0.924
6	4.00	79.41	82.73	-4.18

No.	SPACING (m)	RHO-A (ohm-m) DATA	SYNTHETIC	DIFFERENCE (percent)
7	5.00	92.06	94.18	-2.30
8	6.00	102.5	104.4	-1.87
9	8.00	125.6	121.4	3.33
10	10.00	137.6	134.5	2.18
11	15.00	157.3	155.3	1.29
12	20.00	162.1	164.9	-1.78
13	25.00	161.7	167.7	-3.67
14	30.00	167.5	166.1	0.859
15	40.00	163.8	155.9	4.80
16	50.00	135.7	142.5	-5.00
17	60.00	131.5	129.3	1.71
18	80.00	108.0	108.2	-0.208

PARAMETER RESOLUTION MATRIX:
"F" INDICATES FIXED PARAMETER

P 1	1.00				
P 2	0.00	1.00			
P 3	0.00	0.00	1.00		
T 1	0.00	0.00	0.00	1.00	
T 2	0.00	0.00	0.01	0.00	0.99
	P 1	P 2	P 3	T 1	T 2

DATA SET: OFW-3LYR

CLIENT: UWB
LOCATION: ABER, COLLEGE FARM
COUNTY: GWYNEDD, UK
PROJECT: MSc THESIS, AMEER
ELEVATION: 0.31
SOUNDING COORDINATES: X: 0.0000 Y: 0.0000

DATE: 12-7-95
SOUNDING: 5
AZIMUTH: NE-SW
EQUIPMENT: GEOPULSE

Wenner Configuration

FITTING ERROR: 6.415 PERCENT

L f	RESISTIVITY (ohm-m)	THICKNESS (meters)	ELEVATION (meters)	LONG. COND. (Siemens)	TRANS. RES. (Ohm-m^2)
			0.310		
1	48.44	2.39	-2.08	0.0493	115.8
2	221.1	25.77	-27.85	0.116	5699.4
3	68.28				

ALL PARAMETERS ARE FREE

PARAMETER BOUNDS FROM EQUIVALENCE ANALYSIS

	LAYER	MINIMUM	BEST	MAXIMUM
RHO	1	43.690	48.440	53.065
	2	185.398	221.163	261.662
	3	38.657	68.287	114.752
THICK	1	1.938	2.392	2.880
	2	13.442	25.770	51.007
DEPTH	1	1.938	2.392	2.880
	2	16.213	28.162	53.056

No.	SPACING (m)	RHO-A (ohm-m) DATA	SYNTHETIC	DIFFERENCE (percent)
1	0.500	46.16	48.65	-5.40
2	1.00	51.40	50.05	2.61
3	2.00	58.20	57.69	0.866
4	3.00	78.04	69.33	11.15
5	4.00	75.89	81.71	-7.67
6	6.00	104.3	103.6	0.661

No.	SPACING (m)	RHO-A (ohm-m) DATA	SYNTHETIC	DIFFERENCE (percent)
7	8.00	111.8	120.7	-7.99
8	12.00	143.9	144.0	-0.0162
9	16.00	157.3	157.2	0.0568
10	24.00	185.5	166.1	10.44
11	32.00	150.8	162.2	-7.52
12	64.00	120.6	120.2	0.304

PARAMETER RESOLUTION MATRIX:
"F" INDICATES FIXED PARAMETER

P 1	1.00				
P 2	0.00	1.00			
P 3	0.00	0.00	0.98		
T 1	0.00	0.00	0.00	1.00	
T 2	0.00	0.00	0.02	0.00	0.98
	P 1	P 2	P 3	T 1	T 2

DATA SET: SH4-4LYR

CLIENT: UWB
LOCATION: ABER, COLLEGE FARM
COUNTY: GWYNEDD, UK
PROJECT: MSc THESIS, AMEER
ELEVATION: 0.31
SOUNDING COORDINATES: X: 0.0000 Y: 0.0000

DATE: 12-7-95
SOUNDING: 4
AZIMUTH: NE-SW
EQUIPMENT: GEOPULSE

Schlumberger Configuration

FITTING ERROR: 3.152 PERCENT

L f	RESISTIVITY (ohm-m)	THICKNESS (meters)	ELEVATION (meters)	LONG. COND. (Siemens)	TRANS. RES. (Ohm-m^2)
			0.310		
1	47.16	2.83	-2.52	0.0602	133.9
2	131.2	0.925	-3.45	0.00705	121.4
3	275.8	20.45	-23.90	0.0741	5641.9
4	77.37				

ALL PARAMETERS ARE FREE

PARAMETER BOUNDS FROM EQUIVALENCE ANALYSIS

	LAYER	MINIMUM	BEST	MAXIMUM
RHO	1	43.946	47.160	50.327
	2	59.205	131.240	390.199
	3	228.536	275.840	346.311
	4	52.640	77.376	102.757
THICK	1	2.400	2.840	3.354
	2	0.246	0.926	2.682
	3	12.255	20.454	32.438
DEPTH	1	2.400	2.840	3.354
	2	3.400	3.765	5.292
	3	16.411	24.219	35.973

No.	SPACING (m)	RHO-A (ohm-m) DATA	RHO-A (ohm-m) SYNTHETIC	DIFFERENCE (percent)
1	1.50	52.88	55.04	-4.09
2	2.00	56.66	56.46	0.337

No.	SPACING (m)	RHO-A (ohm-m) DATA	RHO-A (ohm-m) SYNTHETIC	DIFFERENCE (percent)
3	2.50	60.69	58.55	3.51
4	3.00	63.78	61.28	3.91
5	4.00	68.28	68.28	-0.00944
6	5.00	75.96	76.62	-0.868
7	6.00	82.99	85.50	-3.03
8	8.00	102.9	103.0	-0.135
9	10.00	124.4	119.0	4.27
10	6.00	79.98	85.50	-6.91
11	8.00	101.3	103.0	-1.74
12	10.00	124.4	119.0	4.27
13	15.00	155.6	150.9	3.05
14	20.00	172.1	172.8	-0.414
15	25.00	193.6	187.0	3.37
16	30.00	197.0	195.4	0.783
17	40.00	190.5	199.9	-4.92
18	30.00	160.8	165.6	-2.96
19	40.00	161.3	169.3	-4.92
20	50.00	171.5	164.5	4.07
21	60.00	158.3	155.6	1.71
22	80.00	134.5	135.1	-0.450
23	60.00	163.3	160.7	1.59
24	80.00	139.0	139.6	-0.450
25	100.0	121.3	121.6	-0.198

PARAMETER RESOLUTION MATRIX:
"F" INDICATES FIXED PARAMETER

P 1	1.00						
P 2	0.00	0.02					
P 3	0.00	0.01	0.96				
P 4	0.00	0.01	-0.05	0.79			
T 1	-0.01	-0.14	-0.02	-0.02	0.95		
T 2	0.00	-0.01	-0.02	0.00	0.08	0.02	
T 3	0.01	0.01	0.10	0.22	0.04	0.05	0.70
	P 1	P 2	P 3	P 4	T 1	T 2	T 3

DATA SET: WEN4-LYR

CLIENT: UWB
LOCATION: ABER, COLLEGE FARM
COUNTY: GWYNEDD, UK
PROJECT: MSc THESIS, AMEER
ELEVATION: 0.31
SOUNDING COORDINATES: X: 0.0000 Y: 0.0000

DATE: 12-7-95
SOUNDING: 5
AZIMUTH: NE-SW
EQUIPMENT: GEOPULSE

Wenner Configuration

FITTING ERROR: 2.939 PERCENT

L f	RESISTIVITY (ohm-m)	THICKNESS (meters)	ELEVATION (meters)	LONG. COND. (Siemens)	TRANS. RES. (Ohm-m^2)
			0.310		
1	50.11	2.20	-1.89	0.0439	110.4
2	131.4	1.04	-2.94	0.00799	137.9
3	220.5	26.36	-29.30	0.119	5815.1
4	70.01				

ALL PARAMETERS ARE FREE

PARAMETER BOUNDS FROM EQUIVALENCE ANALYSIS

LAYER		MINIMUM	BEST	MAXIMUM
RHO	1	47.910	50.119	52.989
	2	67.798	131.431	354.193
	3	200.980	220.569	239.104
	4	50.418	70.015	90.813
THICK	1	1.860	2.204	2.766
	2	0.171	1.050	3.987
	3	18.903	26.364	38.073
DEPTH	1	1.860	2.204	2.766
	2	2.647	3.253	6.010
	3	22.807	29.617	40.877

No.	SPACING (m)	RHO-A (ohm-m) DATA	SYNTHETIC	DIFFERENCE (percent)
1	1.00	49.80	51.77	-3.97
2	1.50	56.05	54.87	2.08

No.	SPACING (m)	RHO-A (ohm-m) DATA	SYNTHETIC	DIFFERENCE (percent)
3	2.00	61.72	59.41	3.73
4	2.50	65.67	64.88	1.19
5	3.00	71.25	70.82	0.597
6	4.00	79.41	82.88	-4.37
7	5.00	92.06	94.19	-2.31
8	6.00	102.5	104.3	-1.76
9	8.00	125.6	121.2	3.52
10	10.00	137.6	134.3	2.38
11	15.00	157.3	155.1	1.43
12	20.00	162.1	164.8	-1.69
13	25.00	161.7	167.6	-3.61
14	30.00	167.5	166.0	0.911
15	40.00	163.8	155.8	4.87
16	50.00	135.7	142.3	-4.89
17	60.00	131.5	129.1	1.84
18	80.00	108.0	108.1	-0.0604

PARAMETER RESOLUTION MATRIX:
"F" INDICATES FIXED PARAMETER

P 1	1.00						
P 2	0.00	0.09					
P 3	0.00	0.01	1.00				
P 4	0.00	0.01	-0.01	0.96			
T 1	0.00	-0.21	0.00	0.00	0.94		
T 2	0.01	-0.08	-0.02	-0.03	0.06	0.11	
T 3	0.00	0.00	0.01	0.04	0.00	0.08	0.95
	P 1	P 2	P 3	P 4	T 1	T 2	T 3

DATA SET: OFW-4LYR

CLIENT: UWB
LOCATION: ABER, COLLEGE FARM
COUNTY: GWYNEDD, UK
PROJECT: MSc THESIS, AMEER
ELEVATION: 0.31
SOUNDING COORDINATES: X: 0.0000 Y: 0.0000

DATE: 12-7-95
SOUNDING: 5
AZIMUTH: NE-SW
EQUIPMENT: GEOPULSE

Wenner Configuration

FITTING ERROR: 6.209 PERCENT

L #	RESISTIVITY (ohm-m)	THICKNESS (meters)	ELEVATION (meters)	LONG. COND. (Siemens)	TRANS. RES. (Ohm-m^2)
			0.310		
1	47.91	1.82	-1.51	0.0381	87.67
2	97.06	1.68	-3.20	0.0173	163.3
3	226.8	24.29	-27.49	0.107	5510.2
4	68.03				

ALL PARAMETERS ARE FREE

PARAMETER BOUNDS FROM EQUIVALENCE ANALYSIS

	LAYER	MINIMUM	BEST	MAXIMUM
RHO	1	43.139	47.920	53.307
	2	68.590	97.065	426.950
	3	185.657	226.838	263.245
	4	35.918	68.036	110.447
THICK	1	1.439	1.830	2.878
	2	0.195	1.683	3.253
	3	14.548	24.292	48.432
DEPTH	1	1.439	1.830	2.878
	2	2.600	3.513	4.936
	3	18.485	27.804	51.263

No.	SPACING (m)	RHO-A (ohm-m) DATA	SYNTHETIC	DIFFERENCE (percent)
1	0.500	46.16	48.20	-4.42
2	1.00	51.40	49.89	2.92

No.	SPACING (m)	RHO-A (ohm-m) DATA	SYNTHETIC	DIFFERENCE (percent)
3	2.00	58.20	58.06	0.240
4	3.00	78.04	69.29	11.20
5	4.00	75.89	80.83	-6.51
6	6.00	104.3	101.5	2.71
7	8.00	111.8	118.2	-5.67
8	12.00	143.9	141.5	1.68
9	16.00	157.3	155.3	1.28
10	24.00	185.5	165.0	11.00
11	32.00	150.8	161.6	-7.15
12	64.00	120.6	120.0	0.493

PARAMETER RESOLUTION MATRIX:
"F" INDICATES FIXED PARAMETER

P 1	1.00						
P 2	0.00	0.09					
P 3	0.00	0.01	0.98				
P 4	0.00	0.02	-0.04	0.63			
T 1	-0.01	-0.28	0.00	-0.01	0.88		
T 2	0.01	-0.06	-0.04	-0.04	0.11	0.10	
T 3	0.00	0.00	0.06	0.33	0.02	0.11	0.65
	P 1	P 2	P 3	P 4	T 1	T 2	T 3

DATA SET: SCHL4FIX

CLIENT: UWB
LOCATION: ABER, COLLEGE FARM
COUNTY: GWYNEDD, UK
PROJECT: MSc THESIS, AMEER
ELEVATION: 0.31
SOUNDING COORDINATES: X: 0.0000 Y: 0.0000

DATE: 12-7-95
SOUNDING: 4
AZIMUTH: NE-SW
EQUIPMENT: GEOPULSE

Schlumberger Configuration

FITTING ERROR: 2.905 PERCENT

L f	RESISTIVITY (ohm-m)	THICKNESS (meters)	ELEVATION (meters)	LONG. COND. (Siemens)	TRANS. RES. (Ohm-m^2)
			0.310		
1	45.06	1.00 *	-0.690	0.0221	45.06
2	50.87	0.900*	-1.59	0.0176	45.79
3	68.64	2.70 *	-4.29	0.0393	185.3
4	1162.7	2.40 *	-6.69	0.00206	2790.4
5	141.5	53.27	-59.96	0.376	7539.9
6	26.41				

"*" INDICATES FIXED PARAMETER

PARAMETER BOUNDS FROM EQUIVALENCE ANALYSIS

	LAYER	MINIMUM	BEST	MAXIMUM
RHO	1	39.126	45.067	52.048
	2	35.253	50.880	75.137
	3	56.473	68.649	87.705
	4	685.322	1162.707	1758.538
	5	97.121	141.528	228.420
	6	7.522	26.418	66.868
THICK	1	1.000	1.000	1.000
	2	0.900	0.900	0.900
	3	2.700	2.700	2.700
	4	2.400	2.400	2.400
	5	21.314	53.276	109.519
DEPTH	1	1.000	1.000	1.000
	2	1.900	1.900	1.900
	3	4.600	4.600	4.600
	4	7.000	7.000	7.000
	5	28.314	60.276	116.519

No.	SPACING (m)	RHO-A (ohm-m) DATA	SYNTHETIC	DIFFERENCE (percent)
1	1.50	52.88	54.07	-2.25
2	2.00	56.66	56.34	0.561
3	2.50	60.69	59.07	2.65
4	3.00	63.78	62.16	2.52
5	4.00	68.28	69.13	-1.25
6	5.00	75.96	76.90	-1.24
7	6.00	82.99	85.18	-2.64
8	8.00	102.9	102.2	0.637
9	10.00	124.4	118.7	4.53
10	6.00	79.98	85.18	-6.50
11	8.00	101.3	102.2	-0.961
12	10.00	124.4	118.7	4.53
13	15.00	155.6	152.4	2.03
14	20.00	172.1	174.9	-1.62
15	25.00	193.6	188.5	2.64
16	30.00	197.0	195.8	0.610
17	40.00	190.5	198.6	-4.26
18	30.00	160.8	165.8	-3.14
19	40.00	161.3	168.2	-4.26
20	50.00	171.5	163.4	4.70
21	60.00	158.3	155.3	1.85
22	80.00	134.5	136.2	-1.22
23	60.00	163.3	160.5	1.74
24	80.00	139.0	140.7	-1.22
25	100.0	121.3	120.9	0.328

PARAMETER RESOLUTION MATRIX:
"F" INDICATES FIXED PARAMETER

P 1	0.99										
P 2	0.03	0.89									
P 3	-0.01	0.05	0.96								
P 4	0.01	-0.05	0.05	0.83							
P 5	-0.01	0.03	-0.03	0.13	0.90						
P 6	0.00	-0.01	0.01	-0.02	0.00	0.07					
F 1	0.00	0.00	0.00	0.00	0.00	0.00	0.00				
F 2	0.00	0.00	0.00	0.00	0.00	0.00	0.00	0.00			
F 3	0.00	0.00	0.00	0.00	0.00	0.00	0.00	0.00	0.00		
F 4	0.00	0.00	0.00	0.00	0.00	0.00	0.00	0.00	0.00	0.00	
T 5	0.00	-0.02	0.03	-0.14	0.13	0.23	0.00	0.00	0.00	0.00	0.
	P 1	P 2	P 3	P 4	P 5	P 6	F 1	F 2	F 3	F 4	T

DATA SET: WN1-6LYR

CLIENT: UWB DATE: 12-7-95
LOCATION: ABER, COLLEGE FARM SOUNDING: 5
COUNTY: GWYNEDD, UK AZIMUTH: NE-SW
PROJECT: MSc THESIS, AMEER EQUIPMENT: GEOPULSE
ELEVATION: 0.31
SOUNDING COORDINATES: X: 0.0000 Y: 0.0000

Wenner Configuration

FITTING ERROR: 2.537 PERCENT

L f	RESISTIVITY (ohm-m)	THICKNESS (meters)	ELEVATION (meters)	LONG. COND. (Siemens)	TRANS. RES. (Ohm-m^2)
			0.310		
1	46.26	1.00 *	-0.690	0.0216	46.26
2	67.78	0.900*	-1.59	0.0132	61.00
3	83.30	2.70 *	-4.29	0.0324	224.9
4	782.5	2.40 *	-6.69	0.00307	1878.2
5	151.3	40.12	-46.81	0.265	6074.0
6	51.36				

"*" INDICATES FIXED PARAMETER

PARAMETER BOUNDS FROM EQUIVALENCE ANALYSIS

LAYER		MINIMUM	BEST	MAXIMUM
RHO	1	41.064	46.266	51.618
	2	47.794	67.784	99.182
	3	66.998	83.305	109.925
	4	356.508	782.589	1277.388
	5	113.414	151.380	240.603
	6	25.362	51.363	80.282
THICK	1	1.000	1.000	1.000
	2	0.900	0.900	0.900
	3	2.700	2.700	2.700
	4	2.400	2.400	2.400
	5	18.969	40.124	87.649
DEPTH	1	1.000	1.000	1.000
	2	1.900	1.900	1.900
	3	4.600	4.600	4.600

4	7.000	7.000	7.000
5	25.969	47.124	94.649

No.	SPACING (m)	RHO-A (ohm-m) DATA	SYNTHETIC	DIFFERENCE (percent)
1	1.00	49.80	50.44	-1.29
2	1.50	56.05	55.33	1.28
3	2.00	61.72	60.61	1.78
4	2.50	65.67	65.97	-0.459
5	3.00	71.25	71.34	-0.133
6	4.00	79.41	82.11	-3.40
7	5.00	92.06	92.74	-0.741
8	6.00	102.5	102.9	-0.359
9	8.00	125.6	120.9	3.77
10	10.00	137.6	135.3	1.65
11	15.00	157.3	157.3	0.0352
12	20.00	162.1	166.0	-2.45
13	25.00	161.7	167.5	-3.56
14	30.00	167.5	165.0	1.47
15	40.00	163.8	154.8	5.47
16	50.00	135.7	142.3	-4.90
17	60.00	131.5	129.9	1.26
18	80.00	108.0	108.1	-0.0842

PARAMETER RESOLUTION MATRIX:
"F" INDICATES FIXED PARAMETER

P 1	0.99										
P 2	0.03	0.87									
P 3	-0.01	0.07	0.94								
P 4	0.01	-0.09	0.09	0.73							
P 5	0.00	0.03	-0.04	0.13	0.92						
P 6	0.00	0.00	0.00	0.04	-0.06	0.52					
F 1	0.00	0.00	0.00	0.00	0.00	0.00	0.00				
F 2	0.00	0.00	0.00	0.00	0.00	0.00	0.00	0.00			
F 3	0.00	0.00	0.00	0.00	0.00	0.00	0.00	0.00	0.00		
F 4	0.00	0.00	0.00	0.00	0.00	0.00	0.00	0.00	0.00	0.00	
T 5	0.00	-0.02	0.03	-0.16	0.13	0.41	0.00	0.00	0.00	0.00	0.5
	P 1	P 2	P 3	P 4	P 5	P 6	F 1	F 2	F 3	F 4	

Appendix A6.1

DATA SET: OFW-6LYR

CLIENT: UWB DATE: 12-7-95
LOCATION: ABER, COLLEGE FARM SOUNDING: 5
COUNTY: GWYNEDD, UK AZIMUTH: NE-SW
PROJECT: MSc THESIS, AMEER EQUIPMENT: GEOPULSE
ELEVATION: 0.31
SOUNDING COORDINATES: X: 0.0000 Y: 0.0000

Wenner Configuration

FITTING ERROR: 5.545 PERCENT

L #	RESISTIVITY (ohm-m)	THICKNESS (meters)	ELEVATION (meters)	LONG. COND. (Siemens)	TRANS. RES. (Ohm-m^2)
			0.310		
1	44.94	1.00 *	-0.690	0.0222	44.94
2	91.90	0.900*	-1.59	0.00979	82.71
3	62.87	2.70 *	-4.29	0.0429	169.7
4	1383.3	2.40 *	-6.69	0.00173	3320.1
5	100.8	31.13	-37.82	0.308	3138.8
6	80.18				

"*" INDICATES FIXED PARAMETER

PARAMETER BOUNDS FROM EQUIVALENCE ANALYSIS

	LAYER	MINIMUM	BEST	MAXIMUM
RHO	1	40.250	44.941	50.587
	2	50.961	91.909	135.737
	3	51.126	62.872	85.962
	4	648.021	1383.386	2095.852
	5	60.596	100.805	255.261
	6	38.893	80.181	118.778
THICK	1	1.000	1.000	1.000
	2	0.900	0.900	0.900
	3	2.700	2.700	2.700
	4	2.400	2.400	2.400
	5	14.847	31.138	226.709
DEPTH	1	1.000	1.000	1.000
	2	1.900	1.900	1.900
	3	4.600	4.600	4.600

4	7.000	7.000	7.000
5	21.847	38.138	233.709

No.	SPACING (m)	RHO-A (ohm-m) DATA	SYNTHETIC	DIFFERENCE (percent)
1	0.500	46.16	46.09	0.136
2	1.00	51.40	50.73	1.29
3	2.00	58.20	61.89	-6.35
4	3.00	78.04	71.21	8.74
5	4.00	75.89	80.22	-5.71
6	6.00	104.3	99.22	4.91
7	8.00	111.8	117.5	-5.07
8	12.00	143.9	145.4	-0.988
9	16.00	157.3	161.1	-2.45
10	24.00	185.5	169.3	8.72
11	32.00	150.8	162.5	-7.71
12	64.00	120.6	120.6	-0.0199

PARAMETER RESOLUTION MATRIX:
"F" INDICATES FIXED PARAMETER

P 1	1.00										
P 2	0.01	0.94									
P 3	0.00	0.03	0.98								
P 4	0.00	-0.05	0.06	0.77							
P 5	0.00	0.05	-0.05	0.26	0.69						
P 6	0.00	-0.02	0.03	-0.16	0.20	0.60					
F 1	0.00	0.00	0.00	0.00	0.00	0.00	0.00				
F 2	0.00	0.00	0.00	0.00	0.00	0.00	0.00	0.00			
F 3	0.00	0.00	0.00	0.00	0.00	0.00	0.00	0.00	0.00		
F 4	0.00	0.00	0.00	0.00	0.00	0.00	0.00	0.00	0.00	0.00	
T 5	0.00	-0.01	0.01	-0.09	0.16	0.30	0.00	0.00	0.00	0.00	0.0
	P 1	P 2	P 3	P 4	P 5	P 6	F 1	F 2	F 3	F 4	

DATA SET: SCHL1MOR

CLIENT: UWB DATE: 22-6-95
LOCATION: ABER, COLLEGE FARM SOUNDING: 1
COUNTY: GWYNEDD, UK AZIMUTH: NE-SW
PROJECT: MSc THESIS, AMEER EQUIPMENT: GEOPULSE
ELEVATION: 0.31
SOUNDING COORDINATES: X: 0.0000 Y: 0.0000

Schlumberger Configuration

FITTING ERROR: 2.952 PERCENT

L f	RESISTIVITY (ohm-m)	THICKNESS (meters)	ELEVATION (meters)	LONG. COND. (Siemens)	TRANS. RES. (Ohm-m^2)
			0.310		
1	50.52	3.90	-3.59	0.0773	197.4
2	607.8	6.85	-10.45	0.0112	4168.3
3	91.44				

ALL PARAMETERS ARE FREE

PARAMETER BOUNDS FROM EQUIVALENCE ANALYSIS

	LAYER	MINIMUM	BEST	MAXIMUM
RHO	1	49.029	50.525	52.438
	2	357.230	607.873	1254.457
	3	85.233	91.445	100.244
THICK	1	3.589	3.908	4.343
	2	2.993	6.857	12.940
DEPTH	1	3.589	3.908	4.343
	2	7.120	10.766	16.688

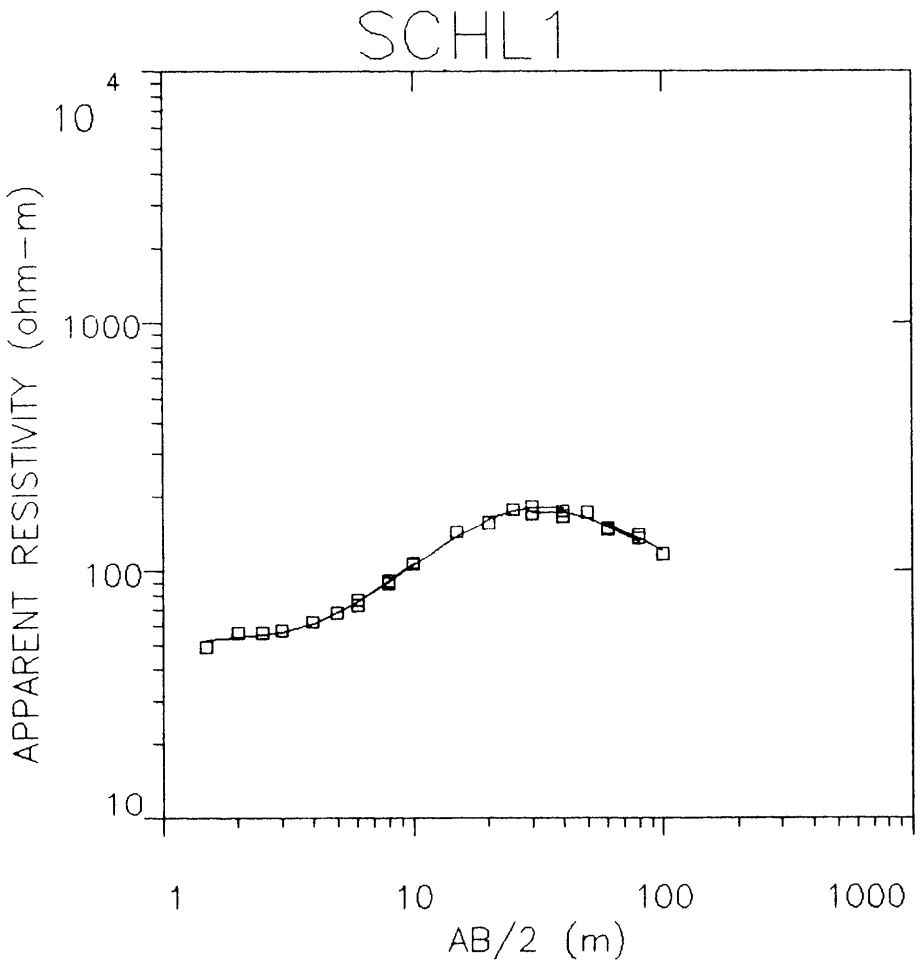
No.	SPACING (m)	RHO-A (ohm-m) DATA	SYNTHETIC	DIFFERENCE (percent)
1	1.50	49.42	52.87	-6.99
2	2.00	55.96	53.71	4.01
3	2.50	56.17	55.00	2.07
4	3.00	57.70	56.76	1.61
5	4.00	62.34	61.67	1.05
6	5.00	67.64	68.11	-0.702

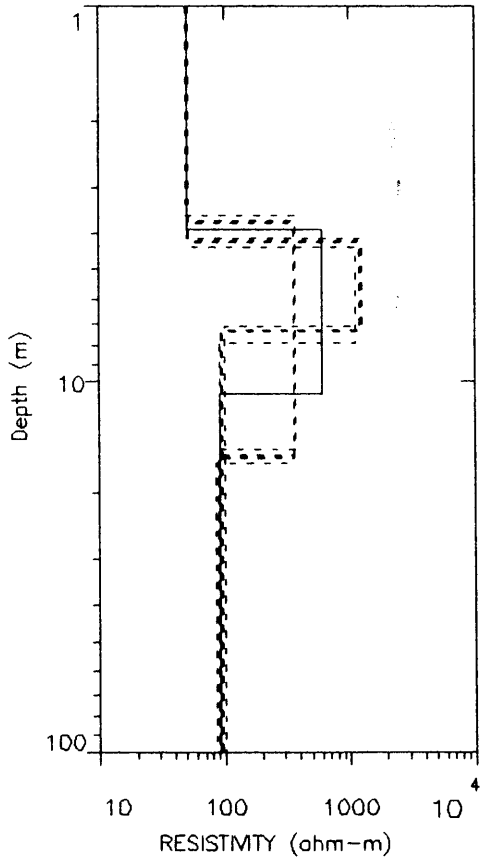
No.	SPACING (m)	RHO-A (ohm-m) DATA	SYNTHETIC	DIFFERENCE (percent)
7	6.00	76.15	75.56	0.762
8	8.00	90.93	91.68	-0.826
9	10.00	107.4	107.4	0.0766
10	6.00	73.17	74.73	-2.14
11	8.00	89.05	90.67	-1.82
12	10.00	106.3	106.2	0.0766
13	15.00	143.6	138.0	3.92
14	20.00	155.8	159.1	-2.13
15	25.00	174.6	171.6	1.70
16	30.00	181.5	177.7	2.11
17	40.00	172.9	177.7	-2.75
18	30.00	168.3	168.9	-0.349
19	40.00	164.4	168.9	-2.75
20	50.00	170.3	161.1	5.43
21	60.00	146.2	150.7	-3.05
22	80.00	135.5	131.0	3.35
23	60.00	148.7	155.0	-4.20
24	80.00	139.4	134.8	3.35
25	100.0	116.8	120.1	-2.84

PARAMETER RESOLUTION MATRIX:
"F" INDICATES FIXED PARAMETER

P 1	1.00				
P 2	0.00	0.79			
P 3	0.00	-0.01	1.00		
T 1	0.00	-0.02	0.00	1.00	
T 2	0.00	0.23	0.01	0.02	0.74
	P 1	P 2	P 3	T 1	T 2

Appendix A6.2





DATA SET: SCHL2MOR

CLIENT: UWB DATE: 22-6-95
LOCATION: ABER, COLLEGE FARM SOUNDING: 2
COUNTY: GWYNEDD, UK AZIMUTH: NE-SW
PROJECT: MSc THESIS, AMEER EQUIPMENT: GEOPULSE
ELEVATION: 0.70
SOUNDING COORDINATES: X: 0.0000 Y: 0.0000

Schlumberger Configuration

FITTING ERROR: 3.154 PERCENT

L #	RESISTIVITY (ohm-m)	THICKNESS (meters)	ELEVATION (meters)	LONG. COND. (Siemens)	TRANS. RES. (Ohm-m^2)
			0.700		
1	261.8	2.33	-1.63	0.00890	610.6
2	347.5	11.96	-13.59	0.0344	4157.3
3	80.55				

ALL PARAMETERS ARE FREE

PARAMETER BOUNDS FROM EQUIVALENCE ANALYSIS

	LAYER	MINIMUM	BEST	MAXIMUM
RHO	1	246.655	261.898	276.999
	2	319.053	347.527	387.080
	3	75.271	80.557	86.791
THICK	1	1.486	2.331	3.714
	2	9.607	11.963	14.390
DEPTH	1	1.486	2.331	3.714
	2	13.043	14.294	15.977

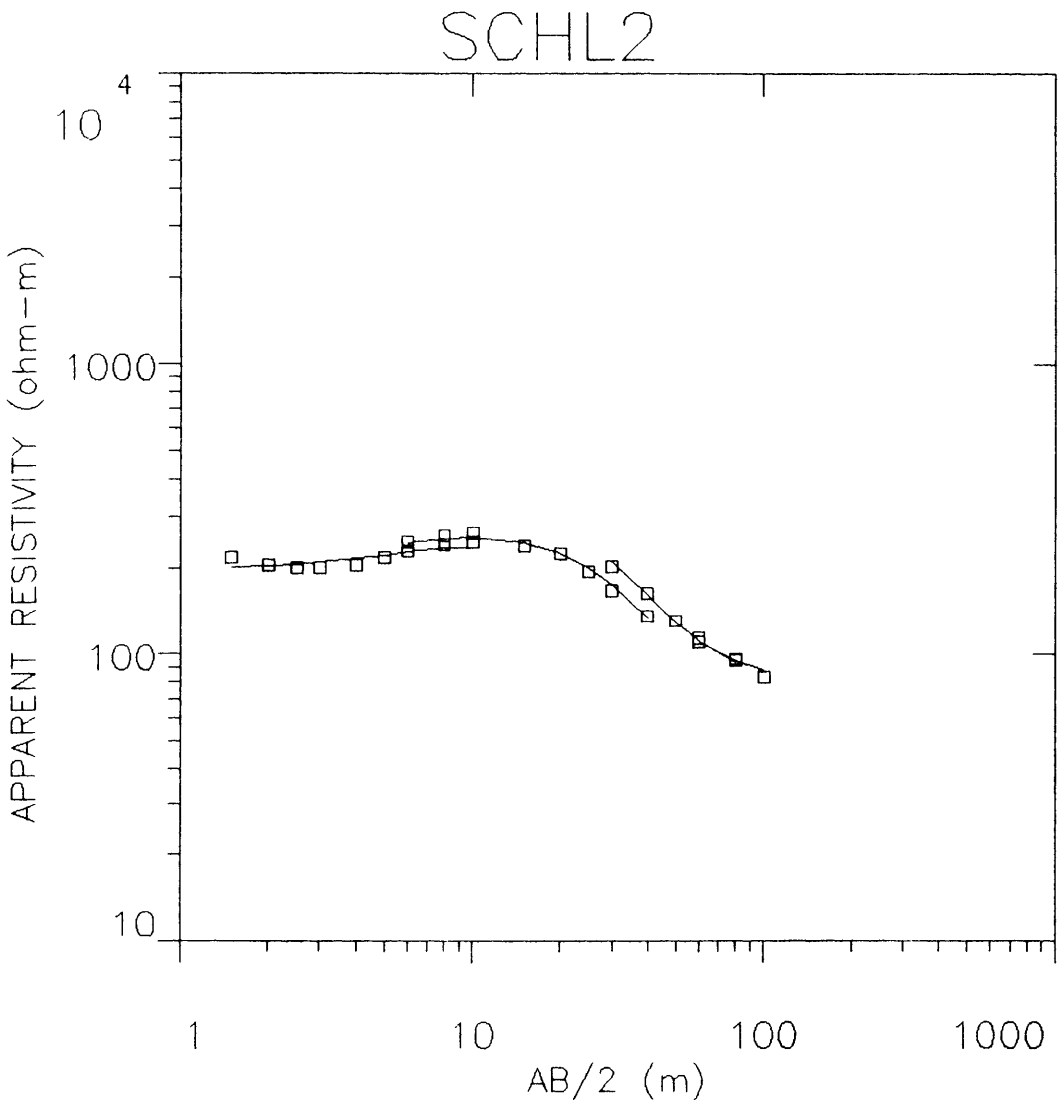
No.	SPACING (m)	RHO-A (ohm-m) DATA	SYNTHETIC	DIFFERENCE (percent)
1	1.50	217.2	202.4	6.84
2	2.00	204.9	204.2	0.360
3	2.50	201.7	206.6	-2.46
4	3.00	200.3	209.5	-4.58
5	4.00	204.8	215.9	-5.44
6	5.00	217.7	222.1	-2.03

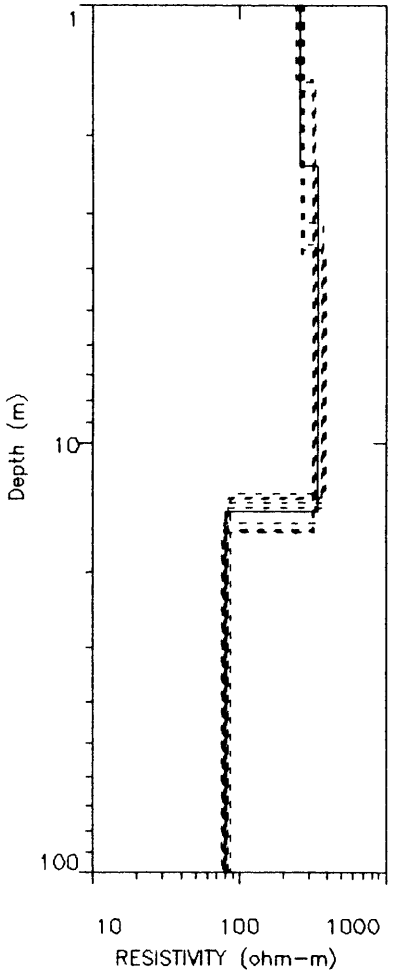
No.	SPACING (m)	RHO-A (ohm-m) DATA	SYNTHETIC	DIFFERENCE (percent)
7	6.00	227.9	227.2	0.310
8	8.00	240.3	233.9	2.67
9	10.00	245.0	236.0	3.67
10	6.00	247.0	245.4	0.626
11	8.00	258.6	252.6	2.35
12	10.00	264.6	254.9	3.67
13	15.00	239.4	245.8	-2.67
14	20.00	224.5	224.7	-0.0954
15	25.00	195.5	199.3	-1.92
16	30.00	167.4	174.4	-4.13
17	40.00	136.6	134.0	1.91
18	30.00	202.3	209.3	-3.47
19	40.00	163.9	160.8	1.91
20	50.00	130.8	129.4	1.02
21	60.00	110.5	110.7	-0.211
22	80.00	95.10	93.40	1.78
23	60.00	114.3	111.3	2.60
24	80.00	95.66	93.95	1.78
25	100.0	82.94	87.62	-5.65

PARAMETER RESOLUTION MATRIX:
"F" INDICATES FIXED PARAMETER

P 1	1.00				
P 2	0.00	1.00			
P 3	0.00	0.00	1.00		
T 1	0.00	0.00	0.00	0.99	
T 2	0.00	0.00	0.00	0.01	1.00
	P 1	P 2	P 3	T 1	T 2

Appendix A6.2





DATA SET: SCHL3MOR

CLIENT: UWB
LOCATION: ABER, COLLEGE FARM
COUNTY: GWYNEDD, UK
PROJECT: MSc THESIS, AMEER
ELEVATION: 0.45
SOUNDING COORDINATES: X: 0.0000 Y: 0.0000

DATE: 22-6-95
SOUNDING: 3
AZIMUTH: NE-SW
EQUIPMENT: GEOPULSE

Schlumberger Configuration

FITTING ERROR: 4.788 PERCENT

L #	RESISTIVITY (ohm-m)	THICKNESS (meters)	ELEVATION (meters)	LONG. COND. (Siemens)	TRANS. RES. (Ohm-m^2)
			0.450		
1	299.8	0.957	-0.507	0.00319	286.9
2	34.57	1.24	-1.75	0.0360	43.11
3	207.0	52.30	-54.05	0.252	10830.7
4	5.23				

ALL PARAMETERS ARE FREE

PARAMETER BOUNDS FROM EQUIVALENCE ANALYSIS

	LAYER	MINIMUM	BEST	MAXIMUM
RHO	1	229.982	299.843	409.843
	2	14.926	34.579	59.394
	3	188.501	207.088	230.147
	4	3.774	5.239	34.717
THICK	1	0.772	0.957	1.180
	2	0.510	1.247	2.192
	3	43.611	52.300	64.194
DEPTH	1	0.772	0.957	1.180
	2	1.604	2.204	3.072
	3	46.083	54.504	66.148

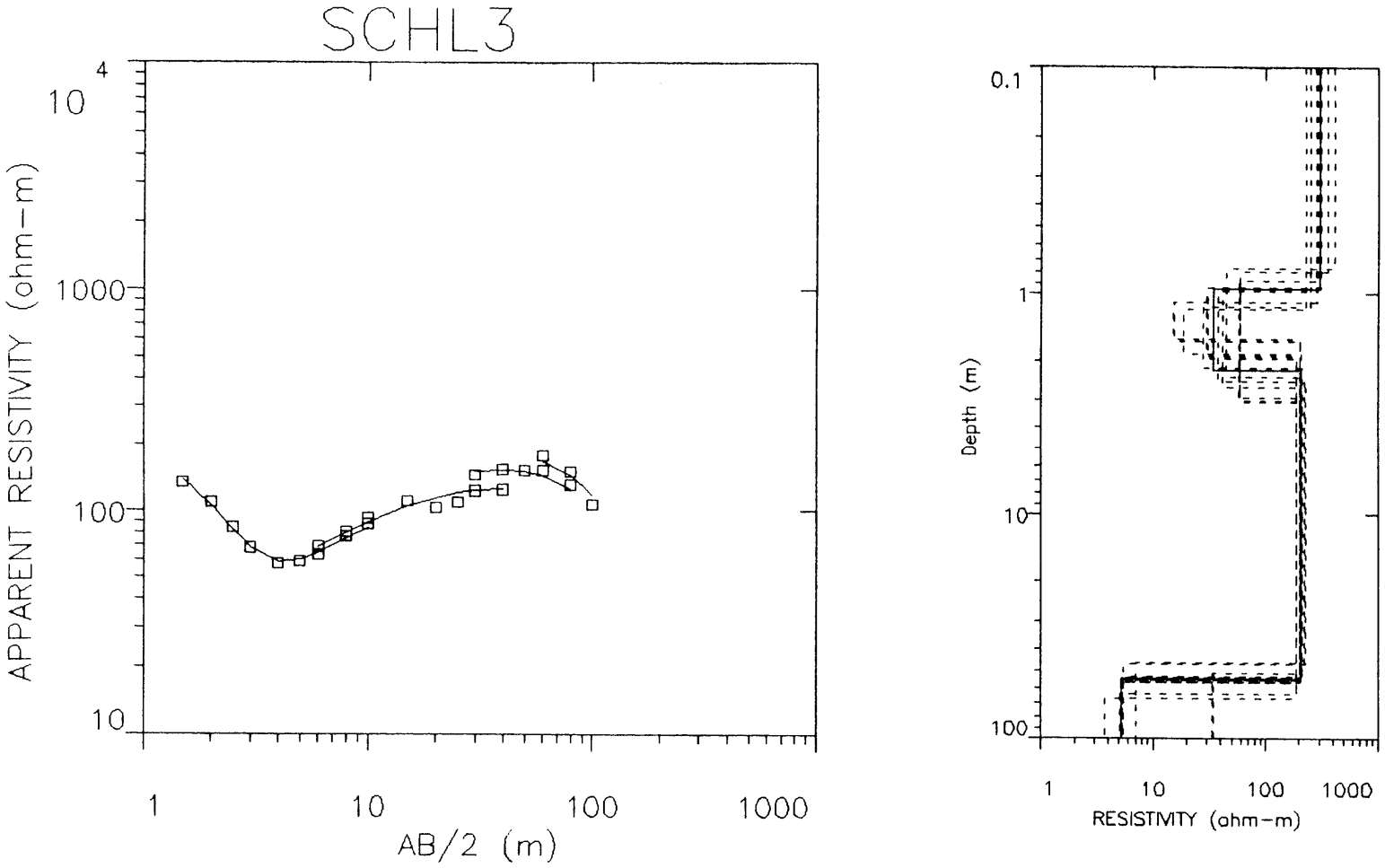
No.	SPACING (m)	RHO-A (ohm-m) DATA	SYNTHETIC	DIFFERENCE (percent)
1	1.50	133.7	137.6	-2.92
2	2.00	109.4	105.8	3.27

No.	SPACING (m)	RHO-A (ohm-m) DATA	SYNTHETIC	DIFFERENCE (percent)
3	2.50	84.07	82.77	1.54
4	3.00	67.63	68.69	-1.57
5	4.00	57.89	58.63	-1.28
6	5.00	58.93	59.91	-1.66
7	6.00	63.23	64.58	-2.14
8	8.00	76.10	74.81	1.69
9	10.00	87.43	83.41	4.59
10	6.00	68.63	68.51	0.171
11	8.00	80.10	79.35	0.928
12	10.00	92.74	88.47	4.59
13	15.00	110.5	104.4	5.54
14	20.00	102.6	114.0	-11.14
15	25.00	109.2	119.9	-9.82
16	30.00	122.4	123.3	-0.768
17	40.00	124.8	125.2	-0.319
18	30.00	144.5	151.1	-4.58
19	40.00	152.9	153.4	-0.319
20	50.00	151.5	150.2	0.858
21	60.00	152.2	143.4	5.78
22	80.00	129.6	123.6	4.61
23	60.00	177.1	166.8	5.80
24	80.00	150.8	143.8	4.61
25	100.0	106.3	117.2	-10.27

PARAMETER RESOLUTION MATRIX:
"F" INDICATES FIXED PARAMETER

P 1	0.97						
P 2	-0.03	0.54					
P 3	0.00	-0.01	0.99				
P 4	0.00	0.00	0.00	0.00			
T 1	0.02	0.08	0.00	0.00	0.97		
T 2	-0.03	-0.48	-0.02	0.00	0.08	0.49	
T 3	0.00	0.01	0.01	0.04	0.00	0.02	0.98
	P 1	P 2	P 3	P 4	T 1	T 2	T 3

Appendix A6.2



DATA SET: SCHL5COR

CLIENT: UWB
LOCATION: ABER, COLLEGE FARM
COUNTY: GWYNEDD, UK
PROJECT: MSc THESIS, AMEER
ELEVATION: 0.31
SOUNDING COORDINATES: X: 0.0000 Y: 0.0000

DATE: 31-7-95
SOUNDING: 7
AZIMUTH: NE-SW
EQUIPMENT: GEOPULSE

Schlumberger Configuration

FITTING ERROR: 3.660 PERCENT

L f	RESISTIVITY (ohm-m)	THICKNESS (meters)	ELEVATION (meters)	LONG. COND. (Siemens)	TRANS. RES. (Ohm-m^2)
			0.310		
1	35.55	1.76	-1.45	0.0495	62.68
2	62.55	1.83	-3.29	0.0294	115.0
3	319.5	13.65	-16.94	0.0427	4361.6
4	85.56				

ALL PARAMETERS ARE FREE

PARAMETER BOUNDS FROM EQUIVALENCE ANALYSIS

LAYER		MINIMUM	BEST	MAXIMUM
RHO	1	32.155	35.559	39.094
	2	42.512	62.551	99.439
	3	237.606	319.533	503.695
	4	62.950	85.561	108.944
THICK	1	1.257	1.763	2.425
	2	0.966	1.840	3.345
	3	6.609	13.650	25.019
DEPTH	1	1.257	1.763	2.425
	2	3.161	3.603	4.775
	3	10.917	17.253	28.556

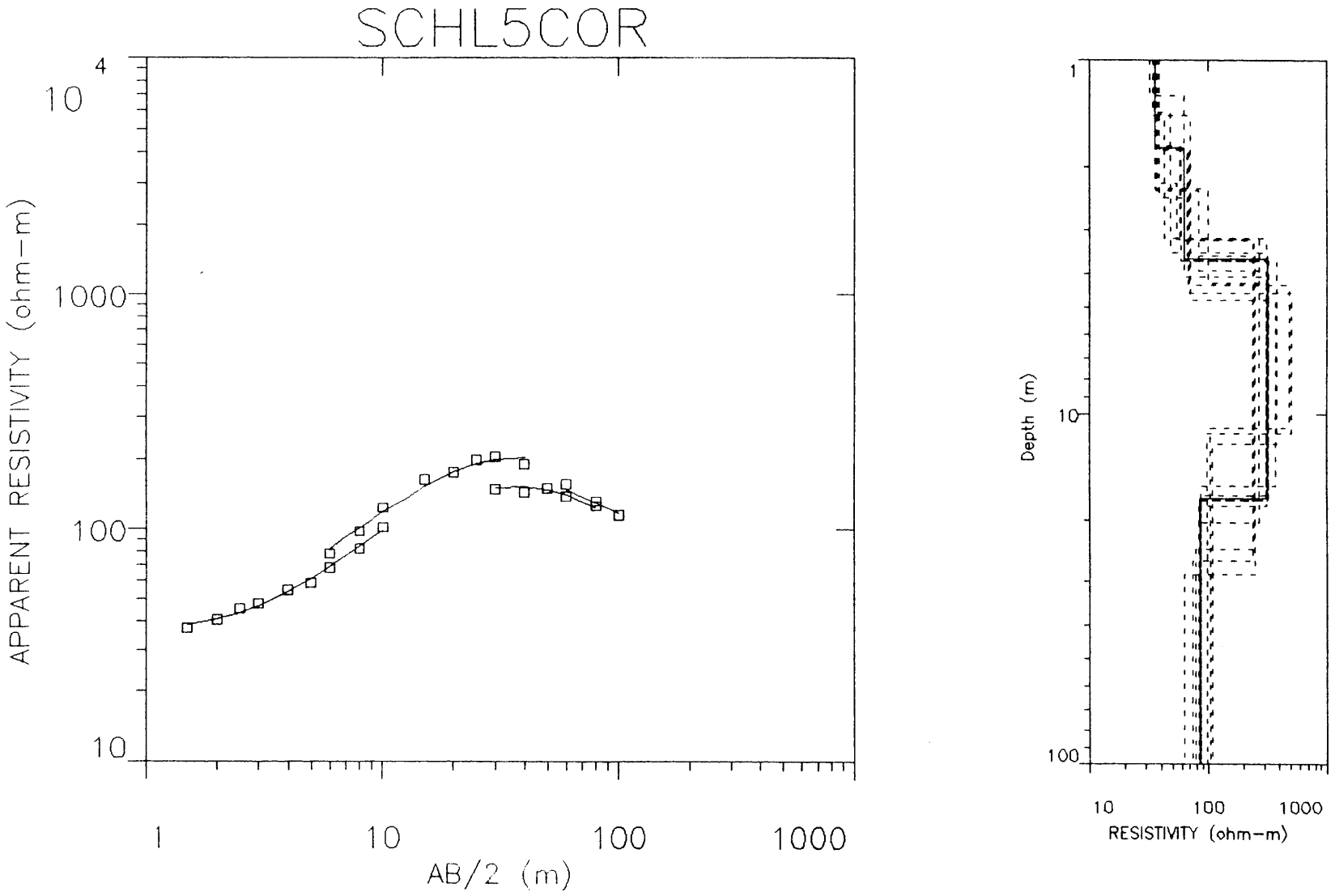
No.	SPACING (m)	RHO-A (ohm-m) DATA	SYNTHETIC	DIFFERENCE (percent)
1	1.50	37.37	38.83	-3.92
2	2.00	40.64	40.74	-0.258

No.	SPACING (m)	RHO-A (ohm-m) DATA	SYNTHETIC	DIFFERENCE (percent)
3	2.50	45.43	43.28	4.71
4	3.00	47.83	46.31	3.16
5	4.00	54.43	53.32	2.02
6	5.00	58.47	60.98	-4.30
7	6.00	67.72	68.84	-1.66
8	8.00	82.72	84.18	-1.77
9	10.00	101.8	98.27	3.51
10	6.00	78.47	83.07	-5.86
11	8.00	98.01	101.5	-3.64
12	10.00	122.9	118.5	3.51
13	15.00	163.3	152.8	6.37
14	20.00	175.4	176.5	-0.626
15	25.00	198.0	191.5	3.24
16	30.00	204.0	200.0	1.96
17	40.00	191.7	203.6	-6.20
18	30.00	149.5	151.4	-1.24
19	40.00	145.1	154.1	-6.20
20	50.00	151.5	149.3	1.48
21	60.00	139.6	141.3	-1.23
22	80.00	125.6	124.6	0.850
23	60.00	157.3	148.4	5.66
24	80.00	131.9	130.8	0.850
25	100.0	114.6	116.9	-2.02

PARAMETER RESOLUTION MATRIX:
"F" INDICATES FIXED PARAMETER

P 1	0.99						
P 2	0.00	0.28					
P 3	0.00	-0.04	0.85				
P 4	0.00	0.01	-0.04	0.94			
T 1	-0.02	-0.40	0.00	0.00	0.63		
T 2	0.03	-0.10	-0.14	-0.01	0.18	0.48	
T 3	0.00	0.05	0.24	0.11	0.01	0.18	0.58
	P 1	P 2	P 3	P 4	T 1	T 2	T 3

Appendix A6.3



DATA SET: SCHL6COR

CLIENT: UWB
LOCATION: ABER, COLLEGE FARM
COUNTY: GWYNEDD, UK
PROJECT: MSc THESIS, AMEER
ELEVATION: 0.31
SOUNDING COORDINATES: X: 0.0000 Y: 0.0000

DATE: 31-7-95
SOUNDING: 8
AZIMUTH: NE-SW
EQUIPMENT: GEOPULSE

Schlumberger Configuration

FITTING ERROR: 4.597 PERCENT

L f	RESISTIVITY (ohm-m)	THICKNESS (meters)	ELEVATION (meters)	LONG. COND. (Siemens)	TRANS. RES. (Ohm-m^2)
			0.310		
1	38.55	3.14	-2.83	0.0815	121.2
2	431.4	9.49	-12.33	0.0220	4098.5
3	79.71				

ALL PARAMETERS ARE FREE

PARAMETER BOUNDS FROM EQUIVALENCE ANALYSIS

LAYER		MINIMUM	BEST	MAXIMUM
RHO	1	36.459	38.560	41.461
	2	259.390	431.500	878.304
	3	68.719	79.713	95.847
THICK	1	2.759	3.144	3.724
	2	3.963	9.498	19.081
DEPTH	1	2.759	3.144	3.724
	2	7.405	12.642	22.025

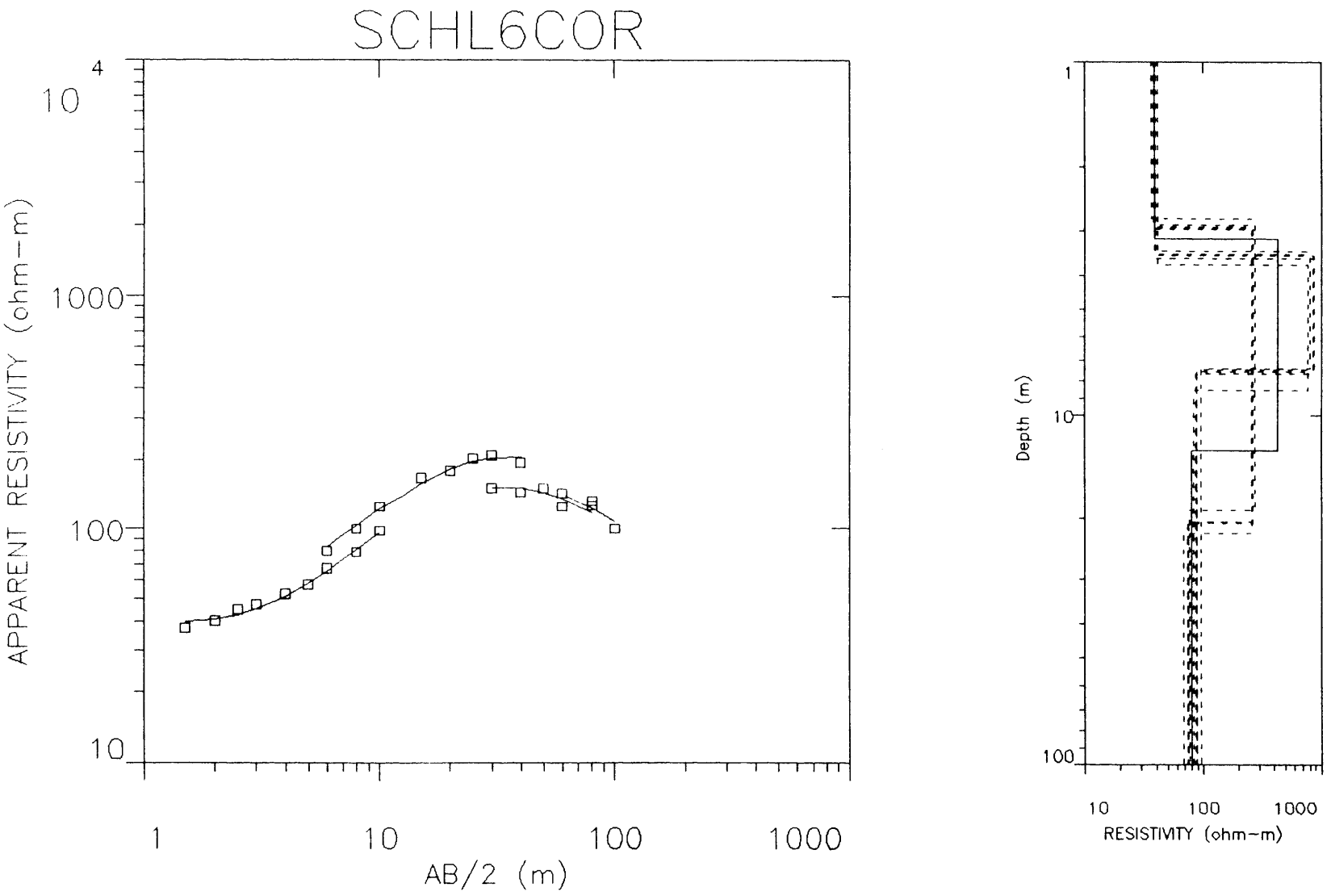
No.	SPACING (m)	RHO-A (ohm-m) DATA	RHO-A (ohm-m) SYNTHETIC	DIFFERENCE (percent)
1	1.50	37.37	39.79	-6.49
2	2.00	40.29	40.93	-1.60
3	2.50	44.86	42.62	4.97
4	3.00	47.28	44.86	5.10
5	4.00	51.95	50.73	2.34
6	5.00	56.91	57.87	-1.68

No.	SPACING (m)	RHO-A (ohm-m) DATA	RHO-A (ohm-m) SYNTHETIC	DIFFERENCE (percent)
7	6.00	66.94	65.62	1.96
8	8.00	78.91	81.25	-2.97
9	10.00	97.77	95.72	2.09
10	6.00	79.73	83.50	-4.73
11	8.00	99.42	103.3	-4.00
12	10.00	124.4	121.8	2.09
13	15.00	166.9	158.5	5.05
14	20.00	179.7	182.9	-1.75
15	25.00	202.8	197.5	2.63
16	30.00	208.3	204.8	1.66
17	40.00	195.5	205.1	-4.91
18	30.00	150.7	152.0	-0.826
19	40.00	145.1	152.2	-4.91
20	50.00	152.0	145.1	4.52
21	60.00	124.8	135.4	-8.51
22	80.00	125.6	116.8	7.06
23	60.00	144.0	142.1	1.26
24	80.00	131.9	122.6	7.06
25	100.0	100.2	108.2	-7.96

PARAMETER RESOLUTION MATRIX:
"F" INDICATES FIXED PARAMETER

P 1	1.00				
P 2	0.00	0.95			
P 3	0.00	-0.01	1.00		
T 1	0.00	-0.01	0.00	1.00	
T 2	0.00	0.06	0.01	0.01	0.93
	P 1	P 2	P 3	T 1	T 2

Appendix A6.3



DATA SET: SCHL7COR

CLIENT: UWB
LOCATION: ABER, COLLEGE FARM
COUNTY: GWYNEDD, UK
PROJECT: MSc THESIS, AMEER
ELEVATION: 0.31
SOUNDING COORDINATES: X: 0.0000 Y: 0.0000

DATE: 31-7-95
SOUNDING: 9
AZIMUTH: NE-SW
EQUIPMENT: GEOPULSE

Schlumberger Configuration

FITTING ERROR: 5.190 PERCENT

L f	RESISTIVITY (ohm-m)	THICKNESS (meters)	ELEVATION (meters)	LONG. COND. (Siemens)	TRANS. RES. (Ohm-m^2)
			0.310		
1	32.07	0.959	-0.649	0.0299	30.78
2	51.10	2.87	-3.52	0.0562	146.8
3	405.9	10.75	-14.27	0.0264	4364.0
4	80.61				

ALL PARAMETERS ARE FREE

PARAMETER BOUNDS FROM EQUIVALENCE ANALYSIS

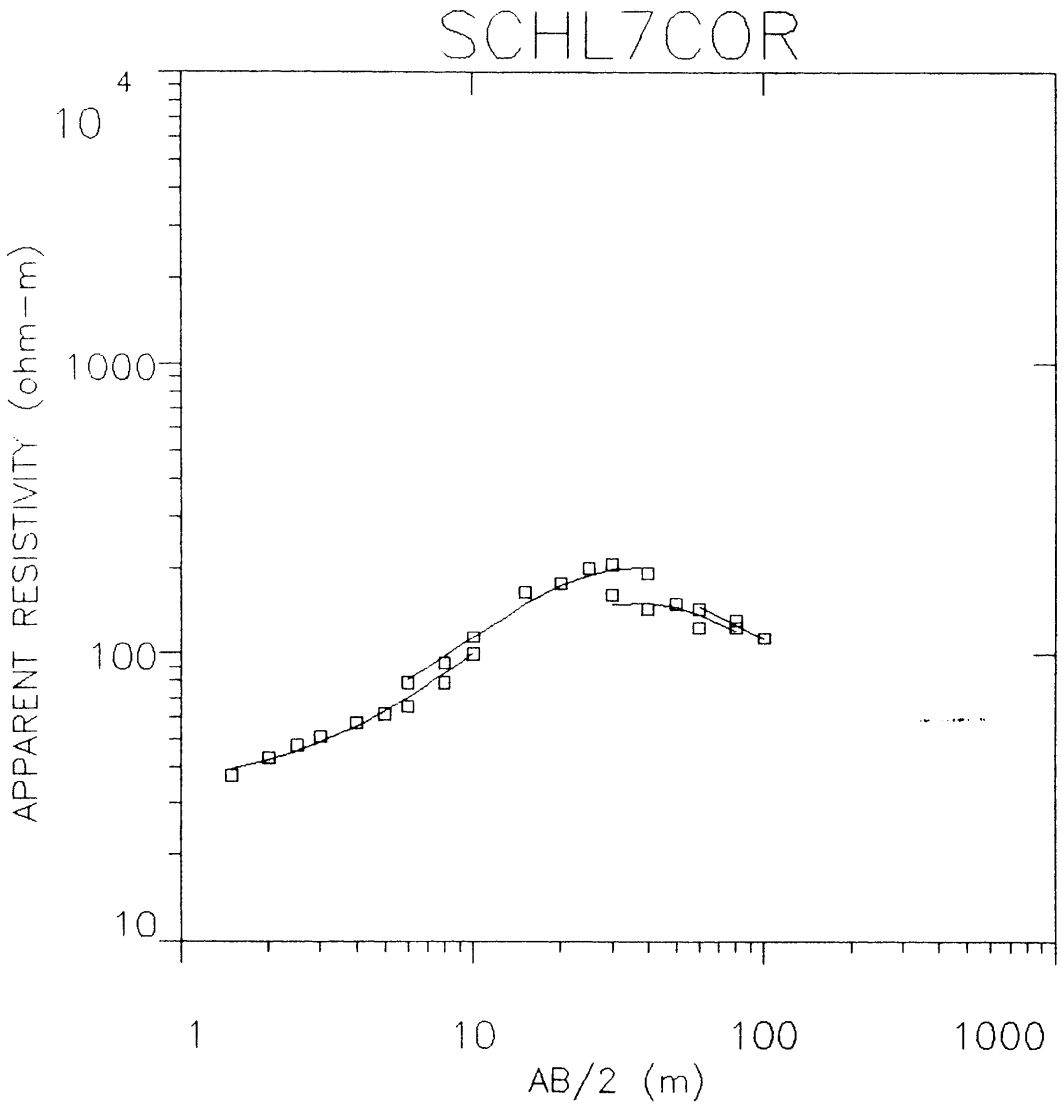
	LAYER	MINIMUM	BEST	MAXIMUM
RHO	1	24.437	32.076	38.792
	2	37.542	51.104	75.502
	3	287.758	405.930	779.348
	4	54.923	80.610	106.926
THICK	1	0.523	0.960	1.718
	2	1.866	2.873	4.220
	3	4.545	10.751	19.587
DEPTH	1	0.523	0.960	1.718
	2	2.933	3.833	5.094
	3	8.438	14.584	23.379

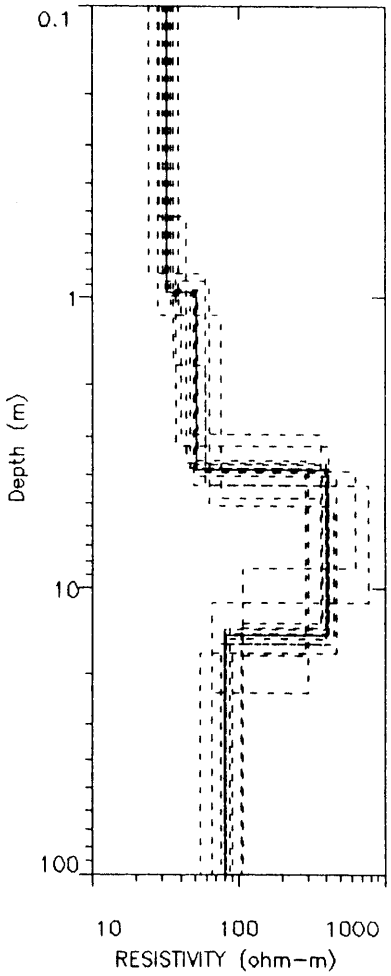
No.	SPACING (m)	RHO-A (ohm-m) DATA	SYNTHETIC	DIFFERENCE (percent)
1	1.50	37.37	39.38	-5.38
2	2.00	43.00	42.49	1.16

No.	SPACING (m)	RHO-A (ohm-m) DATA	SYNTHETIC	DIFFERENCE (percent)
3	2.50	47.69	45.74	4.08
4	3.00	51.41	49.01	4.66
5	4.00	57.40	55.71	2.92
6	5.00	61.58	62.79	-1.97
7	6.00	65.03	70.20	-7.95
8	8.00	78.91	85.36	-8.17
9	10.00	100.3	99.93	0.368
10	6.00	79.47	80.74	-1.60
11	8.00	93.30	98.17	-5.22
12	10.00	115.3	114.9	0.368
13	15.00	165.8	149.9	9.62
14	20.00	178.5	174.4	2.28
15	25.00	200.9	190.1	5.38
16	30.00	206.1	198.9	3.52
17	40.00	193.0	202.5	-4.91
18	30.00	162.1	149.8	7.58
19	40.00	145.3	152.5	-4.91
20	50.00	150.8	147.3	2.29
21	60.00	124.2	138.8	-11.78
22	80.00	124.6	121.0	2.89
23	60.00	144.7	146.9	-1.52
24	80.00	131.9	128.1	2.89
25	100.0	113.8	113.2	0.528

PARAMETER RESOLUTION MATRIX:
"F" INDICATES FIXED PARAMETER

P 1	0.70							
P 2	0.16	0.51						
P 3	-0.02	0.03	0.48					
P 4	0.01	0.00	0.17	0.50				
T 1	-0.17	-0.23	-0.02	0.02	0.13			
T 2	0.08	-0.29	-0.13	0.09	0.13	0.47		
T 3	0.00	-0.02	0.36	0.23	0.01	0.01	0.31	
	P 1	P 2	P 3	P 4	T 1	T 2	T 3	


SCHL7COR
APPARENT RESISTIVITY (ohm-m)
10^4
1000
100
10
1
10
100
1000
AB/2 (m)


0.1
1
10
100
Depth (m)
10
100
1000
RESISTIVITY (ohm-m)

BEAUMARIS

MAY 1995

	HIGH WATER				LOW WATER			
Date	Time	Ht.	Time	Ht.	Time	Ht.	Time	Ht.
1	1134	7.42	2354	7.46	0553	1.17	1808	1.13
2			1211	7.24	0628	1.26	1842	1.32
3	0030	7.29	1249	6.98	0704	1.41	1919	1.57
4	0108	7.04	1330	6.66	0743	1.63	1959	1.87
5	0149	6.73	1415	6.32	0827	1.88	2044	2.18
6	0235	6.40	1507	6.00	0915	2.12	2134	2.46
7	0329	6.12	1609	5.79	1009	2.31	2231	2.64
8	0433	5.97	1719	5.76	1108	2.39	2332	2.68
9	0541	6.01	1822	5.92			1209	2.33
10	0641	6.25	1915	6.24	0034	2.54	1309	2.12
11	0732	6.61	2001	6.64	0133	2.25	1404	1.80
12	0819	7.05	2045	7.08	0225	1.87	1454	1.45
13	0904	7.48	2128	7.50	0315	1.45	1542	1.11
14	0948	7.84	2211	7.84	0402	1.06	1628	0.85
15	1033	8.07	2256	8.05	0450	0.76	1715	0.70
16	1120	8.12	2341	8.10	0538	0.59	1803	0.69
17			1207	7.99	0628	0.57	1852	0.83
18	0029	7.97	1258	7.68	0720	0.70	1945	1.09
19	0121	7.70	1352	7.26	0816	0.94	2040	1.43
20	0217	7.32	1454	6.81	0915	1.24	2140	1.77
21	0319	6.94	1603	6.44	1019	1.51	2245	2.05
22	0430	6.66	1720	6.27	1126	1.68	2353	2.18
23	0544	6.55	1831	6.31			1233	1.73
24	0650	6.59	1930	6.48	0100	2.16	1335	1.67
25	0746	6.72	2020	6.70	0201	2.03	1429	1.55
26	0834	6.86	2102	6.93	0253	1.84	1516	1.44
27	0917	7.00	2141	7.13	0338	1.66	1557	1.35
28	0956	7.12	2218	7.30	0418	1.50	1634	1.28
29	1034	7.18	2254	7.40	0455	1.37	1709	1.25
30	1112	7.19	2330	7.42	0531	1.29	1744	1.27
31	1149	7.13			0607	1.26	1820	1.35

JUNE 1995

	HIGH WATER				LOW WATER			
Date	Time	Ht.	Time	Ht.	Time	Ht.	Time	Ht
1	0007	7.36	1227	7.00	0644	1.30	1857	1.4
2	0044	7.21	1306	6.80	0723	1.41	1936	1.6
3	0122	7.01	1347	6.57	0803	1.57	2018	1.9
4	0203	6.77	1431	6.33	0847	1.76	2102	2.1
5	0249	6.54	1522	6.12	0934	1.94	2151	2.3
6	0342	6.36	1620	6.00	1025	2.07	2245	2.4
7	0443	6.28	1725	6.02	1122	2.12	2344	2.3
8	0549	6.36	1828	6.22			1222	2.0
9	0651	6.60	1925	6.55	0047	2.23	1325	1.8
10	0749	6.93	2018	6.95	0150	1.94	1425	1.5
11	0842	7.30	2108	7.37	0250	1.56	1521	1.2
12	0932	7.63	2156	7.74	0346	1.16	1614	0.9
13	1021	7.86	2244	8.00	0439	0.82	1704	0.7
14	1110	7.95	2332	8.12	0531	0.58	1754	0.7
15	1159	7.88			0622	0.49	1843	0.7
16	0020	8.07	1249	7.66	0713	0.55	1933	0.9
17	0110	7.87	1340	7.33	0804	0.74	2024	1.2
18	0202	7.55	1435	6.93	0857	1.04	2117	1.6
19	0257	7.16	1535	6.56	0953	1.38	2214	1.9
20	0357	6.78	1640	6.28	1051	1.69	2315	2.2
21	0503	6.49	1748	6.17	1153	1.92		
22	0609	6.34	1850	6.21	0019	2.39	1255	2.0
23	0709	6.34	1945	6.37	0124	2.38	1353	2.0
24	0803	6.43	2033	6.60	0222	2.23	1445	1.8
25	0850	6.59	2116	6.84	0312	2.02	1530	1.7
26	0933	6.76	2155	7.07	0355	1.78	1610	1.6
27	1013	6.92	2233	7.26	0434	1.55	1647	1.4
28	1051	7.05	2309	7.39	0511	1.36	1723	1.3
29	1128	7.11	2344	7.44	0547	1.22	1759	1.3
30			1204	7.11	0623	1.15	1835	1.3

Times in G.M.T.
Predicted tidal heights in metres relative to Chart Datum, Beaumaris
Ordnance Datum (Newlyn) is +4.00 m

BEAUMARIS

JULY 1995

	HIGH WATER				LOW WATER			
Date	Time	Ht.	Time	Ht.	Time	Ht.	Time	Ht.
1	0019	7.42	1240	7.04	0700	1.16	1912	1.42
2	0055	7.34	1317	6.92	0737	1.25	1950	1.56
3	0132	7.21	1357	6.75	0817	1.39	2030	1.74
4	0213	7.03	1441	6.55	0900	1.58	2114	1.92
5	0300	6.82	1532	6.35	0947	1.77	2205	2.09
6	0357	6.63	1634	6.22	1041	1.94	2303	2.20
7	0503	6.51	1744	6.23	1144	2.03		
8	0616	6.55	1854	6.44	0011	2.19	1253	1.98
9	0724	6.77	1957	6.80	0124	2.00	1403	1.76
10	0826	7.09	2054	7.24	0234	1.65	1507	1.44
11	0922	7.43	2146	7.66	0337	1.21	1604	1.09
12	1013	7.70	2235	7.99	0432	0.80	1656	0.81
13	1102	7.86	2323	8.18	0524	0.49	1744	0.65
14	1149	7.87			0612	0.35	1831	0.66
15	0009	8.19	1236	7.72	0659	0.39	1917	0.82
16	0055	8.03	1322	7.45	0746	0.59	2002	1.11
17	0141	7.72	1410	7.09	0832	0.93	2048	1.49
18	0229	7.30	1501	6.69	0919	1.35	2137	1.91
19	0321	6.83	1557	6.32	1010	1.77	2230	2.29
20	0419	6.41	1659	6.06	1105	2.13	2331	2.56
21	0524	6.10	1806	5.98			1207	2.37
22	0631	5.99	1909	6.07	0040	2.66	1312	2.42
23	0733	6.06	2004	6.30	0148	2.55	1412	2.31
24	0827	6.25	2052	6.58	0245	2.30	1504	2.10
25	0913	6.51	2133	6.88	0332	1.98	1547	1.85
26	0953	6.77	2211	7.16	0412	1.66	1625	1.60
27	1030	7.00	2245	7.38	0449	1.38	1701	1.39
28	1105	7.18	2319	7.55	0524	1.15	1736	1.24
29	1138	7.29	2352	7.66	0558	1.00	1810	1.16
* 30			1212	7.33	0633	0.94	1845	1.15
31	0026	7.69	1247	7.30	0709	0.97	1921	1.22

AUG 1995

	HIGH WATER				LOW WATER			
Date	Time	Ht.	Time	Ht.	Time	Ht.	Time	Ht.
1	0103	7.63	1324	7.18	0747	1.09	1959	1
2	0143	7.47	1407	6.98	0828	1.29	2043	1
3	0228	7.22	1456	6.71	0915	1.56	2133	1
4	0322	6.90	1555	6.43	1010	1.84	2234	2
5	0429	6.59	1709	6.26	1115	2.05	2347	2
6	0549	6.46	1830	6.36			1232	2
7	0708	6.59	1943	6.71	0108	2.02	1349	1
8	0816	6.92	2044	7.18	0224	1.64	1457	1
9	0914	7.30	2137	7.65	0328	1.16	1554	1
10	1005	7.62	2225	8.01	0423	0.71	1645	0
11	1051	7.83	2310	8.22	0512	0.39	1731	0
12	*1135	7.89	2353	8.24	0557	0.26	1814	0
13			*1217	7.79	0640	0.33	1855	0
14	0034	8.08	1259	7.56	0721	0.57	1936	1
15	0116	7.76	1341	7.22	0802	0.95	2016	1
16	0159	7.32	1425	6.82	0842	1.39	2059	1
17	0245	6.82	1514	6.41	0926	1.86	2146	2
18	0337	6.33	1612	6.05	1015	2.28	2242	2
19	0440	5.93	1721	5.85	1114	2.60	2352	2
20	0554	5.75	1832	5.87			1226	2
21	0704	5.81	1935	6.08	0109	2.73	1337	2
22	0803	6.04	2026	6.39	0214	2.46	1435	2
23	0850	6.36	2108	6.73	0304	2.10	1521	2
24	0930	6.69	2145	7.07	0346	1.73	1600	1
25	1005	7.00	2219	7.38	0422	1.39	1635	1
26	1038	7.26	2251	7.65	0456	1.11	1709	1
27	1110	7.47	2324	7.85	0530	0.90	1742	1
* 28	1143	7.61	2359	7.96	0604	0.78	1817	0
29			*1218	7.64	0640	0.78	1853	0
30	0036	7.95	1256	7.55	0718	0.89	1933	1
31	0117	7.78	1339	7.32	0801	1.12	2018	1

Times in G.M.T.
Predicted tidal heights in metres relative to Chart Datum, Beaumaris
Ordnance Datum (Newlyn) is +4.00 m

DATA SET: SCHL1

CLIENT: UWB
LOCATION: Landfill Site
COUNTY: Gwynedd, UK
PROJECT: MSc Thesis, Ameer
ELEVATION: 0.00
SOUNDING COORDINATES: X: 0.0000 Y: 0.0000

DATE: 17-7-95
SOUNDING: 1
AZIMUTH: 11.5 Deg N-NE
EQUIPMENT: Geopulse

Schlumberger Configuration

FITTING ERROR: 2.944 PERCENT

L #	RESISTIVITY (ohm-m)	THICKNESS (meters)	ELEVATION (meters)	LONG. COND. (Siemens)	TRANS. RES. (Ohm-m^2)
			0.0		
1	14.29	3.19	-3.19	0.223	45.75
2	65.75				

ALL PARAMETERS ARE FREE

PARAMETER BOUNDS FROM EQUIVALENCE ANALYSIS

	LAYER	MINIMUM	BEST	MAXIMUM
RHO	1	13.784	14.298	14.717
	2	60.377	65.751	70.270
THICK	1	2.898	3.200	3.439
DEPTH	1	2.898	3.200	3.439

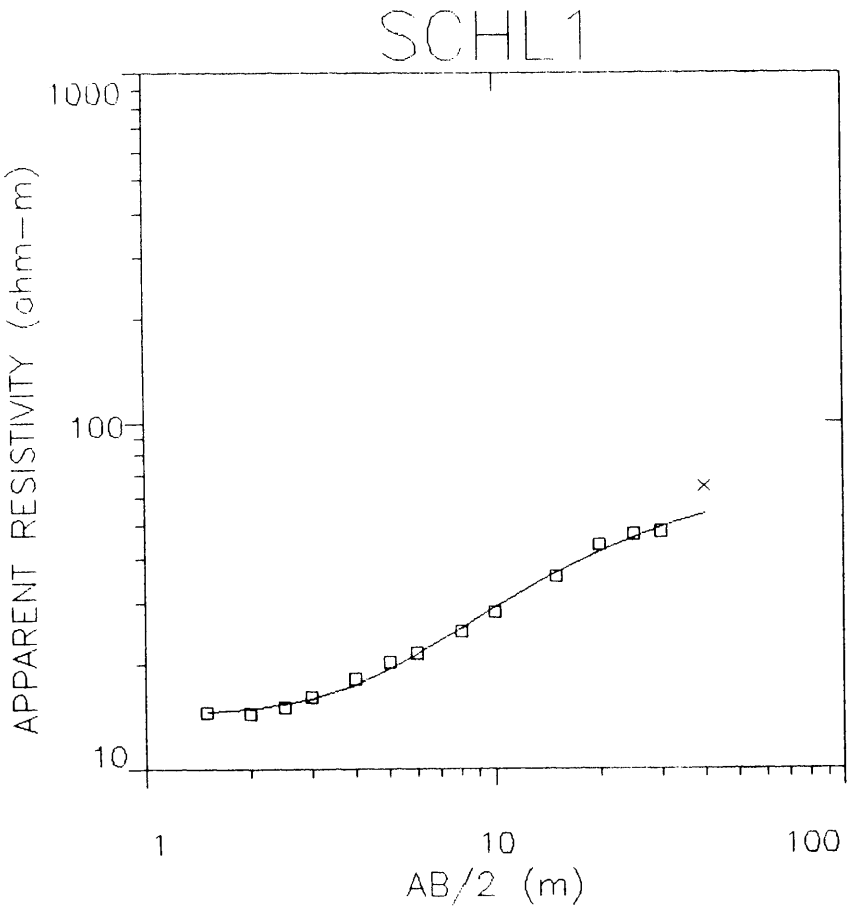
No.	SPACING (m)	RHO-A (ohm-m) DATA	SYNTHETIC	DIFFERENCE (percent)
1	1.50	14.57	14.53	0.242
2	2.00	14.37	14.83	-3.21
3	2.50	14.97	15.27	-2.04
4	3.00	16.08	15.86	1.35
5	4.00	18.06	17.39	3.65
6	5.00	20.14	19.26	4.32
7	6.00	21.34	21.28	0.273
8	8.00	24.73	25.32	-2.37
9	10.00	27.95	29.02	-3.83
10	15.00	35.37	36.45	-3.05

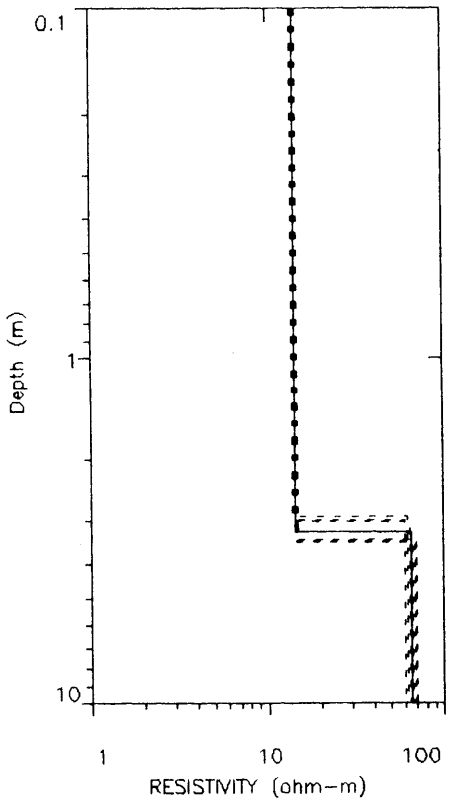
No.	SPACING (m)	RHO-A (ohm-m) DATA	SYNTHETIC	DIFFERENCE (percent)
11	20.00	43.69	41.89	4.12
12	25.00	46.98	45.98	2.13
13	30.00	47.70	49.12	-2.97
14	40.00	64.35	53.58	16.73

PARAMETER RESOLUTION MATRIX:
"F" INDICATES FIXED PARAMETER

P 1	1.00		
P 2	0.00	1.00	
T 1	0.00	0.00	1.00
	P 1	P 2	T 1

Appendix A6.5





DATA SET: SCHL2

CLIENT: UWB
LOCATION: Landfill Site
COUNTY: Gwynedd, UK
PROJECT: MSc Thesis, Ameer
ELEVATION: 0.00
SOUNDING COORDINATES: X: 0.0000 Y: 0.0000

DATE: 17-7-95
SOUNDING: 1
AZIMUTH: 11.5 Deg N-NE
EQUIPMENT: Geopulse

Schlumberger Configuration

FITTING ERROR: 2.687 PERCENT

L #	RESISTIVITY (ohm-m)	THICKNESS (meters)	ELEVATION (meters)	LONG. COND. (Siemens)	TRANS. RES. (Ohm-m^2)
			0.0		
1	38.22	10.88	-10.88	0.284	416.2
2	224.3				

ALL PARAMETERS ARE FREE

PARAMETER BOUNDS FROM EQUIVALENCE ANALYSIS

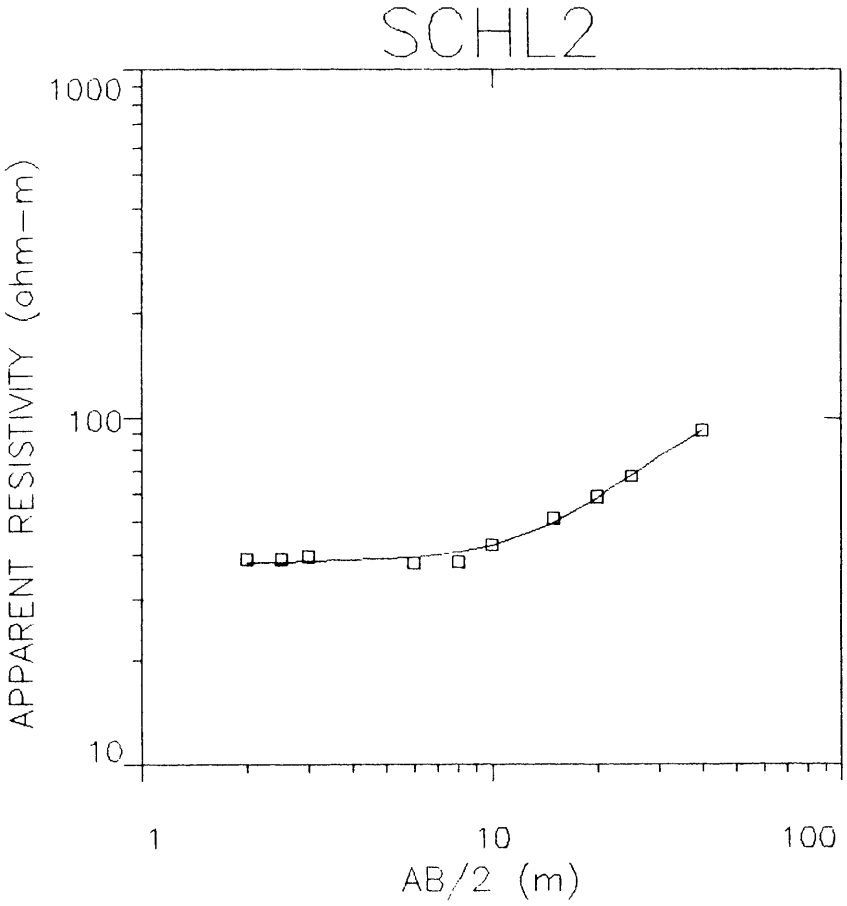
	LAYER	MINIMUM	BEST	MAXIMUM
RHO	1	37.470	38.225	38.993
	2	175.560	224.376	308.252
THICK	1	9.897	10.890	12.124
DEPTH	1	9.897	10.890	12.124

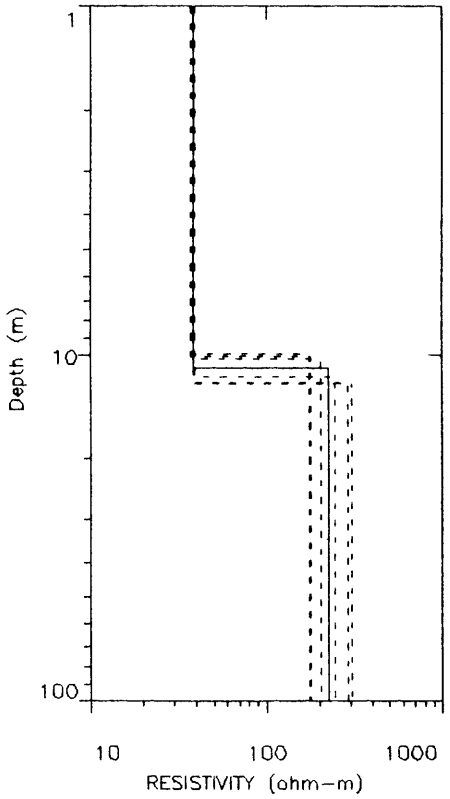
No.	SPACING (m)	RHO-A (ohm-m) DATA	SYNTHETIC	DIFFERENCE (percent)
1	2.00	38.99	38.26	1.86
2	2.50	39.02	38.30	1.82
3	3.00	39.58	38.36	3.05
4	6.00	38.10	39.34	-3.27
5	8.00	38.35	40.70	-6.15
6	10.00	42.60	42.67	-0.172
7	15.00	51.02	49.75	2.48
8	20.00	59.09	58.58	0.861
9	25.00	67.31	67.78	-0.708
10	40.00	92.51	92.66	-0.166

PARAMETER RESOLUTION MATRIX:
"F" INDICATES FIXED PARAMETER

P 1	1.00		
P 2	0.00	0.99	
T 1	0.00	0.00	1.00
	P 1	P 2	T 1

Appendix A6.5





DATA SET: SCHL3

CLIENT: UWB DATE: 25-7-95
LOCATION: LANDFILL SITE SOUNDING: 3
COUNTY: GWYNEDD, UK AZIMUTH:
PROJECT: MSc THESIS, AMEER EQUIPMENT: GEOPULSE
ELEVATION: 0.00
SOUNDING COORDINATES: X: 0.0000 Y: 0.0000

Schlumberger Configuration

FITTING ERROR: 2.108 PERCENT

L #	RESISTIVITY (ohm-m)	THICKNESS (meters)	ELEVATION (meters)	LONG. COND. (Siemens)	TRANS. RES. (Ohm-m^2)
			0.0		
1	38.22	2.85	-2.85	0.0748	109.3
2	261.1				

ALL PARAMETERS ARE FREE

PARAMETER BOUNDS FROM EQUIVALENCE ANALYSIS

	LAYER	MINIMUM	BEST	MAXIMUM
RHO	1	36.698	38.223	39.711
	2	240.611	261.143	286.135
THICK	1	2.644	2.860	3.072
DEPTH	1	2.644	2.860	3.072

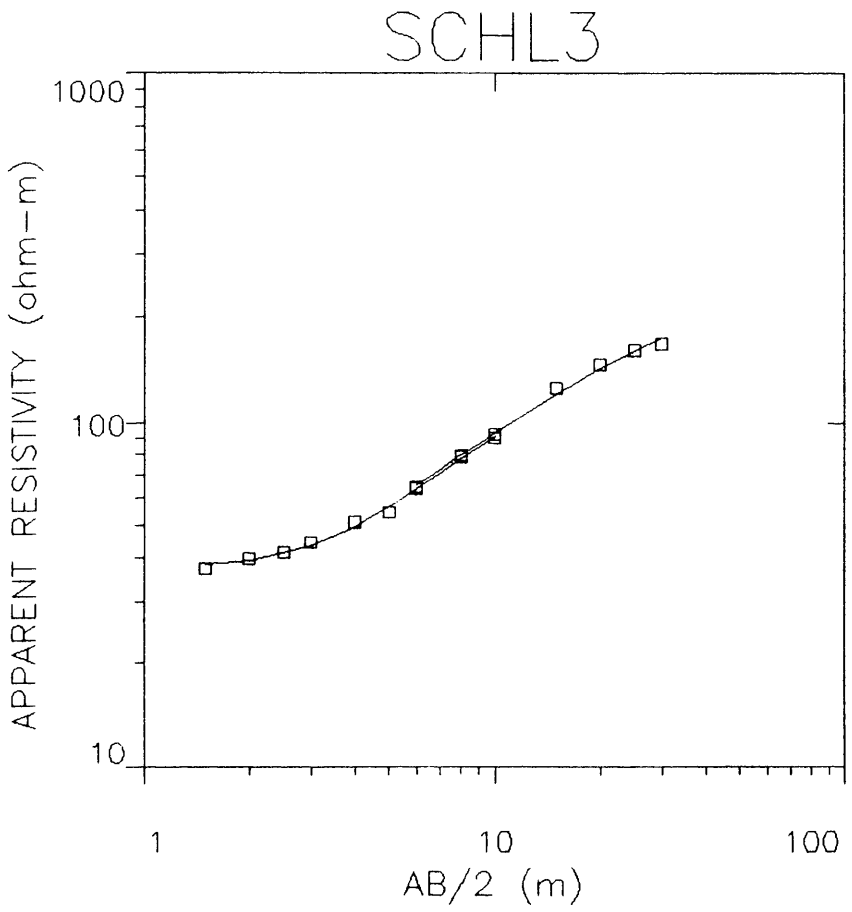
No.	SPACING (m)	RHO-A (ohm-m) DATA	SYNTHETIC	DIFFERENCE (percent)
1	1.50	37.37	38.33	-2.58
2	2.00	39.82	39.57	0.611
3	2.50	41.85	41.38	1.10
4	3.00	44.53	43.73	1.79
5	4.00	50.96	49.68	2.50
6	5.00	54.43	56.65	-4.08
7	6.00	64.35	64.00	0.538
8	8.00	78.91	78.40	0.636
9	10.00	90.56	91.58	-1.13
10	6.00	64.59	65.54	-1.47

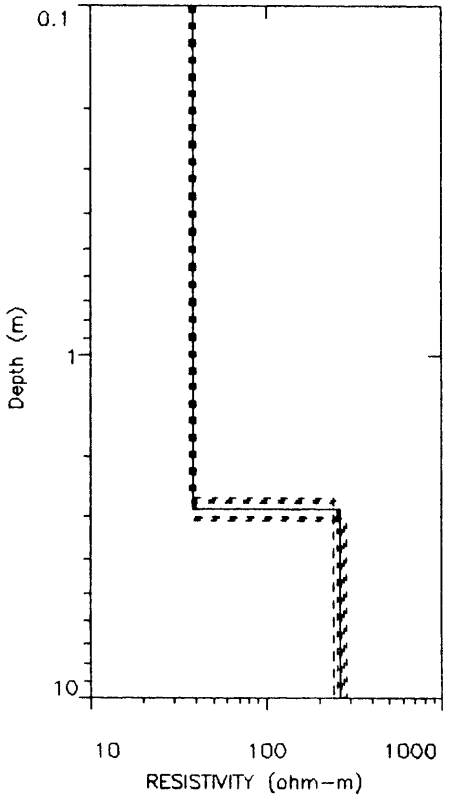
No.	SPACING (m)	RHO-A (ohm-m) DATA	SYNTHETIC	DIFFERENCE (percent)
11	8.00	80.10	80.29	-0.244
12	10.00	92.74	93.79	-1.13
13	15.00	126.3	121.7	3.63
14	20.00	146.4	143.2	2.17
15	25.00	161.4	160.2	0.722
16	30.00	168.1	173.9	-3.39

PARAMETER RESOLUTION MATRIX:
"F" INDICATES FIXED PARAMETER

P 1	1.00		
P 2	0.00	1.00	
T 1	0.00	0.00	1.00
	P 1	P 2	T 1

Appendix A6.5





DATA SET: SCHL4

CLIENT: UWB
LOCATION: Landfill Site
COUNTY: Gwynedd, UK
PROJECT: MSc Thesis, Ameer
ELEVATION: 0.00
SOUNDING COORDINATES: X: 0.0000 Y: 0.0000

DATE: 25-7-95
SOUNDING: 4
AZIMUTH: 11.5 Deg N-NE
EQUIPMENT: Geopulse

Schlumberger Configuration

FITTING ERROR: 5.281 PERCENT

L f	RESISTIVITY (ohm-m)	THICKNESS (meters)	ELEVATION (meters)	LONG. COND. (Siemens)	TRANS. RES. (Ohm-m^2)
			0.0		
1	23.17	0.784	-0.784	0.0338	18.17
2	7.95	9.81	-10.59	1.23	78.02
3	4051.1				

ALL PARAMETERS ARE FREE

PARAMETER BOUNDS FROM EQUIVALENCE ANALYSIS

	LAYER	MINIMUM	BEST	MAXIMUM
RHO	1	17.548	23.171	32.489
	2	7.123	7.951	8.641
	3	347.371	4051.119	44054.578
THICK	1	0.577	0.784	1.071
	2	8.372	9.814	11.067
DEPTH	1	0.577	0.784	1.071
	2	9.374	10.598	11.719

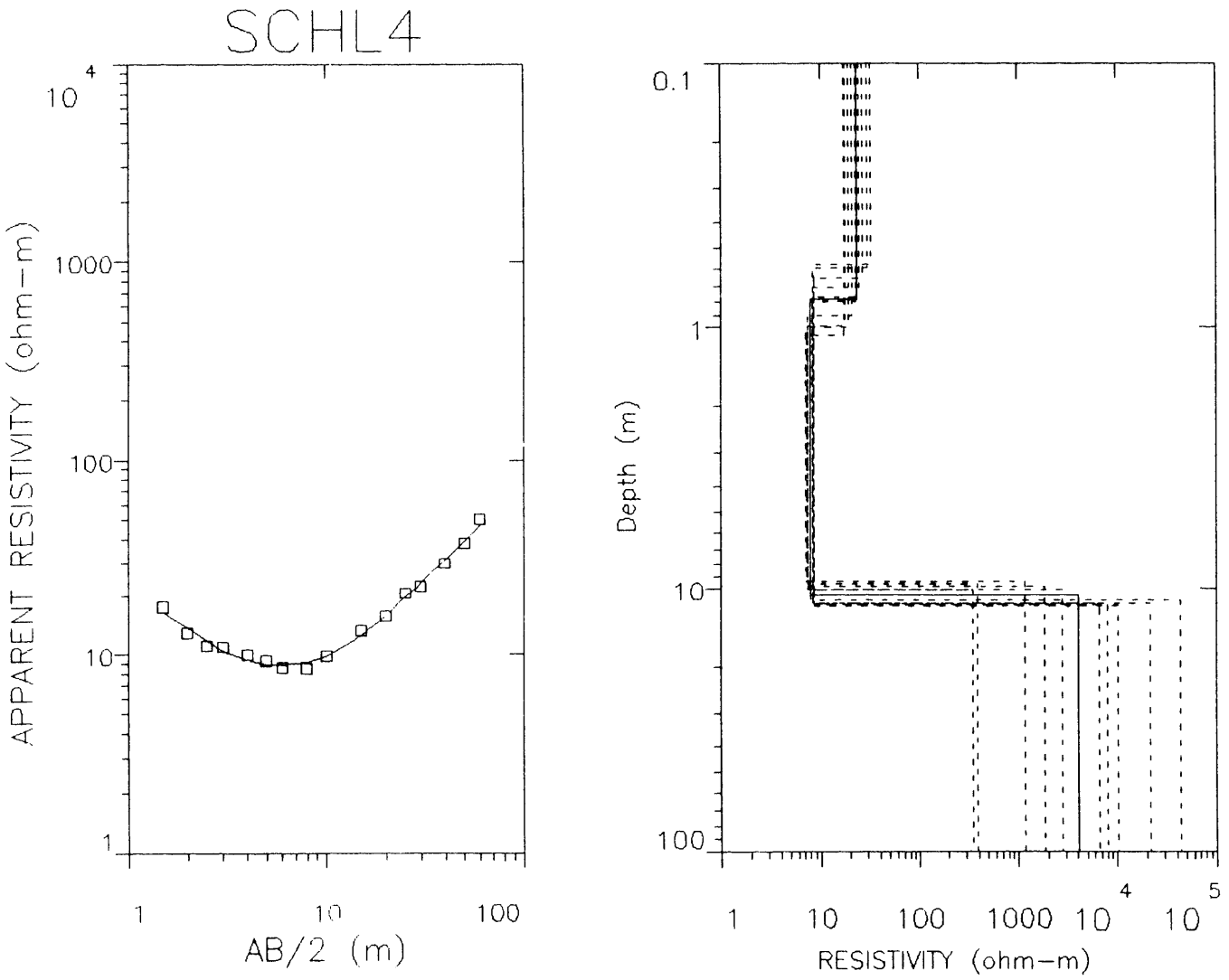
No.	SPACING (m)	RHO-A (ohm-m) DATA	RHO-A (ohm-m) SYNTHETIC	DIFFERENCE (percent)
1	1.50	17.46	16.53	5.29
2	2.00	12.84	13.69	-6.63
3	2.50	11.16	11.74	-5.20
4	3.00	10.91	10.50	3.68
5	4.00	9.99	9.30	6.84
6	5.00	9.25	8.90	3.77

No.	SPACING (m)	RHO-A (ohm-m) DATA	RHO-A (ohm-m) SYNTHETIC	DIFFERENCE (percent)
7	6.00	8.55	8.82	-3.20
8	8.00	8.42	9.14	-8.53
9	10.00	9.78	9.80	-0.280
10	15.00	13.15	12.43	5.48
11	20.00	15.75	15.84	-0.571
12	25.00	20.71	19.56	5.55
13	30.00	22.51	23.38	-3.86
14	40.00	29.81	31.09	-4.27
15	50.00	37.78	38.79	-2.67
16	60.00	50.43	46.46	7.86

PARAMETER RESOLUTION MATRIX:
"F" INDICATES FIXED PARAMETER

P 1	1.00				
P 2	0.00	1.00			
P 3	0.00	0.00	0.63		
T 1	0.00	0.00	0.00	1.00	
T 2	0.00	0.00	-0.01	0.00	1.00
	P 1	P 2	P 3	T 1	T 2

Appendix A6.5



DATA SET: SCHL4

CLIENT: UWB
LOCATION: Landfill Site
COUNTY: Gwynedd, UK
PROJECT: MSc Thesis, Ameer
ELEVATION: 0.00
SOUNDING COORDINATES: X: 0.0000 Y: 0.0000

DATE: 25-7-95
SOUNDING: 4
AZIMUTH: 11.5 Deg N-NE
EQUIPMENT: Geopulse

Schlumberger Configuration

FITTING ERROR: 3.974 PERCENT

L #	RESISTIVITY (ohm-m)	THICKNESS (meters)	ELEVATION (meters)	LONG. COND. (Siemens)	TRANS. RES. (Ohm-m^2)
			0.0		
1	94.47	0.354	-0.354	0.00375	33.49
2	11.56	1.64	-1.99	0.142	19.00
3	6.93	7.89	-9.89	1.13	54.74
4	842.6				

ALL PARAMETERS ARE FREE

PARAMETER BOUNDS FROM EQUIVALENCE ANALYSIS

	LAYER	MINIMUM	BEST	MAXIMUM
RHO	1	52.383	94.476	229.360
	2	10.385	11.562	13.029
	3	6.008	6.932	7.596
	4	374.423	842.670	3774.338
THICK	1	0.281	0.355	0.422
	2	1.205	1.643	2.393
	3	6.412	7.897	9.094
DEPTH	1	0.281	0.355	0.422
	2	1.540	1.998	2.768
	3	9.163	9.895	10.697

No.	SPACING (m)	RHO-A (ohm-m) DATA	RHO-A (ohm-m) SYNTHETIC	DIFFERENCE (percent)
1	1.50	17.46	17.28	1.02
2	2.00	12.84	13.04	-1.55

No.	SPACING (m)	RHO-A (ohm-m) DATA	RHO-A (ohm-m) SYNTHETIC	DIFFERENCE (percent)
3	2.50	11.16	11.51	-3.15
4	3.00	10.91	10.69	1.99
5	4.00	9.99	9.67	3.13
6	5.00	9.25	9.07	1.85
7	6.00	8.48	8.77	-3.50
8	8.00	8.29	8.79	-6.07
9	10.00	9.68	9.34	3.42
10	15.00	12.89	11.95	7.23
11	20.00	15.43	15.34	0.581
12	25.00	20.29	18.95	6.58
13	30.00	21.00	22.60	-7.66
14	40.00	29.00	29.87	-3.02
15	50.00	37.00	37.03	-0.0989
16	60.00	46.00	44.08	4.16

PARAMETER RESOLUTION MATRIX:
"F" INDICATES FIXED PARAMETER

P 1	0.18							
P 2	-0.09	0.96						
P 3	-0.01	-0.02	0.96					
P 4	0.00	0.00	-0.02	0.08				
T 1	0.21	0.05	0.01	0.00	0.93			
T 2	0.08	0.10	0.11	0.04	-0.07	0.61		
T 3	-0.03	-0.04	-0.06	-0.06	0.03	0.17	0.91	
	P 1	P 2	P 3	P 4	T 1	T 2	T 3	

REFERENCES

Al-Ruwaih, F.M. (1992). The feasibility of the resistivity sounding method for detecting the brackish/saline water interface in Kuwait. ***Journal of the University of Kuwait (Sci.)***, v. 19, pp 117-131.

Archie, G. E. (1942). The electrical resistivity log as an aid in determining some reservoir characteristics. ***Petrolum Technology Report 1422, American Institute of Mining and Metallurigical Engineering.***, pp 54-62.

Barker, R.D. (1981). The Offset system of electrical resistivity sounding and its use with a multicore cable. ***Geophysical Prospecting***, v. 29, pp 128-143.

Barker, R. D. (1992). A simple algorithm for electrical imaging of the subsurface. ***First Break***, v. 10, (2), pp 53- 62.

Bhattacharya, P. K. & Patra, H. P. (1968). Direct current geoelectric sounding, principles and interpretation., p.135. **Elsevier.** New York.

Carpenter, E.W. & Habberjam, G.M. (1956). A tri-potential method of resistivity prospecting., ***Geophysics***, v. 21, 455-469.

CGIL (Campus Geophysical Instruments Limited). (1992). Instruction manual of the Campus Geopulse (an earth resistance meter). **CGIL, Institute of Research and Development**. Birmingham. UK.

Cooper, Jr. H. H. (1959). A hypothesis concerning the dynamic balance of fresh water & salt water in a coastal aquifer. ***Journal of Geophysical Research***, v. 64, No. 4, pp 461-467.

Cooper, H. H., Jr., Kohout, F. A., Henry, H. R. & Glover, R. E. (1964). Seawater in coastal aquifers. **U.S. Geological Survey Water Supply Paper** 1613-C., pp C12-C32.

Dakhnov, V. V.(1953). Electrical prospecting for petroleum and natural gas deposits. 497p. **Gostoptekhzat**. Moscow.

Davis, P. A., Greenhalga, S. A. & Merrick, N. P. (1980). Resistivity sounding computations with any array using a single digital filter. ***Bull. Aust. Soci. Explor. Geophys.***, 11, pp 54-62.

Dey, A. & Morrison, H. F. (1979). Resistivity modelling for arbitrary shaped two-dimensional structures. ***Geophysical Prospecting***, v. 27, pp 106- 136.

Elwaheidi, M. M.; Merlanti, F. & Pavan, M. (1992). Geoelectrical resistivity survey of the central part of Azraq basin (Jordan) for identifying saltwater fresh-water interface. ***Journal of Applied Geophysics***, v. 29, No. 2, pp 125-133.

Fitterman, D. V. (1987). Examples of transient sounding for ground-water exploration in sedimentary aquifers. ***Ground Water***, v. 25, No. 6, pp 685-692.

Freeze, R. A. & Cherry, J. A. (1979). Groundwater., p. 604. **Prentice-Hall, Inc**. London.

Frohlich, R. K. (1974). Combined geoelectrical & drill-hole investigations for detecting fresh-water aquifers in Northwestern. ***Geophysics***, v. 39, No. 3, pp. 340-352.

GDC (Groundwater Development Consultant). (1980). Umm er Radhuma study, Bahrain assignment. **Ministry of Commerce and Agriculture**, Bahrain.

Ghyben, W. B. (1888). Nota in verband met de voorgenomen putboring nabij Amsterdam. **Tijdschrift van let Koninklijk Inst**. Van Ing.

Gilchrist, Z. (1993). Site investigation of College Aber Farm. In situ seismic wave velocity measurements. **Unpublished BSc Project, School of Ocean Sciences, University College of North Wales, Bangor**. UK.

Glovtsin, V. N. (1963) Elecktrorazvedka (Electrical prospecting)., p. 361 **Kiev, Akademiya Nauuk Ukrainiskoi ssr**.

Gonzalez, A. & Romero, E. (1991). Influence of pumps on salinity of a coastal aquifer with legal protection (A zone in the north of Isla-Cristina, Huelva, Spain). ***Water Science and Technology***, v. 24, No. 11, pp 251-260.

Goswami, A. B. (1968). A study of salt water encroachment in the coastal aguifer at Digha, Midnapore district, West Bengal, India. ***Bull. Int. Assoc. Hydrol.***, v. 13 (3), pp 77-87.

Griffiths, D. H. & Barker, R. D. (1993). Two-dimensional resistivity imaging and modeling in areas of complex geology. ***Journal of Applied Geophysics***, v. 29, pp 211- 226.

Griffiths, D. H. & Turnbull, J. (1985). A multi-electrode array for resistivity surveying. ***First Break***, 3 (7), pp. 16- 20.

Griffiths, D. H., Turnbull, J. & Olayinka, A. I. (1990). Two dimensional resistivity mapping with a computer-controlled array. ***First Break***, v. 8, pp 121- 129.

Hallof, P. G. (1957). On the interpretation of resistivity and induced polarization measurements. **Ph.D thesis, Massachusetts Institute of Technology.**

Harris, W. H. (1967). Stratification of fresh & salt water on Barrier Islands as a result of differences in sediment permeability. ***Water Resources Research***, v. 3, No. 1, pp 89-97.

Henry, H. R. (1960). Salt water intrusion into a coastal aquifer. ***International Association Society of Hydrology*, Publ**. v. 52, pp. 478-487.

Herzberg, B. (1901). Die wasserversorgung einiger Nordseebader. ***Jour. Gasbeleuchtung und Wasserversorgung***, Munich, v. 44, pp 815-819, 842-844.

Hubbert, M.K. (1940). The theory of groundwater motion. ***Jour. Geology***., v. 48, pp 785-944.

Inman, J. R. (1975). Resistivity inversion with ridge regression. ***Geophysics***, v. 40, pp 798-817.

Interpex Ltd. (1992). Resistivity data interpretation software: Resix Plus, version 2.0: User's Manual. ***Interpex Limited. Golden***, *Colorado*, USA.

Jackson, P.D. (1975). An electrical resistivity method for evaluating the In-situ porosity of clean marine sands. ***Marine Geotechnology***, v. 1, No. 2, pp 91-115.

Keary, P. & Brooks, M. (1991). An introduction to geophysical exploration. **Blackwell Scientific Publications**, London.

Keller, G. V. & Frischknecht, F. C. (1966). Electrical methods in Geophysical prospecting., p. 519. **Pergamon Press.** Oxford.

Kelly, W. E. (1976). Geoelectric sounding for delineating groundwater contamination. ***Groundwater***, v. 14, No. 1, pp. 6-10.

Koefoed, O. (1976). Progress in the direct interpretation of resistivity soundings: an algorithm. ***Geophysical Prospecting***, v. 24, pp 233-240.

Kohout, F. A. (1964) The flow of fresh water and salt water in the Biscayne aquifer of the Miami area, Florida, in Sea water in coastal Aquifer, U.S. ***Geological survey water - Supply paper 1613C***, pp. 12-32.

Kosinski, W. K. and Kelly, W. E. (1981). Geoelectric soundings for predicting aquifer properties. ***Ground Water***, v. 19, No. 2, pp 163-171.

Kunetz, G. (1966). Principle of direct current resistivity prospecting., p. 103 **Gebrüder Borntraeger**. Berlin.

Loke, M. H. & Barker, R. D. (1994). Rapid least-squares inversion of resistivity pseudosections: **56th Annual Meeting, European Association of Exploration Geophysicists, Expanded Abstracts, I002.**

Mills, T.; Hoekstra, P.; Blohm, M., and Evans, L. (1988). Time domain electromagnetic soundings for mapping sea-water intrusion in Monterey County, California. ***Ground Water***, v. 26, No. 6, pp 771-782.

Nawawi, M. N. M. & Loke, M. H. (1995). Mapping voids and other man-made subsurface structures using 2D resistivity imaging technique. **An Abstract presented to the EAGE 57 Conference and Technical Exhibition - Glasgow, Scotland, 29 May-2 June 1995, v 1, ISBN 90-73781-06-x**. Glasgow, UK.

Overmeeren, R. A. (1989). Aquifer boundaries explored by geoelectrical measurements in the coastal plain of Yemen: A case of equivalence. ***Geophysics***, v. 54, No. 1. pp 38-48.

Sandberg, S. K. (1993). Examples of resolution improvement in geoelectrical soundings applied to groundwater investigations. ***Geophysical Prospecting***, v. 41, pp 207-227.

Sarma, K. S. S., Chandrasekharan, H., Datta, D., Mookerji, P., & Das, D. K. (1993). Geo-electrical investigation on sub-surface configuration & groundwater salinity in Indira Gandhi Canal command, western Rajasthan. ***Annals of Arid Zone***, v. 32; No. 3, pp 145-150.

Singh, S. P. & Stammer, W. N. (1989). A potential theory-based finite element algorithm for freshwater recharge of saline aquifers: A sharp interface model. ***Water Resources Research***, v. 25, No. 1, pp 1685-1694.

Soomro, S. A. (1993). Detection of saline intrusion in coastal and estuarine sediments. **Ph.D thesis, University College of North Wales, Bangor**, UK.

Telford, W. M., Geldart, L. P., Sheriff, R. E. (1990). Applied geophysics. **Cambridge University press,** USA.

Todd, D. K. (1959). Ground Water Hydrology., p. 336 **John Wiley & Sons, Inc.** London.

Todd, D. K., (1980). Groundwater Hydrology. 2nd edition. 245 p. **John Wiley and Sons**. New York.

Tonks, D. M; Hunt, S. D; and Bayne, J. M. (1993). Use of the conductivity probe to evaluate groundwater contamination. ***Ground Engineering***, pp 24-29.

Turnbull, J. (1986). A field and interpretation technique for resistivity surveys in two-dimensional structures. **Ph.D thesis, University of Birmingham**, UK.

Volker, R. E., & Ruston, K. R. (1982). An assessment of the importance of some parameters for seawater intrusion in aquifer modelling approaches. ***Journal of Hydrology***, v. 56, pp 239-250.

Wenner F.(1916). A method of measuring earth resistivity. ***U.S. Buearu of Standard Bull.***, 12 pp. 469-478.

Worthington, P. F. (1976). Hydrogeophysical equivalence of water salinity, Porosity & Matrix conduction in arenaceous aquifers. ***Ground Water***, v. 14, No. 4, pp 224-232.

Wu, J. C., Xue, Y. Q., Liu, P.M., Wang, J. J. Jiang, Q. B. and Shi, H. W. (1993). Sea-water intrusion in the coastal area of Laizhon Bay, China. 2. Sea-water intrusion monitoring. ***Ground Water***, v. 31, No. 5, pp. 740-745.

Zohdy, A. A. R, Eaton, G. P. & Maby, D. R. (1974). Application of surface geophysics to groundwater investigation. **Techniques of Water-Resources Investigations of the United States Geological Survey. Book 2, Chapter D1. U.S. Geological Survey. Government Printing office**, Washington, DC.

Zohdy, A. A. R. (1989). A new method for the automatic interpretation of Schlumberger & Wenner sounding curves. ***Geophysics***, v. 54, No. 2, pp 245-253.